University of Alberta

The Howell Creek suite, southeastern British Columbia - mid-Cretaceous alkalic intrusions and related gold deposition in the Canadian Cordillera

by

Elspeth M. Barnes

A thesis submitted to the Faculty of Graduate Studies and Research in partial fulfillment of the requirements for the degree of Master of Science

Department of Earth and Atmospheric Science

Edmonton, Alberta

Spring 2002

National Library of Canada
Acquisitions and Bibliographic Services
395 Wellington Street
Ottawa ON K1A 0N4
Canada

Bibliothèque nationale du Canada
Acquisitions et services bibliographiques
395, rue Wellington
Ottawa ON K1A 0N4
Canada

Your file Votre référence

Our file Notre référence

The author has granted a non-exclusive licence allowing the National Library of Canada to reproduce, loan, distribute or sell copies of this thesis in microform, paper or electronic formats.

L'auteur a accordé une licence non exclusive permettant à la Bibliothèque nationale du Canada de reproduire, prêter, distribuer ou vendre des copies de cette thèse sous la forme de microfiche/film, de reproduction sur papier ou sur format électronique.

The author retains ownership of the copyright in this thesis. Neither the thesis nor substantial extracts from it may be printed or otherwise reproduced without the author's permission.

L'auteur conserve la propriété du droit d'auteur qui protège cette thèse. Ni la thèse ni des extraits substantiels de celle-ci ne doivent être imprimés ou autrement reproduits sans son autorisation.

0-612-69684-7

Canada

University of Alberta

Library Release Form

Name of Author: Elspeth M. Barnes

Title of thesis: The Howell Creek suite, southeastern British Columbia - mid-Cretaceous alkalic intrusions and related gold deposition in the Canadian Cordillera.

Degree: Master of Science

Year this Degree Granted: 2002

Permission is hereby granted to the University of Alberta library to reproduce single copies of this thesis and to lend or sell such copies for private, scholarly or scientific research purposes only.

The author reserves all other publication and other rights in association with the copyright in the thesis, and except as herein before provided, neither the thesis nor any substantial portion thereof may be printed or otherwise reproduced in any material form whatever without the author's prior written permission.

E.M. Barnes

Appt. 704.
11147-82 Avenue
Edmonton
AB T6G 0T5

31st January 2002

University of Alberta

Faculty of Graduate Studies and Research

The undersigned certify that they have read, and recommend to the Faculty of Graduate Studies and Research for acceptance, a thesis entitled 'The Howell Creek suite, southeastern British Columbia - mid-Cretaceous alkalic intrusions and related gold deposition in the Canadian Cordillera' submitted by Elspeth M. Barnes in partial fulfillment of the requirements for the degree of Master of Science

Dr. J. P. Richards

Dr. R. A. Burwash

Dr. S. Frimpong

28th January 2002

Abstract

The mid-Cretaceous alkalic Howell Creek suite of southeastern British Columbia, consists of coeval, hypabyssal, intrusions of alkali feldspar syenite, foid syenite, megacrystic syenite, and gabbro, with associated intrusive breccias. These rocks are spatially associated with low-grade gold mineralisation.

The results of x-ray fluorescence analysis (XRF) and inductively coupled plasma mass-spectrometry (ICP-MS) provide trace and rare earth element data which indicate a geochemical association between the intrusive phases. This augments the results of $^{40}Ar/^{39}Ar$ dating of K-feldspar phenocrysts which confirms coeval emplacement of the intrusions at ~102 Ma.

The Howell Creek suite and its associated style of mineralisation bears similarities to other mid-Cretaceous intrusive suites occurring along the Canadian Cordillera resulting from anatectic melting of thickened crustal rocks.

The Howell Creek area lies in a unique position proximal to a crustal lineament, and its potential influence on the location and geochemistry of the Howell Creek suite is discussed.

Table of Contents

Introduction	Page 1
Professional contributions	Page 4
Previous work	Page 5
Structure	Page 6
Igneous rocks	Page 10
Mineralisation	Page 11
Fieldwork	Page 12
Geology of mapped area	Page 13
Stratigraphy	Page 13
Late Proterozoic	Page 13
Cambrian	Page 14
Devonian	Page 14
Mississippian	Page 14
Permian-Pennsylvanian	Page 15
Triassic	Page 15
Upper Cretaceous	Page 15
Fossils	Page 16
Igneous rocks and intrusive breccias	Page 16
Alkali feldspar syenite	Page 16
Foid syenite	Page 17
Megacrystic syenite	Page 18
Gabbro	Page 19
Intrusive breccias	Page 19
Mineralogy	Page 20
Phenocrysts and xenocrysts	Page 20
Feldspar	Page 20

Nepheline Page 21
Garnet Page 22
Pyroxene Page 22
Analcite Page 22
Titanite Page 23
Hornblende Page 23
Apatite Page 23
Textures Page 23
Alteration minerals of the intrusive phases Page 24
Feldspar alteration Page 24
Mafic mineral alteration Page 24
Other alteration products Page 25
Alteration of the host rock Page 25
Mineralisation of the intrusive rocks Page 25
Mineralisation of the country rock Page 27

Geochemistry Page 27
Major element analyses Page 28
Interpretation Page 32
Trace and rare earth element analyses Page 34
Multi-element profile and interpretation Page 34
Rare earth element profile and interpretation Page 35
Elemental ratios and their relevance Page 35

Geochronology Page 38
Method for $^{40}Ar/^{39}Ar$ analysis Page 39
$^{40}Ar/^{39}Ar$ age data Page 39
Inverse isochron data Page 42
Plateau data Page 43
Interpretation of $^{40}Ar/^{39}Ar$ data Page 43

Discussion Page 44

Regional igneous geology of southeastern British Columbia

Pre-Mesozoic Page 44

Mesozoic – Southern Omineca Belt Page 45

Mesozoic – Foreland Belt Page 46

Mid-Cretaceous magmatism of the Canadian Cordillera Page 48

Tombstone pluton Page 49

Mineralisation Page 51

Cassiar batholith Page 52

Bayonne Suite Page 53

Crowsnest Formation Page 56

Mesozoic-Cenozoic magmatism of Montana Page 60

Mineralisation Page 62

Basement rock composition and structure Page 62

The Howell Creek suite – synthesis

Setting Page 65

Intrusions Page 68

Mineralisation and alteration Page 70

Further studies Page 72

Conclusions Page 75

Acknowledgements Page 76

Bibliography Page 80

List of Appendices

Appendix 1.	Stratigraphic column of sedimentary rock lithologies	Page 90
Appendix 2.	Chronological list of fossils	Page 91
Appendix 3.	Petrographic observations	Page 92
Appendix 4.	Table of geochemical data	Page 98-99
Appendix 5.	Table of geochronological data	Page 100

List of Tables

Table 1.	Electron microprobe data of the feldspar crystals of EB1301	Page 21
Table 2.	Compositional variations between Howell Creek suite samples and averages of comparable rock types	Page 29
Table 3.	CIPW normative values for Howell Creek suite samples	Page 31-32
Table 4.	Elemental ratio variations between Howell Creek suite samples and average source rock compositions	Page 37
Table 5.	Elemental ratios of Howell Creek suite samples	Page 37-38
Table 6.	Howell Creek suite and Tombstone pluton major oxide abundances	Page 50
Table 7.	Cassiar batholith and Bayonne Suite lithologies	Page 54
Table 8.	Phenocrysts of the Crowsnest Formation	Page 57
Table 9.	Howell Creek suite and Crowsnest Formation major oxide abundances	Page 58

List of Figures

Map	Howell Creek area	In pocket
Figure 1.	Map of western Canada	Page 2
Figure 2.	Map of igneous intrusions in the Howell Creek area	Page 5
Figure 3.	Schematic plans of Howell Creek faults	Page 7
a)	after Price (1965)	
b)	after Legun (1993)	
c)	after Brown and Cameron (1999)	
Figure 4.	Schematic cross-sections of Howell Creek faults	Page 7
a)	after Price (1965)	
b)	after Labreque and Shaw (1973)	
Figure 5.	TAS diagram of Howell Creek samples	Page 29
Figure 6.	Shand Index diagram of Howell Creeks samples	Page 30
Figure 7.	Harker diagrams of Howell Creek samples	Page 33
Figure 8.	Multi-element plot of Howell Creek samples	Page 34
Figure 9.	Rare earth element profiles of Howell Creek samples	Page 36
Figure 10.	$^{40}Ar/^{39}Ar$ diagrams for sample 1301A	Page 40
a)	inverse isochron plot	
b)	plateau data plot	
Figure 11.	$^{40}Ar/^{39}Ar$ diagrams for sample EB1810	Page 41
a)	inverse isochron plot	
b)	plateau data plot	
Figure 12.	Map of selected intrusions of the Canadian Cordillera	Page 46
Figure 13.	Schematic map of tectonic features and igneous intrusions of the Howell Creek area	Page 47
Figure 14.	Multi-element plot comparing Howell Creek and Tombstone pluton samples	Page 51
Figure 15.	Multi-element plot comparing Howell Creek and Cassiar Batholith samples	Page 53
Figure 16.	Multi-element plot comparing Howell Creek, Cassiar Batholith, and Bayonne Suite samples	Page 55

Figure 17. Multi-element plot comparing Howell Creek and Crowsnest Formation samples Page 59
Figure 18. Multi-element plot comparing Howell Creek and Highwood Mountains samples Page 61

List of Plates

Plate 1. Inset from 1:44 444 scale map of Eastern Outlier Page 77

Plates 2-6. Page 78

2. Cretaceous fossils
3. Alkali feldspar syenite
4. Pink alkali feldspar syenite
5. Xenolithic megacrystic syenite
6. Foid syenite

Plates 7-10. Page 79

7. Megacrystic syenite
8. Fluorite vein
9. Pyrite and calcite mineralisation
10. Quartz stockwork veining

List of Symbols and Abbreviations

$^{40}Ar/^{39}Ar$, $^{36}Ar/^{39}Ar$	Ratios of argon isotopes measured in this study to calculate the age of the igneous rocks
CIPW	Cross, Iddings, Pirsson and Washington
EDS	energy dispersive spectra
Ga	billion years
GSC	Geological Survey of Canada
HFSE	high field strength element
ICP-MS	inductively coupled plasma mass-spectrometry
Kd	Nernst distribution coefficient
LILE	large ion lithophile element
LREE	light rare earth element
Ma	million years
MREE	medium rare earth element
MSWD	mean square of weighted deviates
NewPet	geochemical data handling and plotting software
PM	primitive mantle
REE	rare earth element
UTM	Universal Transverse Mercator
XRF	X-ray fluorescence

Introduction

For the last thirty years, exploration work has investigated the occurrence of low-grade gold mineralisation in the Howell Creek area of southeast British Columbia (Fig. 1; Williams and James 1971; Netolitzky, 1972; Goble, 1973; Noakes, 1984; Casselman and Termuende, 1987; Fox and Cameron, 1986, 1987, 1989). The mineralisation is spatially associated with a suite of mid-Cretaceous hypabyssal, alkalic intrusions (the Howell Creek suite; Woodsworth et al. 1991), emplaced in Proterozoic to Mesozoic miogeoclinal sedimentary strata (Price, 1962, 1965; Skupinski and Legun, 1989; Legun, 1993; Brown and Cameron, 1999; Lefebure et al., 1999. The British Columbia Geological Survey identified the area as an example of intrusion-related and sediment-hosted, disseminated gold mineralisation (Poulsen, 1996; Brown and Cameron, 1999; Lefebure et al., 1999), and proposed the study reported here.

In order to understand the geological significance of the Howell Creek suite, this study has undertaken detailed studies of the various intrusive phases, supported by geological mapping, x-ray fluorescence analyses (XRF), and inductively coupled plasma mass-spectrometry (ICP-MS) of eighteen whole rock samples from three of the intrusive phases. In addition, transmitted and reflected light microscopy was undertaken on all samples and energy dispersive spectrometry (EDS) was conducted on selected mineral phases. The results have provided information on the nature and petrogenesis of the intrusive suite.

The results of $^{40}Ar/^{39}Ar$ dating, utilising the laser-induced step-heating procedure, confirm that the intrusions form a coeval suite, emplaced during a magmatic event occurring ~102 Ma.

To place the Howell Creek suite within a regional geological context, a comparison is made with the geochemical signatures of selected mid-Cretaceous intrusions occurring along the Canadian Cordillera and younger intrusions in Montana. The results show similarities between these suites, with a particularly strong resemblance to the geochemistry of the Tombstone pluton, part of the Tombstone Range, Yukon (Olade and Goodfellow, 1979; Anderson, 1987; Woodsworth et al., 1991; Mortenson et al. 1996). This discovery strengthens the link between the two areas suggested by Brown and Cameron (1999) and Schroeter and Cameron (1996) in a comparison of their styles of

Figure 1.

Map of western Canada (with inset map of Canada), showing study area, terrane boundaries, and the Omineca Belt (one of five morphogeological divisions of western Canada). After Wheeler and McFeely (1991).

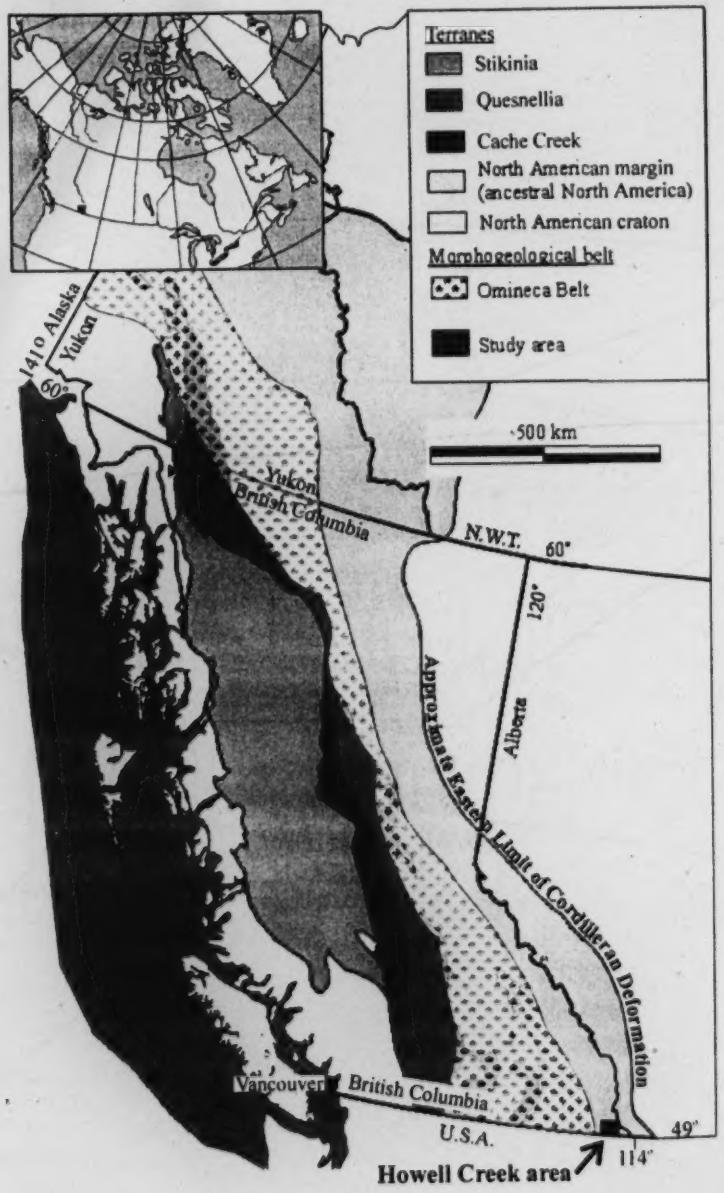

mineralisation. The Canadian examples used in this study are believed to result from anatexis of the underlying crust resulting from compression and thickening of the western edge of the North American craton during the Mesozoic period (Brandon and Lambert, 1990 and 1993; Driver et al., 2000). The results of this study suggest that the influence of Mesozoic deformation on the formation of crustally-associated alkalic magma may have extended along the entire length of the Canadian Cordillera, and furthermore extends the area of prospectivity for associated mineralisation.

The Howell Creek suite lies to the south of the 'Crowsnest Deflection' (Fig. 2; Norris, 1969), within the Front Ranges of the Rocky Mountain Fold and Thrust Belt, and is the most westerly of several regional occurrences of discrete mid-Cretaceous alkalic intrusions and volcanic rocks within an area of <100 km^2 (Pearce, 1970; Ferguson and Edgar, 1978; Dingwall and Brearley, 1985; Goble et al., 1993, 1999b; Peterson and Currie, 1993; Peterson et al., 1997). This area experienced intense compression from the west during the Mesozoic period due to terrane accretion, and the resulting structural complexity in the vicinity of the Howell Creek suite has been studied and debated extensively (1:44 444 scale map and Plate 1; e.g. Price, 1965; Labrecque and Shaw, 1973; Jones, 1977; Skupinski and Legun, 1989; Legun, 1993). This unique region of the Rocky Mountains is underlain by a major crustal lineament (Kanasewich et al., 1969; McMechan, 1981; Ross et al., 1991, 2000, Villeneuve et al., 1993; Eaton et al., 1999; Lemieux et al., 2000) whose potential influence on the structural and magmatic history of the area is discussed in this study.

This thesis begins by reviewing previous studies, outlining the debate regarding the structural complexities, and introducing the various intrusive phases and styles of mineralisation occurring in the area. There follows an account of the mapping component of the study, which includes descriptions of the igneous and sedimentary rocks and fossils as identified in the field. Descriptions of the mineralogy of selected samples are given, prior to the presentation of the results of litho-geochemical analyses and geochronological analyses of two key samples. Finally, the regional context of the Howell Creek suite is discussed, including an outline of the igneous history of the area, a review of work undertaken on the basement rocks, and comparisons with other intrusive suites. The discussion concludes with a synthesis of the emplacement of the Howell

Creek suite, its possible influence on post-emplacement faulting, and processes involved in the mineralisation and alteration of the intrusions and host rocks.

Professional contributions

Elspeth Barnes (University of Alberta): mapping, petrography, $^{40}Ar/^{39}Ar$ sample preparation, microprobe and EDS analysis, literature search, data and literature interpretation.

Dr. Jeremy P. Richards (University of Alberta): thesis supervision.

Mike Villeneuve (Geological Survey of Canada, Ottawa): grain selection for $^{40}Ar/^{39}Ar$ dating, $^{40}Ar/^{39}Ar$ dating.

XRAL (University of Saskatchewan): XRF data.

Dr. Q. Xie (University of Saskatchewan): ICP-MS data.

Dr. Charles Stelck (University of Alberta), Dr. R. Hall, and Chris Collom (University of Calgary): paleontological identifications.

Lang Shi (formerly of University of Alberta): microprobe assistance.

Don Resultay and Mark Labbe (University of Alberta): thin section and polished slab preparation.

Figure 2.

Map showing mid-Cretaceous igneous rocks in the Howell Creek area and the surrounding region. After Price (1962), Brown and Cameron (1999), and Goble et al., (1999b).

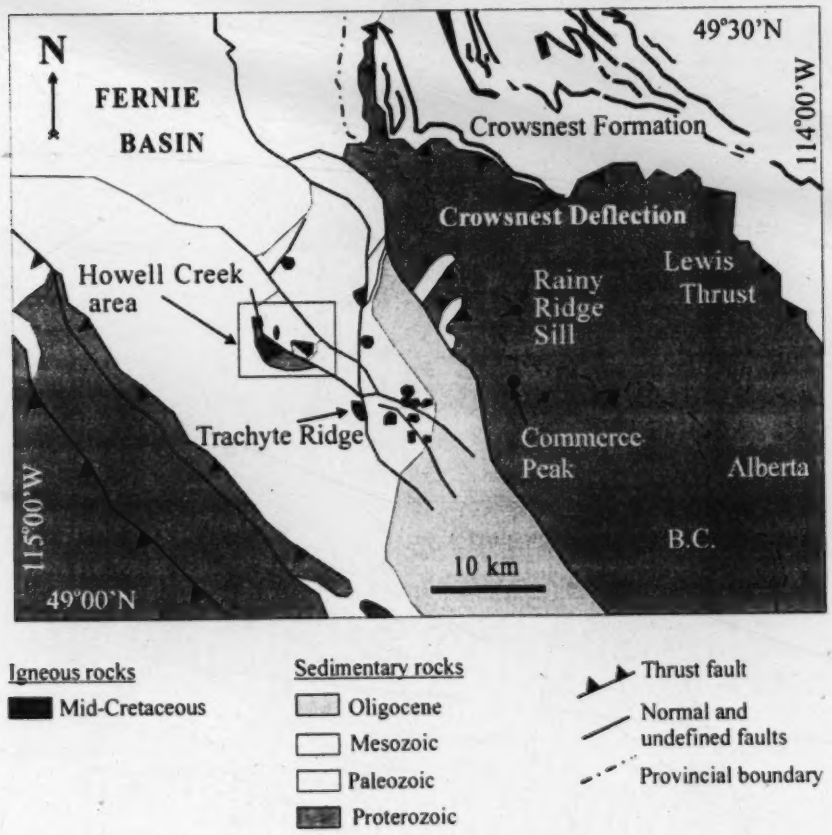

Previous work

The southern Canadian Rocky Mountains have been the subject of geological interest for 150 years. The regional structural and stratigraphical aspect has been the subject of many papers written by numerous geologists including: Daly (1912), Price (1959, 1962, 1965), Clark (1964), Hume (1932, 1964), Hunt (1964), Jones (1964, 1969, 1977), Oswald (1964a, b), Bally et al. (1966), Dahlstrom (1970), Labrecque and Shaw (1973), Skupinski and Legun (1989), Legun (1993), Brown and Cameron (1999), and Lefebure et al. (1999). In brief, the present day structural configuration of the area is the result of

compression generated by Mesozoic terrane accretion in the west, which initiated Late Cretaceous to Early Tertiary (Bally et al., 1966) thin-skinned tectonic responses in the Proterozoic to Cretaceous strata of the miogeocline.

Structure

In the Howell Creek area sequences of Proterozoic and Paleozoic miogeoclinal strata have been thrust east over younger strata (Fig. 2). The complexity of the Howell Creek structure (HCS; Price, 1965) lies in the relationship between Upper Cretaceous sedimentary rocks in contact with Proterozoic to Paleozoic rocks to the west and Paleozoic rocks to the east. The nature of the contacts between a faulted sequence of Proterozoic to Paleozoic strata within the Upper Cretaceous block and the faults abutting its southeastern boundary (Price, 1965; Skupinski and Legun, 1989; Legun, 1993) adds to the intricacy of what has been called one of the most structurally enigmatic areas of the Canadian Cordillera (Jones, 1977).

Price (1965) determined the Howell Fault to be a relatively young thrust fault striking northeast, dipping northwest. This fault underlies and truncates a steeply dipping portion of a southeast striking thrust, which Price suggested is a section of the Lewis Thrust (Figs. 3a, 4a, 1:44 444 scale map). Kirk Osadetz, of the Geological Survey of Canada (personal communication, 2000) and Dahlstrom (1970) concur with Price on the interpretation of the Lewis Thrust. Price (1965) proposed that Cretaceous Alberta Group sedimentary rocks which outcrop in the central portion of the map rode on the Howell Fault, and thin to the east due to wedging out against the Lewis Thrust above them. He corroborated his interpretation of the Howell Creek area by comparison to regional structures. From outcrop mapping, Legun (1993) re-interpreted the fault that Price claimed to be the Lewis Thrust to be a steep reverse fault with a 70° southwest dip, and renamed it the Twenty Nine Mile Creek Fault (Fig. 3b). Both Price (1965) and Skupinski and Legun (1989) mapped a number of additional minor thrust faults in the same orientation and to the east of the Twenty Nine Mile Creek Fault (see 1:44 444), in the area known now as the Western Outlier. Brown and Cameron (1999) made further

Figure 3.

Schematic representations of interpretations of the major faults in the Howell Creek area. (a) after Price (1965), (b) after Legun (1993), and (c) after Brown and Cameron (1999).

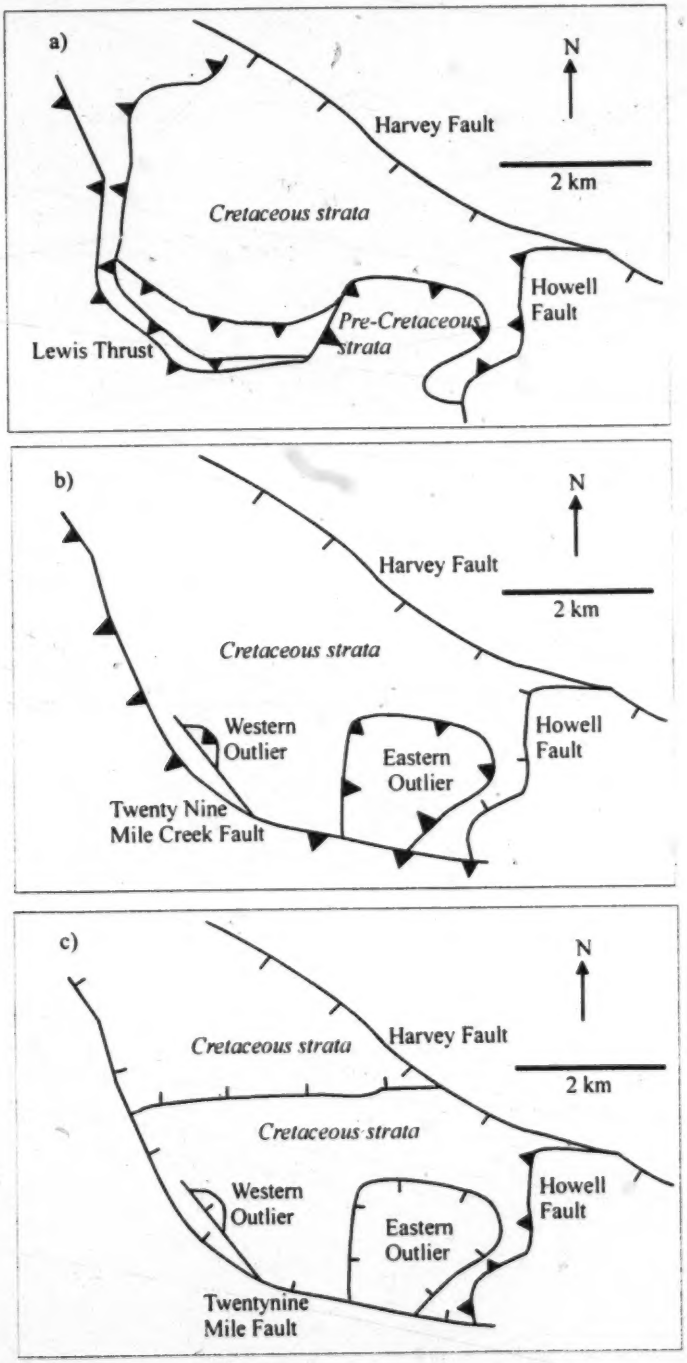

Figure 4.

Schematic representations of the interpretations of the major faults in the Howell Creek area. (a) after Price (1965), (b) after Labreque and Shaw (1973).

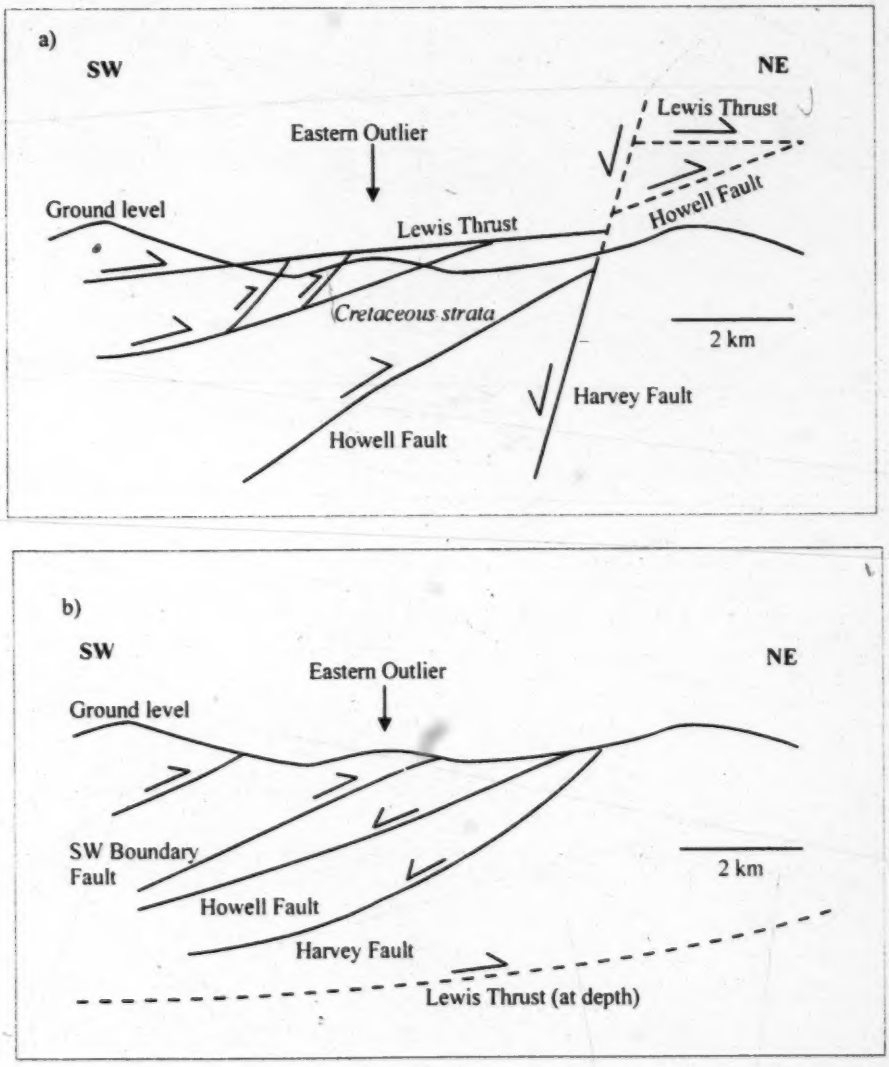

reinterpretations, renaming the Twenty Nine Mile Creek Fault, the Twentynine Mile Fault and designating it as a normal fault (Fig. 3c).

Price (1965) interpreted the Harvey Fault as a normal fault striking northwest, dipping to the southwest, which cuts both the Howell Fault and the Lewis Thrust (see Figs. 3a and 4a). Labrecque and Shaw (1973) interpreted seismic sections of the Howell Creek area and reported drill core logging results from an Imperial Oil drill hole Cigol-IOE et al. Howell a-16-B, in the northeast corner of the Howell Creek structure, proximal and west of the Harvey Fault (see 1:44 444 scale map). Their work suggested that the Harvey Fault and the Howell Fault are both normal faults, which would have converged above the present day surface (Fig. 4b). They reinterpreted the fault that Price (1965) had identified as the Lewis Thrust, renaming it the SW Boundary Fault, and suggesting that the Lewis Thrust underlay the entire area and emerged nearly 5 km to the east. However, the authors added that the evidence is open to interpretation due to the complexity and changeability of the structures along strike.

The presence of Proterozoic to Paleozoic sedimentary rocks within the central area of the map (Western and Eastern Outliers; Plate 1, figs. 3b, c, 4a, b, and 1:44 444 scale map) have also been variously interpreted. In Price's (1965) map, the pre-Cretaceous strata in the west of the area, form part of a thrust slice encompassed by the Lewis Thrust which is shown to veer progressively northeast, east, and southwest in order to realign with the main southeast orientation of the fault (Fig. 3a).

Jones (1977) re-evaluated the presence of the Cretaceous sedimentary rocks and concluded that they are the result of a huge rockslide, depositing the strata essentially undisturbed into a valley. He proposed that the Western and Eastern Outliers (Plate 1, figs. 3b,c, 4a,b, and 1:44 444 scale map) are large slump blocks deposited after the emplacement of the rock fall.

According to Legun (1993), the Twenty Nine Mile Creek Fault continues to trend southeast throughout and the discrete areas of older strata are structural outliers, with thrust faults encompassing the Eastern Outlier and part-surrounding the Western Outlier (Fig. 3b). He further suggested that the Howell Fault was a normal fault and that the Eastern Outlier was originally part of the hanging wall of the Twenty Nine Mile Creek Fault, unlike the Western Outlier, whose origin is undetermined.

In the map accompanying Brown and Cameron's (1999) paper (based in part on an unpublished map by Cameron) the sense of movement of several of the faults have been re-interpreted (Plate 1, figs. 3c and 1:44 444 scale map). As mentioned above, the previously named 'Twenty Nine Mile Creek Fault' is renamed the Twentynine Mile Fault by Brown and Cameron (1999) and is designated a normal fault, as is the fault on the western boundary of the Western Outlier and the faults surrounding the Eastern Outlier. In addition, the Howell Fault was re-designated a thrust fault as in Price's (1965) map.

Brown and Cameron's (1999) re-interpretation of Legun's map (1993) provided the basis for the 1:44 444 scale map and Plate 1 produced for this study.

In consideration of the debate concerning the most westerly major fault in the area it will be referred to as the Twentynine Mile Fault / Lewis Thrust in this text and on the enclosed 1:44 444 scale map.

Igneous rocks

Price (1962, 1965) described relatively small stocks and dykes of trachyte and syenite in the Howell Creek area, whose distinctive mineralogy and texture resembled lithic fragments, found in the Crowsnest Formation and Blairmore Group to the northeast.

During the 1960s, the hydrocarbon potential of the Howell Creek area was under investigation. In their studies, Shell obtained a K-Ar date of 89±3 Ma (Gordy and Edwards, 1962) for the alkali feldspar syenite phase of the Howell Creek suite from east of the Twentynine Mile Fault / Lewis Thrust. The Geological Survey of Canada (GSC) dated a similar phase sampled from west of the fault and obtained a K-Ar date of 129±9 Ma (Leech et al., 1963). The date obtained by Leech et al. (1963) has been recalculated to correct original computational errors in GSC data prior to 1965. A U-Pb (zircon) age of 98.5±5 Ma (2σ) was obtained from a sample of syenite from the Flathead Grid A anomaly, the most westerly intrusion in the Trachyte Ridge area (Fig. 2), collected by Dave Grieve of the Ministry of Energy, Mines and Petroleum Resources in 1987, and analysed at the GSC by Donald Murphy (Skupinski and Legun, 1989; Legun, 2001, personal communication). The two data points display a significant contribution of inherited Early Proterozoic zircon (2347±22 Ma, 2σ), which Murphy reported as concurring with results from other intrusions in the area.

$^{40}Ar/^{39}Ar$ dating of two phases of the Howell Creek Suite undertaken for this study yielded apparent ages for the megacrystic syenite of 102.5±1.0 Ma (2σ), and for the foid syenite of 101.3±1.0 Ma (2σ). Both of the sample sites lie west of the Twentynine Mile Fault / Lewis Thrust.

From unpublished? data, Armstrong (1988) reported initial $^{87}Sr/^{86}Sr$ ratios for the Howell Creek intrusions of between 0.703 and 0.705, and commented that they represent an eastward decrease from the highly radiogenic Cretaceous intrusions of the southern Omineca Belt, which commonly range above 0.707. Peterson et al. (1997) determined a higher initial $^{87}Sr/^{86}Sr$ ratio (0.71018) for a trachyte from the Howell Creek area.

Skupinski and Legun (1989) included detailed petrographic descriptions of the alkalic rocks, differentiating them into: alkali trachyte, tinguaite, diabase, and dacite. Brown and Cameron (1999) renamed the separate phases, using plutonic rock nomenclature (Le Maitre et al., 1989), as syenite, alkali feldspar syenite, foid syenite, and gabbro, also differentiating a phase of megacrystic syenite, and associated intrusive breccias.

Mineralisation

The alkalic intrusions of the Howell Creek area described by Price (1962, 1965) promoted interest in the possibility of gold mineralisation. Work by exploration companies in the 1970s, included investigations of lead, gold, silver, zinc, and arsenic anomalies in the study area, to the east on Trachyte Ridge (Fig. 2), and in the region around Commerce Peak (Williams and James 1971; Netolitzky, 1972; Goble, 1973). During the 1980s, Fox Geological Consultants Ltd. and others undertook geological, geophysical, and geochemical surveys for Cominco Ltd., Dome Exploration (Canada) Ltd., and Placer Dome Inc. (Noakes, 1984; Casselman and Termuende, 1987; Fox and Cameron, 1986, 1987, 1989). Skupinski and Legun (1989) noted the presence of fluorite, barite, minor pyrite, chalcopyrite, sphalerite, and malachite. The late 1980s and 1990s brought interest from Eastfield Resources Ltd. and Commerce Resources Corp., and at present they, together with Placer Dome Inc., hold title to claims within the Howell Creek area.

The presence of pyritised, silty carbonate sequences associated with gold, silver, arsenic, antimony, tungsten and tellurium anomalies prompted the British Columbia Geological Survey to include Howell Creek in a project instigated in 1997, to determine the potential for intrusion-related sediment-hosted gold deposits within British Columbia (Lefebure et al., 1999; Brown and Cameron, 1999).

Fieldwork

Fieldwork was undertaken on an approximately 25 km^2 area in the Howell Creek region, covered by map sheets 82 G/2 and 82 G/7 (Plate 1, figs. 2, and 1:44 444 scale map).

The primary purpose of the field work component of this study was to map, and obtain samples of various phases of the Howell Creek intrusive suite suitable for detailed petrographic descriptions, geochemical analyses, and $^{40}Ar/^{39}Ar$ age dating.

Previous geological maps (Brown and Cameron, 1999; Skupinski and Legun, 1989; and Legun, 1993) and aerial photographs of the area, supplied by the British Columbia Geological Survey, were used for initial orientation within the area. Several previously unmapped outcrops of various igneous phases and Cretaceous fossil sites, as well as new structural data obtained from sedimentary rocks, have been included on the enclosed 1:44 444 scale map. In addition, sedimentary rock outcrops within the Western Outlier were identified as Cambrian Flathead and Elko Formation rocks in contrast to Proterozoic strata as designated in previous geological maps (Skupinski and Legun, 1989; Legun, 1993; Brown and Cameron, 1999).

The mapped area is in southeastern British Columbia, 40 km southeast of Fernie and 15 km west of the British Columbia/Alberta provincial border. The International Boundary with the USA is 25 km to the south.

Access to the area is from Highway 3, 13 km south of Fernie, following the Morrissey, Lodgepole, and Harvey Road system of active logging roads. Turning due south at the 58 km marker on the Harvey Road the road becomes less well maintained and unless on foot, a 4 x 4 truck is advised for the final 5 km. Old gravel roads, drill trails, and new paths provide easy vehicle or foot access within the study area.

The Howell Creek and Twentynine Mile Creek flow southeast, down broad glacially eroded valleys, from cliffs of Paleozoic carbonate rocks that surround the study

area to the west and northwest. Piaysoo Ridge, consisting of well-stratified Paleozoic sedimentary rocks forms the eastern mapping boundary. The fieldwork concentrated on the areas of relief (up to 2200 m) within these boundaries.

Fieldwork was undertaken in 1999 and 2000. One week's reconnaissance of the area was made in August 1999 with members of the British Columbia Ministry of Energy and Mines, Victoria and Cranbrook offices, and geologists from Eastfield Resources Ltd.

Geological mapping was undertaken in 2000 between 21 July and 14 August 2000. Five days were spent reconnoitring regional Cretaceous intrusions, data from which does not form part of this study.

Samples were gathered during 18 traverses planned using topographic and geological maps, and air photographs. Located drill core samples were collected from abandoned core boxes in the area (UTM E670300 N5453400). Station locations were determined with a global positioning system accurate to ±30 m.

Eastfield Resources Ltd. kindly permitted access to the area, as well as providing comparative rock samples from Trachyte Ridge (Fig. 2), and unpublished geological maps and sections of the area.

Geology of mapped area

Various systems of nomenclature have been applied to the sedimentary and igneous rocks found in the study area (Price, 1959, 1962, 1965; Skupinski and Legun, 1989; Legun, 1993; and work by Fox Geological Consultants Ltd., in the 1980s). Revision by Brown and Cameron (1999) simplified the stratigraphic and igneous rock divisions and it is this system which will be adhered to in this work (stratigraphy, Appendix 1).

Stratigraphy

Late Proterozoic

Miogeoclinal sedimentary rocks of the Gateway, Roosville, and Phillips Formations belonging to the Purcell Supergroup, are the oldest rocks in the Howell Creek area. These formations consist of distinctive green or maroon siltite to argillite occurring with thin beds of resistant quartzite to quartz arenite, and with minor argillaceous carbonate. The rocks crop out west of the Twentynine Mile Fault/Lewis Thrust, and along the ridge of

the Eastern Outlier. Glacial deposits within the valleys have obscured much of the bedrock, making it difficult accurately to identify contacts between units.

Cambrian

The Cambrian Flathead and Elko Formations crop out close to the peak of the Eastern Outlier. The Flathead Formation quartzite and quartz arenite lie unconformably on the Purcell Supergroup, below a recessive shale unit at the base of the Elko Formation dolomite. The Elko Formation dolomite is pale grey to brown, moderately crystalline with localised areas of vuggy porosity, and sparry calcite-filled veins (< 1 cm wide). A strong sulfurous smell is commonly apparent when rocks of the Elko Formation are struck, implying the presence of hydrocarbons. Quartzite of the Flathead Formation, and highly altered Elko Formation having a sulfurous smell and displaying hydrocarbon residues were also observed within the Western Outlier (UTM E667944 N5454804).

Devonian

The Devonian Fairholme Group consists of pale to dark grey, to buff coloured, finely crystalline, argillaceous limestone. This unit crops out on the north slope and peak of the Eastern Outlier, and with the Cambrian limestone forms vertical cliffs on the south side of the outlier. Cambrian strata are thrust over the Fairholme Group within the Eastern Outlier.

Mississippian

Pale to dark grey calcarenite of the Rundle Group crops out in the east of the mapped area. Lower sections of this unit are highly bioclastic, showing numerous bivalves and broken crinoid stems, whereas up sequence, ripple marks and trace fossils become apparent (e.g., UTM E670708 N5453616). Weathered surfaces show good examples of rillenkarren, with sharply edged, linear flutes and ridges. Areas affected by hydrothermal alteration (~10 cm wide chalcedony and calcite veins) commonly form prominent outcrops, where the secondary minerals have increased the resistance of the host rocks (e.g., UTM E670791 N5453757).

Permian-Pennsylvanian

Massive, pale to dark grey to buff coloured, fairly well-rounded, well-sorted, fine grained quartzite of the lower section of the Rocky Mountain Group crops out on the eastern ridge of the Eastern Outlier, and in the southeast of the map area. Mid-grey to buff coloured, fossiliferous, locally silicified, and locally highly brecciated dolomite constitutes the upper section of the Rocky Mountain Group in this area. Black hydrocarbon residues commonly occur in vugs and cavities in the dolomite (e.g., UTM E671079 N5455070), providing evidence of hydrocarbon passage through this porous lithology.

Triassic

Dense vegetation prohibited confirmation of the presence of the Spray River Formation reported by Price (1965; p.55) to be a recessive "rust-brown to dark grey…siltstone and silty shale" cropping out to the southeast of the Howell Fault.

Upper Cretaceous

Alberta Group strata are bounded by the Harvey, Howell, and Twentynine Mile Fault / Lewis Thrust and occur at relatively low elevations in comparison to the peaks of the Western and Eastern Outliers. Units consist of dark grey to dark grey-brown siltstone, fissile shale, and fine-grained sandstone containing variable amounts of feldspar, mica, and lithic and mafic rock fragments. Locally, the shale beds contain numerous trace fossils and bioclastic fragments. Brown to orange ovoid concretions (5-20 cm in diameter) are common in the shale beds, and where present represent ~5-25% of the rock. Locally, sandstones exhibit distinct ripple marks and possible dessication cracks (UTM E670495 N5455909).

On the north side of the Eastern Outlier (e.g., UTM E669876 N5455193), dark grey pebble beds occur consisting of rounded to angular siltstone, feldspar, and mafic igneous? clasts up to 3 cm in diameter, with ~20% matrix. This unit is apparently in sequence with other sandstones as seen throughout the mapped area. The only other occurrence of pebble beds was upslope of the Eastern Outlier (UTM E670222 N5455147), where a sequence of pale grey sandstone, pebble beds, and concretion-rich

shale was noted as rubbly float. The composition and sequence of the strata is identical to the competent beds occurring at lower elevations. However, the incompetent nature of these units makes their origin debatable, and they have not been included on the map. Jones (1977) reported anomalous conglomerate masses (not identified in this study) on the ridge of the Eastern Outlier, visually similar to the Kishenehn Formation, which were determined as Upper Eocene to Lower Oligocene.

Fossils

Fossils collected on traverse, from the banks of Howell Creek (UTM; E669314 N5456258, station 0402; E670684 N5455647, station 1403) were studied by Dr. Charles Stelck (University of Alberta), and Dr. Russell Hall and Chris Collom (Department of Geology and Geophysics, University of Calgary). They have been identified as ammonites and bivalves (mostly inoceramid), from the Wapiabi Formation, and are of Middle Coniacian, Early Santonian, and Late Santonian age, from the Muskiki, Dowling, and Thistle Members respectively (Plate 2 and Appendix 2). The fossil sites are believed to be proximal to those described by Price (1965; p. 67) from which J. A. Jeletzky of the Geological Survey of Canada identified *Scaphites ventricosus* and *Inoceramus* sp.

Igneous rocks and intrusive breccias

Brown and Cameron (1999) divided the intrusions found in the Howell Creek area into five categories as follows (the corresponding units as described by Skupinski and Legun, 1989, are bracketed): alkali feldspar syenite (alkali trachyte), foid syenite (tinguaite and dacite), megacrystic syenite, gabbro (diabase), and intrusive breccia (petrographic observations, Appendix 3.

Alkali feldspar syenite

Examples: EB0610, EB1901, HA1-154/6, HA7-169, HA7-169/171, HE1-50/56, HE1-26, HE1-68, HE2-59, HE3-38.7, HE4-94, HE4-198.

Alkali feldspar syenite is the most common intrusive phase, cropping out west of the Twentynine Mile Fault / Lewis Thrust, within Proterozoic strata and in the Western and Eastern Outliers (1:44 444 scale map and Plate 1), where it occurs as sills and stocks hosted predominantly by Cambrian to Devonian country rocks.

Leucocratic, dark to pale grey, porphyritic syenite contains between 10 to 85%, white to grey coloured, subhedral to euhedral alkali feldspar laths (2 mm to occasionally >20 mm in length) in a microcrystalline groundmass. The phenocrysts commonly show a trachytic texture, being subaligned to aligned (Plate 3). Variations in the percentage and size of the phenocrysts seen at different outcrops suggest that several mineralogically similar magmatic pulses may have been responsible for these intrusions. Phenocrysts of other minerals are minor.

Mineralogically similar but texturally distinct leucocratic, pink, holocrystalline syenite with a trachytic texture, containing alkali feldspar laths up to 5 mm in length is included in this category. It is a volumetrically minor phase intruded by the megacrystic syenite (UTM E667242 N5453102, station 1301; Plate 4), and occurs as xenolithic rounded cobbles within a matrix of the megacrystic syenite proximal to the Western Outlier (UTM E667192 N5454553, station 1202; Plate 5).

The K-Ar date of 129±9 Ma obtained by Leech et al. (1963) for the alkali feldspar syenite west of the Twentynine Mile Fault / Lewis Thrust (UTM E666240 N5455222) is the oldest date obtained for any of the Howell Creek suite phases. Although the date is not precise, it is consistent with field observations that the alkali feldspar syenite is commonly crosscut by other phases, in particular the megacrystic phase, and generally shows a higher degree of alteration.

Foid syenite

Examples: EB0202, EB1809, EB1810.

Foid syenite occurs as sills in strata of the same age as the alkali feldspar syenite but is less common. Two distinct phases are included in this category.

The first phase outcrops on the ridge to the southeast of the Eastern Outlier within the Triassic Spray River Formation (UTM; E671260 N5453989, station 1809; E671107 N6565128, station 1810), and is cut by the Howell Fault. This phase is a mid grey to mid to dark green, fine to medium grained foid syenite (Plate 6) containing approximately 30% alkali feldspar as fine laths, showing a trachytic texture. Fine needles of pyroxene, rounded analcite crystals, and minor garnet are also visible in hand sample.

The second foid syenite phase occurs on the southern slope of the Eastern Outlier within the Mississippian Rundle Group (UTM E670708 N5453616, station 0202). It is dark grey, porphyritic and predominantly holocrystalline, comprising of <30% euhedral pink orthoclase phenocrysts (5–10 mm in length), and 10% white plagioclase crystals, slightly smaller than the alkali feldspar crystals, and <10% nepheline crystals. Relict hornblende constitutes 15-20% of the rock.

Brown and Cameron (1999) mention that nosean is suspected to be present in the foid syenite, but this mineral was not observed in this study.

Megacrystic syenite

Examples: EB1202, EB1301, EB0603.

This phase commonly crosscuts both grey and pink alkali feldspar syenite and occurs proximal to the Western Outlier (e.g., UTM; E667192 N5454552, station 1202; E667287 N5454355) on the western end of the ridge of the Eastern Outlier (e.g., UTM; E668864 N5454976; E670568 N5454592), and to the south of the mapped area (e.g., UTM; E667242 N5453102, station 1301; E666771 N5452795 and E666847 N5452806 (outwith 1:44 444 scale map area)).

The rock is red-brown to grey, porphyritic syenite (Plates 4, 5, and 7), containing up to 40% tabular, euhedral, pinkish orthoclase phenocrysts up to 70 mm in length (Brown and Cameron, 1989), but commonly between 15 to 30 mm in length. Altered hornblende phenocrysts (3-10 mm in length) recognised by their crystal form, comprise <7% of the rock. Clinopyroxene in the form of augite and aegirine-augite, constitute up to 10% of the rock. Locally, the rock is up to 1% vesicular, with round vesicles <2 mm in diameter.

A good example of the commonly xenolithic nature of this phase occurs proximal to the Western Outlier (UTM E667192 N5454552, station 1202), where it hosts subangular to rounded cobbles (30 to 70 mm in diameter) of laminated siltstone and fine grained pink alkali feldspar syenite (Plate 5; see above).

On the north side of the Eastern Outlier, a mineralogically similar phase occurs (UTM E670582 N5454970, station 0603) containing well aligned, pink, tabular, orthoclase phenocrysts which constitute 35% of the rock.

Gabbro

Gabbro was not positively identified during fieldwork for this study, but is reported as occurring on the ridge of the Eastern Outlier by Skupinski and Legun (1:44 444 scale map; 1989; p. B33). It is described as '...dark green with diffuse pale spotting and a remnant felted fabric', with <55% plagioclase, and <25% pyroxene, <12% magnetite, and possible miarolitic cavities. Intensely altered, the secondary minerals include zeolites, chlorite, epidote, zoisite, sericite, and albite.

A small outcrop (<2 m width) of a doleritic phase hosted by undifferentiated Proterozoic strata was noted in the field (UTM E667176 N5452984), occurring close to station 1301. This dark green-grey, finely crystalline dolerite contains ~40% plagioclase, 45-55% clinopyroxene, and shows chloritic alteration. It may be an analogue to the outcrops reported elsewhere on the Eastern Outlier.

Intrusive breccias

Large areas (up to 1000m by 300 m) of intrusive breccias are commonly associated with the previously described intrusive phases. The intrusive breccias occur throughout the mapped area with the highest concentration on the Eastern Outlier (e.g., UTM E669184 N5454870, E670508 N5454863, E670571 N5454832, E669711 N5455053). Commonly concordant with the host sedimentary strata, several breccias cut the strata prior to becoming concordant at higher levels (Brown and Cameron, 1999).

Compositional diversity of the clasts is dependent on the lithologies affected by the brecciation. Examination of clasts from various outcrops identified Proterozoic green argillite and quartz arenite, Paleozoic limestone and dolomite, Mesozoic shale and siltstone, as well as examples of the intrusions described above.

The composition of the matrix varies between being wholly magmatic to dominantly carbonate rich. On the north side of the Eastern Outlier (UTM E670280 N5455011, station 0607) the matrix of the interior of an intrusive breccia is composed of alkali syenite, showing distinct flow layering textures (Plate 3). The matrix becomes progressively carbonate rich over a distance of <2 m, towards the contact with the Devonian Fairholme Group host rock.

The clasts are rounded to angular, ranging from millimetres to decimetres in length. Angular clasts are commonly seen at the periphery of the intrusive breccias, suggesting that they became entrained into the matrix due to local fracturing of the country rock, in comparison to rounded clasts which experienced more intensive comminution. However, both angular and rounded clasts are commonly intermingled.

Alteration of the intrusive breccias is common, with clasts commonly showing limonitic alteration (Skupinski and Legun, 1989), and dissolution of the carbonate rich matrix.

Mineralogy

Thin sections of the eighteen samples of intrusive rocks chosen for geochemical and/or age dating purposes were studied petrographically (Appendix 3). In addition, to help discriminate between alkali feldspar, plagioclase, and nepheline, polished slabs of each sample were etched with hydrofluoric acid for approximately 30 seconds and then placed in a solution of sodium cobaltnitrate for a further 20-30 seconds before being rinsed in water. This procedure produced a yellow stain on potassium feldspar, sericite, and clay, leaving other minerals unstained.

The first section below provides detailed descriptions of the phenocryst and xenocryst assemblages, including results from electron microprobe and EDS (energy dispersive spectrometer) analyses of phenocrysts from samples EB1301 and EB1810, the two samples used for $^{40}Ar/^{39}Ar$ dating. A note is also made of the textures observed at the hand sample and outcrop scale.

The second and third sections provide descriptions of the alteration and mineralisation assemblages occurring in the intrusions and the country rock.

Phenocrysts and xenocrysts

Feldspar - Alkali feldspar syenite, foid syenite and megacrystic syenite

Feldspar as orthoclase, sanidine, and oligoclase phenocrysts constitute the most abundant mineral (20 – 50%) occurring in the Howell Creek suite. Commonly also occurring as oikocrysts, alkali feldspar crystals can variously encompass randomly oriented plagioclase, pyroxene, apatite, and titanite crystals. The euhedral to subhedral

alkali feldspar crystals range in length from ~1 mm up to 20 mm with the majority ranging between 5 – 15 mm in length. However, Brown and Cameron (1999) identified alkali feldspar phenocrysts up to 70 mm in length in the megacrystic syenite. Distinct, sequential growth bands produced by compositional variations are common in the larger crystals, electron microprobe analyses show Ba to be increasingly substituted for K during the growth of each zone. Carlsbad twinning is common, with parallel twins more common than interpenetrant twins. Manebach and rare Baveno twins are also seen. The perthitic textures are rare, with only some alkali feldspar crystals from samples HE4-198, EB0603A, EB1809, and EB1810 showing crypto- to microperthitic textures, giving a rare bluish iridescence.

Plagioclase to calcic plagioclase crystals, determined microscopically to be of composition An 60-80 (labradorite to bytownite) range between ~1 mm and 20 mm in length, more commonly occurring in the range 5-10 mm in length.

Representative electron microprobe analyses of feldspar crystals from this study show the compositional variation between orthoclase and oligoclase in sample EB1301 (Table 1).

Table 1.

Electron microprobe analyses of feldspar crystals from sample EB1301.

Sample 1301	SiO_2	TiO_2	Al_2O_3	FeO total	MgO	BaO	CaO	Na_2O	K_2O	H_2O	Total
*Orthoclase	63.0	0	19.51	0.14	0	1.53	0.32	3.24	11.15	0	98.89
**Oligoclase	63.4	0	23.86	0.20	0	0.12	4.74	7.60	1.57	0	98.49

* Average of 9 measurements.
** Average of 3 measurements.

Nepheline - Foid syenite

Nepheline (approximately 2 mm in diameter) is ubiquitously highly altered. Identification of this mineral is commonly dependent on the identification of its euhedral, hexagonal crystal form.

Garnet - Foid syenite

Rare intensively altered (sodic-calcic amphiboles and possibly eucolite) and resorbed titanian andradite, is found in sample EB1810 (composition from EDS measurements). The highly resorbed nature of the andradite in sample EB1810 indicates that garnet is out of equilibrium. There is a lack of zonation in contrast to the majority of compositionally similar andraditic garnet found in the Crowsnest Formation (Dingwall and Brearley, 1985).

Pyroxene - Alkali feldspar syenite, foid syenite, and megacrystic syenite

The clinopyroxene augite (composition from EDS measurements) occurs in a stubby to prismatic, distinctly zoned euhedral form. Aegerine-augite occurs most commonly in the foid syenite as subhedral, acicular crystals. Both pyroxenes occur in the groundmass and as inclusions within the alkali feldspar crystals. In such settings, augite tends to appear closer to the core of the feldspar crystals in contrast to aegerine-augite which occurs at the actual rim or at the outside edge of an earlier growth zone within the feldspar. Deer et al. (1992) report that the crystallisation of Ca-rich augite followed by Na-rich aegerine-augite is a common phenomenon, as crystallisation of the magma progresses. The occurrence of acicular pyroxenes within zoned feldspar grains is a feature of magmatic crystallisation common in alkali syenites (Sørenson, 1974).

Pyroxene is commonly altered in the alkali feldspar and megacrystic syenite, but may be identified by its crystal form in addition to its replacement by uralite.

Analcite - Foid syenite

Altered analcite is found only in sample EB1810. EDS examination of unaltered remnants confirmed analcite, while examination of altered portions of the phenocrysts determined strontianite (?). Due to the extensive alteration, it is difficult to confirm whether analcite is a primary mineral or secondary mineral.

Analcite can occur as a primary mineral in magma at ~600°C and 28-50 km depth (Deer et al., 1992), and rare examples include those from the regional Crowsnest Formation volcanic rocks (Pearce, 1970; Ferguson and Edgar, 1978; Dingwall and Brearley, 1985; Goble et al., 1993; Peterson and Currie, 1993). It is however, more

common as a secondary mineral, produced by the hydrothermal alteration of nepheline (Deer et al. 1992).

Titanite - Alkali feldspar syenite, megacrystic syenite

Subhedral to euhedral crystals of titanite (<1 mm to 3 mm in length), commonly showing simple twinning, occur as grains within feldspar crystals and within the groundmass.

Hornblende - Alkali feldspar syenite, foid syenite, and megacrystic syenite

Highly altered hornblende, commonly replaced by chlorite and possibly uralite, is identified by its relict crystal form when other diagnostic indicators, such as pleochroism, twinning or cleavage traces, are absent. This may have resulted in misidentification as augite in some cases due to its similar, stubby morphology.

Apatite - Alkali feldspar syenite, foid syenite, and megacrystic syenite

Subhedral to euhedral crystals of apatite (<1 mm to 4 mm in length), occur randomly oriented in feldspar oikocrysts, as disseminated individual crystals, and as clotted masses within the groundmass.

Textures

Trachytic textures, with feldspar crystals sub- to well-aligned, are more evident in the sanidine-rich samples of the alkali feldspar syenites. In very fine-grained examples of the syenites, flow textures are apparent in the contrasting colours of bands of magma of slightly differing compositions, for example in the matrix of an intrusive breccia close to drillhole HA1 (Plates 1 and 3; 1:44 444 scale map). Skupinski and Legun (1989) also report protoclastic textures from thin section study.

Miarolitic cavities (<1%) occur in sample EB0610 (alkali feldspar syenite) as reported for this lithology by Skupinski and Legun (1989).

Alteration minerals of the intrusive phases

Feldspar alteration

Sericitic alteration of the feldspar crystals is widespread, occurring in variable degrees in all samples. Sericite and minor muscovite are commonly spatially associated with saussuritisation of the feldspar phenocrysts and groundmass, together representing between <1-5%, and rarely up to 10% of the rock volume.

Pale green, argillic alteration occurring in sample EB0610 (alkali feldspar syenite) may be illite. Thompson and Robitaille (1998) conducted PIMA short wave infrared studies of the clay minerals from samples from drill holes HA1, HA2, HA4, HA6, HA8, HE2 and HE3 identifying illite in both intrusions and the host rock, kaolinite and smectite in the intrusions, and chlorite in the breccias.

Mafic mineral alteration

The secondary minerals are described in order of abundance. The original minerals are named where positive identification was possible.

Red-brown, clotted, subhedral to euhedral secondary biotite, commonly chloritised, occurs commonly in areas proximal to, and probably as a replacement of, mafic minerals, in samples EB1901, EB1202A, EB0202, and HE1-26.

Uralitisation of pyroxene (and hornblende?) occurs in samples EB0610, EB1810, and HE4-198. However, the fine-grained habit of the uralite makes its identification difficult, and it may therefore be more common than reported.

Fine-grained chlorite (possibly also uralite) occurs in samples EB0202 and EB1202, after hornblende.

Epidote is rare, occurring in association with rutile in one mineralised sample (HE1-50/56), which shows argillic alteration. Rutile also occurs in EB0202, EB0610, EB1301A, HE1-50/56, HE1-26, and HE3-38.7.

From EDS measurements the secondary minerals mantling the garnet in sample EB1810 appear to be a combination of sodic-calcic amphiboles and possibly eucolite.

Other alteration products

Natrolite and prehnite occur in minor miarolitic cavities and areas of increased porosity possibly due to hydrothermal fracturing, in sample EB0610.

Secondary euhedral nepheline occurs in sample EB0202, where it has formed in contact with a resorbed feldspar phenocryst.

Proximal to the contact with carbonate host rocks, the matrix of the intrusive breccias is partially to wholly replaced by sparry calcite.

Alteration of the host rock

Proximal to veins, the carbonate host rock is commonly coarsely crystalline, reflecting recrystallisation due to hydrothermal alteration. However, the widespread occurrence of coarse recrystallisation, especially in the Cambrian Elko Formation, implies that regional recrystallisation, unassociated with the intrusions, has also taken place.

Thompson and Robitaille (1998) reported illite in impure carbonate rocks from drill hole HE2.

Mineralisation of the intrusive rocks

Brown and Cameron (1999) report that gold mineralisation in the Howell Creek area is associated with fine-grained disseminated and fracture-controlled pyrite, and highlight the value of 219 ppb Au from pyritic gouge in drillcore from hole HE2 (see 1:44 444 scale map) at a depth of 65.5 m. Back scattered electron imaging, undertaken for this study, was unable to determine the presence of gold in any sample, in association with pyrite or not.

Fine-grained (<1 mm to 2 mm), subhedral to euhedral, disseminated opaque minerals occur throughout the groundmass of all phases, but more commonly in the megacrystic phase, with pyrite > marcasite, > magnetite = hematite >> chalcopyrite.

Larger veins (up to 2 cm in width) are commonly lined with euhedral, coarse-grained pyrite, and / or marcasite, and have a core of euhedral, coarse-grained calcite (Plate 9). Late, barren, coarsely crystalline calcite veins (millimetre to centimetre width) are common in the igneous intrusions and the country rocks. Euhedral pyrite (<1 mm) and calcite are also commonly associated in areas of mafic mineral replacement.

Localised quartz stockwork and veins occur proximal to the Twentynine Mile Fault / Lewis Thrust within the alkali feldspar syenite. Sheeted, milky coloured to clear quartz veins (0.5-3 cm in width) predominate in the area, forming up to 20% of the rock volume (Brown and Cameron, 1999), with wider veins (up to 10 – 20 cm in width) consisting of euhedrally terminated, clear quartz crystals, concentrated within an area of 100 m^2. The host rock is intensely altered and bleached, and in association with the larger quartz veins forms a gossan (due to Fe-sulfide oxidation). This area is also associated with a crosscutting intrusion of the megacrystic phase, containing a high percentage of xenoliths (up to 50% rock volume) and is associated with a molybdenum soil anomaly (Brown and Cameron, 1999).

Intense silicification of the alkali feldspar syenite occurs locally throughout the mapped area commonly associated with hydrothermal quartz veining (as described above). Silicification may be being locally augmented by remobilisation of silica in areas of quartz-rich country rock, as seen in the intense silicification of the intrusions in contact with Cambrian quartzite in the Western Outlier (UTM E667931 N5455320, station 1901).

Dark blue to red purple fluorite±pyrite±silicification occurs most commonly west of the Twentynine Mile Fault / Lewis Thrust in the alkali feldspar syenite (e.g. UTM E665346 N5455837), and to a lesser extent in the carbonate country rocks. Its form varies between discrete veins, veinlets (Plate 8), and patches (up to 5 cm, but commonly approximately 1 cm in diameter), to widespread flooding of the rock. An area of the fluorite alteration in the northwest was the target of a drilling programme (drill holes HE1- 4, see 1:44 444 scale map) due to a Au soil anomaly, but elevated Au levels were not found at depth.

Microscopic adularia occurs in samples EB0202, EB1202A, EB1301A, EB1901, HA1-154/6, and HE3-38.7. Adularia is commonly seen in association with calcite ± chlorite ± pyrite in areas of mafic mineral alteration and replacement.

Alteration of the intrusive breccias occurs within the matrix, and consists of calcification, fine-grained pyrite, and areas of silicification (e.g. UTM E669830 N5455033).

Mineralisation of the country rock

Euhedral to subhedral pyrite is commonly found in the carbonate and clastic rocks, as either fine-grained, disseminated grains throughout the rock mass or more commonly as coarsely crystalline grains concentrated at vein selvages.

Locally, the carbonate lithologies display concentrated patches of, and/or disseminated dark purple fluorite in areas associated with fluoritisation of the intrusions, i.e. proximal to the HE drill holes, in the northwest of the mapped area.

The occurrence of calcite, and to a lesser degree quartz and chalcedony, veins are widespread within the carbonate lithologies of all ages, and are commonly associated with intrusions and/or faults. In general, calcite veins (<1 cm in width) ± pyritic >> chalcopyrite mineralisation, are randomly oriented, and tend to have parallel, straight sides. Examples include the Mississippian Rundle Group on the south side of the Eastern Outlier (UTM E670791 N5453757), where randomly oriented, fine (millimetre to centimetre sized) calcite veins occur in the micritic limestone, while chalcedony veins (approximately 10 cm wide) are conformable with the bedding planes. On the north side of the Eastern Outlier, Devonian Fairholme Group limestone exhibits crystalline, calcite filled fractures (<2 mm wide) spatially associated with the intrusive breccias (e.g. UTM E670571 N5454832). Proximal to the eastern fault on the Western Outlier, both milky quartz (<10 cm wide), and sparry calcite veins (<5 cm wide) cut the Cambrian Flathead and Elko Formations (redesignated this study). Alteration occurring in such close proximity to faults suggests that late-stage hydrothermal veining may have occurred, during movement along the fault or reusing the fault as a conduit.

Geochemistry

Major and minor element analyses, including rare earth elements (REE), were obtained from 18 samples, representing the alkali feldspar syenite, foid syenite, and megacrystic syenite phases of the intrusions from the Howell Creek area (Appendix 4). Care was taken to select the freshest samples available, although petrographical observation confirmed that all samples had undergone some degree of alteration, with variable saussuritic alteration of the feldspar phenocrysts being the most common form. However, the feldspar phenocrysts in all the samples were competent, and commonly displayed

vitreous crystal faces. Other alteration minerals, more common in the groundmass, are listed in order of decreasing abundance; sericite, calcite, albite and pyrite, marcasite and arsenopyrite. Samples were analysed in order of increasing alteration to decrease the possibility of cross-contamination by sulphides and carbonates.

Hydrothermal alteration (e.g. saussuritisation, sericitisation, addition of hydrothermal adularia) or weathering processes will cause some elements, especially the LILE (large ion lithophile elements; e.g. K, Sr, Ba) to become mobilised. The measured values for the mobile elements may therefore not reflect the original abundances of those elements in the magma. This is a serious concern for the classification of these rocks and the interpretation of the magma petrogenesis. In an effort to identify the influence of secondary minerals the extent of alteration of the samples has been indicated on the geochemical diagrams. In addition, consideration of the extent and type of alteration has been made throughout and instances where alteration is believed to have affected the data to the extent of influencing the interpretation have been noted where appropriate.

Major element analyses

The 18 samples of the Howell Creek suite chosen for analysis are of intermediate composition, having a range of SiO_2 between 57.8-63.7 wt.% (60.8-65.0 wt.% SiO_2, normalised to 100% volatile free; Appendix 4). Five samples plot within the phonolite field (volcanic equivalent of foidal syenite; Sørenson, 1974) of a total alkali-silica diagram, and the other 13 plot within the trachyte field (volcanic equivalent of syenite; Sørenson, 1974; Fig. 5). The least altered samples are similarly distributed. With reference to compositional averages from selected comparable rock types (Table 2) the Howell Creek suite samples have variable K_2O (4.4-12.7 wt.%), and Na_2O (0.5-7.4 wt.%) concentrations and K_2O/Na_2O ratios (0.9-24.0).

The least altered samples (EB1809, EB1810, EB1301A, and HA1 154-6) have a more restricted range of K_2O (4.4-10.0 wt.%), Na_2O (2.6-7.4 wt.%), K_2O/Na_2O ratios (0.9-3.82) and relatively high Al_2O concentrations (17.1-20.1 wt.%). K_2O concentrations

Figure 5.

Total alkali vs. SiO_2 diagram for 18 samples of the Howell Creek suite. After Le Maitre (1989). Recalculated 100% volatile free.

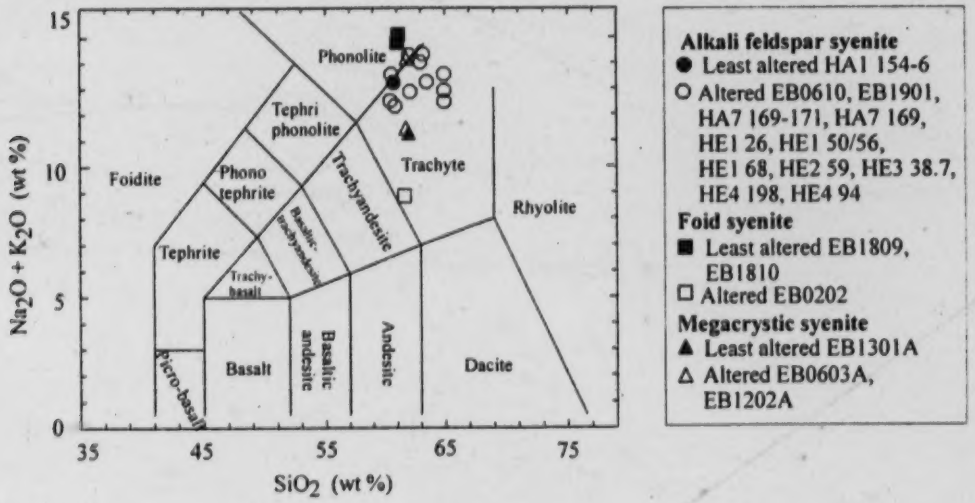

Table 2.

Compositional variations between the Howell Creek suite and averages of comparable rock types.

LOI included	SiO_2 wt.%	Na_2O wt.%	K_2O wt.%	K_2O/Na_2O	Al_2O_3 wt.%
Howell Creek					
-all samples	57.8-63.7	0.5-7.4	4.4-12.7	0.9-24.0	17.1-20.6
-least altered	58.0-60.3	2.6-7.4	4.4-10.0	0.9-3.8	17.1-20.1
-altered	57.8-63.7	0.5-5.4	7.2-12.7	1.0-24.0	18.1-20.6
***Alkali syenite**	61.9	5.5	5.9	1.1	16.9
****Syenite**	58.6	5.2	5.0	1.1	16.6
*****Tinguaite**	54.0	8.1	5.2	0.7	18.7

LOI = loss on ignition

* Average of 25 samples. Reported in Sørenson (1974, p.32)

** Average of 102 samples. Reported in Olade and Goodfellow (1979).

*** Average of 93 samples. Reported in Olade and Goodfellow (1979).

in the more highly altered samples overlap and exceed the values for the least altered samples (7.2-12.7 wt%), whereas N_2O concentrations overlap and fall short of the least altered sample values (0.5-5.4 wt.%). The K_2O/Na_2O ratios vary greatly (1.0-24.0).

The more highly altered samples therefore appear to reflect variable loss of Na and gain of K.

From the Shand Index diagram (Fig. 6) eight samples are strongly peraluminous ($Al_2O_3/CaO + Na_2O + K_2O > 1.1$), three are weakly peraluminous ($Al_2O_3/CaO + Na_2O + K_2O = 1.0$-$1.1$), and seven are metaluminous ($Al_2O_3/CaO + Na_2O + K_2O < 1.0$).

The metaluminous field contains all of the least altered samples. Petrographic observation confirmed a relatively high content of secondary calcite in the altered samples which plot on the left of the least altered samples, suggesting that they may originally have been less strongly metaluminous. The spread of results for the altered samples within the peraluminous field suggests that alkali loss may also have occurred.

The low magnesium-iron ratio ($100 \times Mg/(Mg + Fe^{total}) = 0$-$30.1$) reflects the leucocratic nature of the intrusions (Appendix 4). The range of Fe^{3+}/Fe^{2+} ratios (1.5-4.1)

Figure 6.

Shand Index of 18 samples of the Howell Creek suite. After Maniar and Piccoli (1989). Recalculated 100% volatile free.

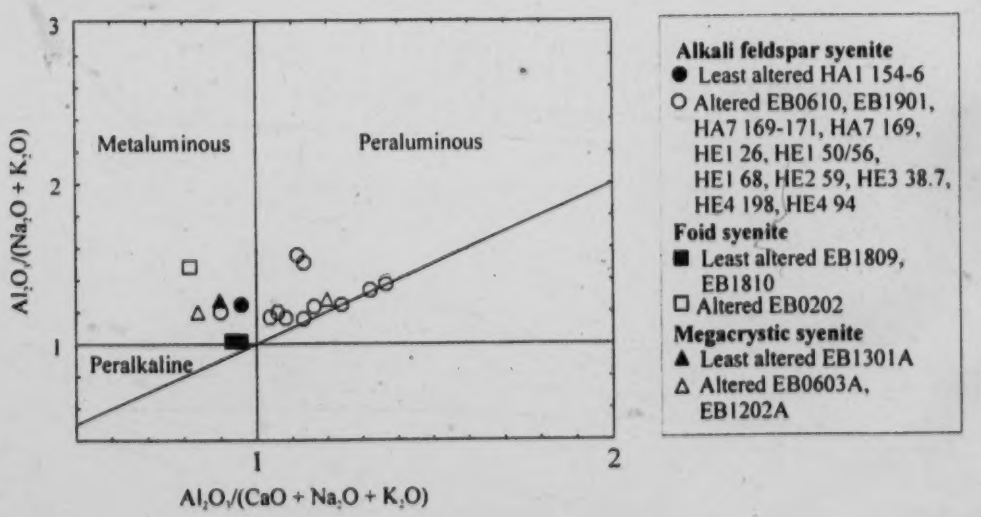

of the least altered samples (EB1809, EB1810, EB1301A, HA1 154-6; Appendix 4), is consistent with the presence of magnetite in the mineralogy and suggests a relatively oxidised magma.

CIPW norm calculations (Table 3) indicate that the majority of the samples contain normative quartz, commonly in the range 1-10 wt%. From petrographic study, the high level of normative quartz occurring in alkali feldspar sample EB1901 (11.47 wt%) is assumed attributable to silicification. The relatively high aluminium content is reflected in normative corundum occurring in most samples. The foid syenite samples, EB1809 and EB1810, are nepheline normative and together with EB1301A, EB1202A and EB0202 are the only samples lacking normative corundum. Only sample EB1809 contains normative olivine, confirming its more mafic composition.

The more highly calcitised samples, EB0603A, EB1901, HA1 154-6, and HE3 38.7 all show normative calcite.

Table 3.

CIPW normative values for 18 samples of the Howell Creek suite.

	EB0202	EB0603A	EB0610	EB1202A	EB1301A	EB1809	EB1810	EB1901	HA7 169-71	HA1 154-6	HA7 169	HE1 26	HE1 50-6	HE1 68	HE2 59	HE3 38.7	HE4 198	HE4 94
Quartz	9.14	4.24	9.79	0.16	2.87			11.47	4.36	2.88	5.24	5.30	1.11	4.57	1.31	2.9	5.51	4.96
Corundum		4.02	5.00					4.69		3.60	1.95	3.58	0.94	2.59		3.21	1.34	2.11
Zircon	0.02	0.06	0.05	0.03	0.03	0.07	0.07	0.03	2.14	0.06	0.07	0.03	0.03	0.03	0.04	0.02	0.02	0.02
Orthoclase	26.87	76.09	71.68	34.44	39.68	52.93	41.92	76.67	0.03	61.81	68.01	76.70	74.82	72.87	51.88	62.65	43.42	45.96
Albite	36.13	10.62	9.20	47.31	38.19	29.07	37.85	4.57	67.9	23.13	6.57	11.22	13.41	14.00	34.29	24.56	43.07	43.06
Anorthite	15.71	1.04	1.61	8.55	11.15	0.87	1.05	0.81	8.39	0.62	15.62	1.02	6.12	3.06	7.36		3.67	1.58
Nepheline						12.14	14.50		13.88									
Acmite																		
Diopside	4.85			3.21	3.74	2.59	0.91								0.18			
Wollastonite	1.77			2.81	0.94		1.69											
Hypersthene		0.94	0.69					0.66		2.86	0.72	0.31	1.14	0.57	0.97	0.35	0.31	
Olivine						0.06			0.82									
Magnetite	4.41	0.97		3.10	3.19	1.36	1.09			2.11			0.69		0.42	1.61		
Hematite		1.33	2.11	0.15		0.83	0.94	0.76			2.03	1.91	1.53	2.17	3.65	0.85	2.71	2.50
Ilmenite	0.91	0.38	0.43	0.60	0.66	0.34	0.28	0.26	2.57	0.40	0.04	0.22	0.36	0.31	0.57	0.43	0.06	

Table 3. cont.

Rutile								0.25	0.26		0.21	0.06		0.02			0.15	0.16
Apatite	0.55	0.11	0.08	0.23	0.23	0.11	0.05	0.11	0.11	0.11	0.18	0.04	0.1	0.08	0.15	0.13	0.16	0.16
Calcite		0.88						0.03	0.16	5.06						6.14		
Magnesite																0.78		
Spodumene	0.07	0.07	0.13	0.07	0.06	0.12	0.07	0.08	0.07	0.21	0.09	0.16	0.12	0.11	0.52	0.14	0.01	0.01

Harker diagrams of the major oxides compared to increasing SiO_2, (normalised to 100% volatile-free) show a wide spread of values for phases with <63 wt.% SiO_2, with no distinct fractionation trends. In phases with >63 wt.%. SiO_2 (altered samples), trends occur with a decrease of MgO, CaO, and Na_2O with increasing SiO_2 (Fig. 7).

Interpretation

The observed contrasts in the alkali content between the more highly and the least altered samples would be compatible with the loss of Na due to alteration of the more albitic feldspars (and possibly nepheline), while the common occurrence of sericite in the samples could explain the high K abundance. Although the altered nature of the majority of the samples makes interpretation of major oxide relative abundances debatable, data from samples <63 wt.% SiO_2 (100% volatile free) suggest that the Howell Creek intrusions do not represent a comagmatic fractionation suite, although the decrease in MgO, CaO, and Na_2O with increasing SiO_2 (>63 wt.%, 100% volatile free) would be compatible with minor pyroxene or amphibole fractionation. The intrusions may therefore have pooled and fractionated before separating into small leucocratic pulses with only a minor degree of fractionation occurring after separation. The compositions may also reflect the heterogeneity of the source rock composition. Peterson et al. (1997) suggested that the magma composition of the regional Crowsnest Formation was controlled by the source rock mineralogy, and disputed the application of a fractional crystallisation model between the phonolites and trachytes (Pearce, 1970).

Figure 7.

Harker diagrams of 18 samples of the Howell Creek suite. Recalculated 100% volatile free.

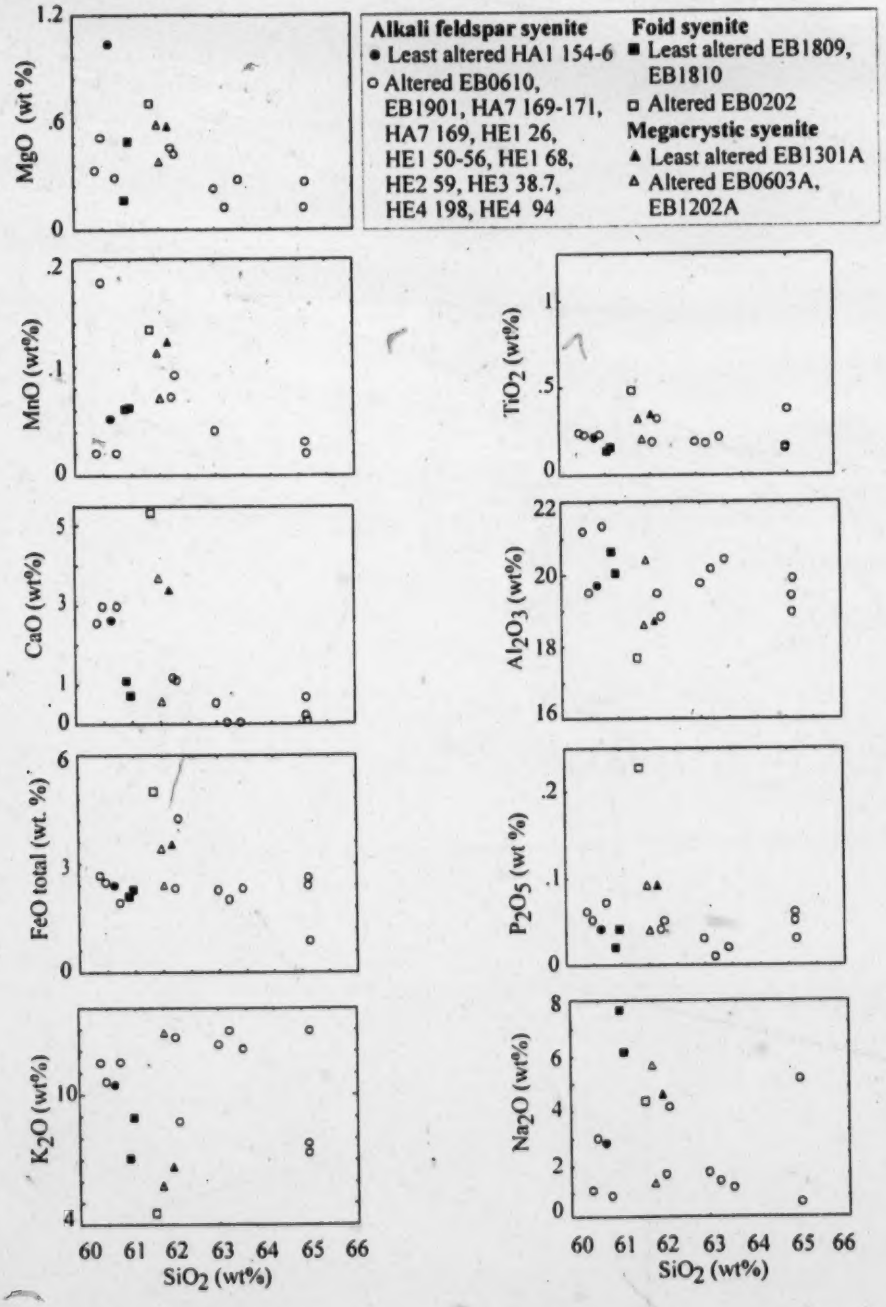

Trace and rare earth element analyses

Immobile trace and rare earth elements are often more useful for petrogenetic studies than the major oxides, which tend to be more mobile during hydrothermal alteration. Trace element abundances, whose usage was originally applied to basaltic rocks, can be applied with caution, to the interpretation of felsic and porphyritic rock petrogenesis (Rollinson, 1993).

Multi-element profile and interpretation

A primitive mantle (PM) normalised multi-element profile (Fig. 8) shows similar patterns for all the samples, with a high abundance of large ion lithophile elements (LILE) (e.g.

Figure 8.

Primitive mantle-normalised multi-element plot showing the profiles of 18 samples of the Howell Creek suite. Normalised to values from Jenner (NewPet; 1987-94).

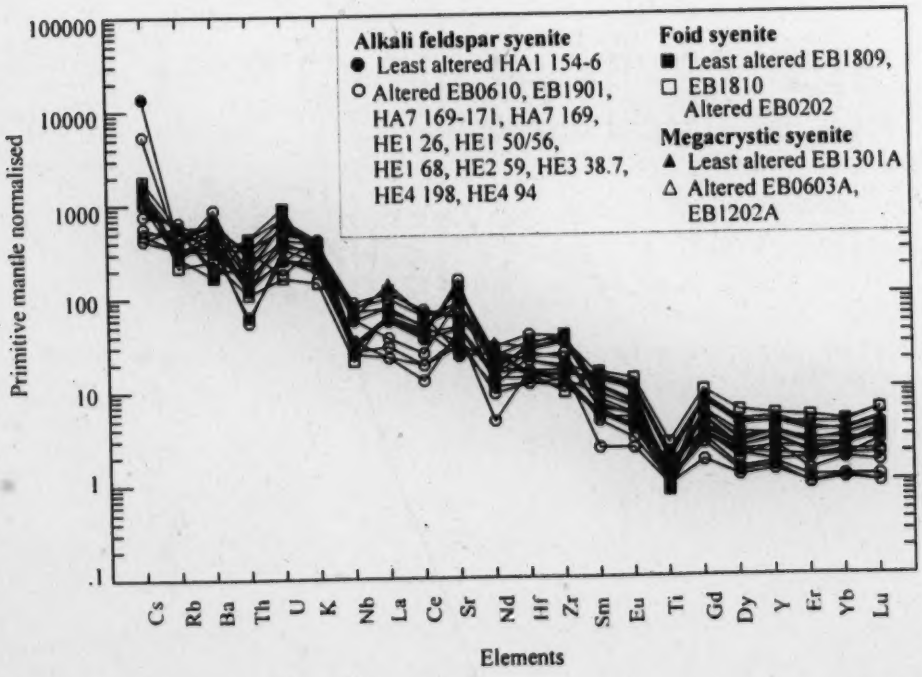
Alkali feldspar syenite
● Least altered HA1 154-6
○ Altered EB0610, EB1901, HA7 169-171, HA7 169, HE1 26, HE1 50/56, HE1 68, HE2 59, HE3 38.7, HE4 198, HE4 94
Foid syenite
■ Least altered EB1809,
□ EB1810
Altered EB0202
Megacrystic syenite
▲ Least altered EB1301A
△ Altered EB0603A, EB1202A
Primitive mantle normalised
100000
10000
1000
100
10
1
.1
Cs Rb Ba Th U K Nb La Ce Sr Nd Hf Zr Sm Eu Ti Gd Dy Y Er Yb Lu
Elements

Cs, 300-10500 x PM values) and light rare earth elements (LREE), in contrast to the low abundance of the high field strength elements (HFSE), (e.g. Lu, 1-7 x PM values).

In the profiles, deviations from a smooth curve occur with elevated values for Sr and relative depletions of Th, Nb, and Ti.

The abundance of Sr in the Howell Creek suite is compatible with the presence of plagioclase. Sr has a relatively high Kd with regard to plagioclase in intermediate magmas (Pearce and Norry, 1979).

Kd or Nernst distribution coefficient is defined as:

Kd = concentration of a specific element within a mineral / concentration of the same element within the corresponding melt

and is a function of temperature, pressure, and composition. It is based on Henry's Law, which, at equilibrium, relates the activity of a trace element (of average concentration) to the composition of the mineral it forms part of, given that the element has non-essential rôle within that mineral (Rollinson, 1993).

Rare earth element profile and interpretation

The REE profiles (Fig. 9), of the samples form relatively similar, shallow listric patterns which flatten off at Gd and have a slight upward curve at Yb and Lu.

Hornblende fractionation would be compatible with the listric patterns seen in the profiles. Hornblende is the main control on the MREE levels (Sm to Ho) in a melt (Rollinson, 1993), and its presence is associated with high MREE abundance. The profiles level off at Ho, with a slight upward curve at the tail of the profiles caused by an increase in the levels of Lu. This increase may be due to the presence of hornblende and apatite. Zircon has a higher Nernst distribution coefficient (Kd) for Lu than apatite (Fujimaki, 1984), but was not identified in any of the samples.

Elemental ratios and their relevance

The degree of REE fractionation within the Howell Creek suite (Fig. 9) is quantified in the ratios La/Yb (17.5-79), La/Sm (6.6-20.6) and Gd/Yb (1.5-3.2).

The Eu/Eu* ratio ($Eu_N/\sqrt{[(Sm_N).(Gd_N)]}$ where N denotes a normalised value) falls close to unity for all the samples (0.85-1.2; Appendix 4), suggesting moderately oxidising magmatic conditions (Cox et al., 1979), which is supported by the Fe^{3+}/Fe^{2+} ratios (1.5-4.1) and the presence of plagioclase in the samples. La/Nb, Ba/Nb, Ba/Th, Rb/Nb, Th/Nb, Th/La, and Ba/La ratios (Table 4) for the phases of the Howell Creek suite show that the lower values are comparable with those for average crust composition, while the ratio (Zr/Nb), encompasses the range determined from crust enriched by subduction processes (Rollinson, 1993).

Figure 9.

Chondrite normalised rare earth element profiles of 18 samples of the Howell Creek suite. Normalisation values from Jenner (NewPet; 1987-94).

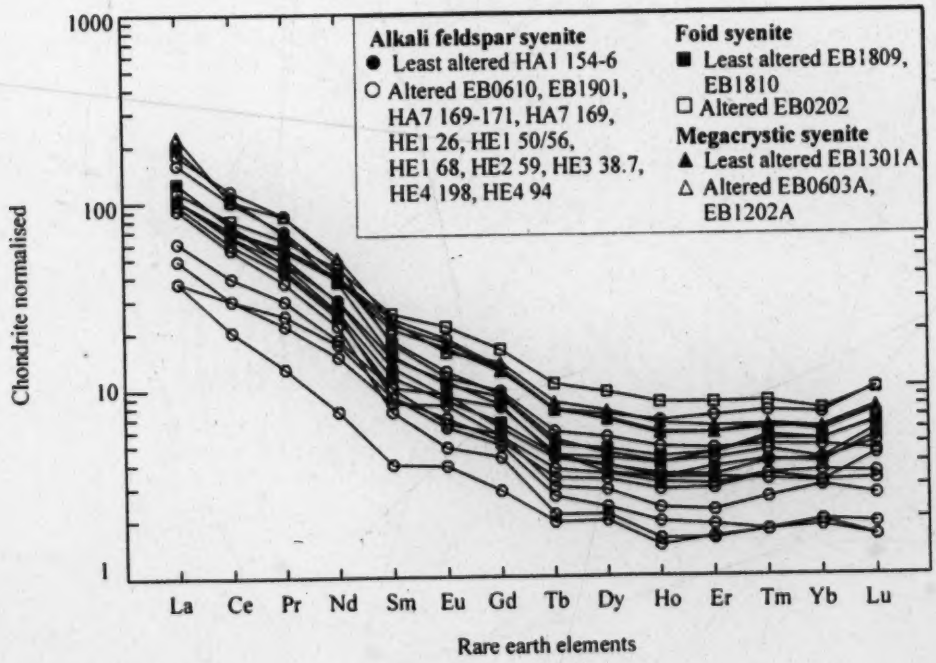
Alkali feldspar syenite
● Least altered HA1 154-6
○ Altered EB0610, EB1901, HA7 169-171, HA7 169, HE1 26, HE1 50/56, HE1 68, HE2 59, HE3 38.7, HE4 198, HE4 94
Foid syenite
■ Least altered EB1809, EB1810
□ Altered EB0202
Megacrystic syenite
▲ Least altered EB1301A
△ Altered EB0603A, EB1202A
1000
100
10
1
Chondrite normalised
La Ce Pr Nd Sm Eu Gd Tb Dy Ho Er Tm Yb Lu
Rare earth elements

Table 4.

Elemental ratios of the Howell Creek suite compared to average source rock compositions.

	La/Nb	Ba/Nb	Ba/Th	Rb/Nb	Th/Nb	Th/La	Ba/La	Zr/Nb
Howell Creek samples	0.6 – 3.2	23.3 – 276	27.7 – 534	3.4 – 17.7	0.3 – 0.9	0.2 – 0.8	22.0 – 176	3.2 – 10.6
***Continental crust average**	2.2	54	124	4.7	0.44	0.204	25	16.2
***Enriched mantle**	0.89 – 1.09	7.3 – 13.3	67 - 84	0.59- 0.85	0.111 – 0.157	0.122 – 0.163	8.3 – 11.3	4.5-7.3

*Reported in Rollinson (1993).

Because alteration processes readily affect LILE, interpretation of their ratios must be applied with caution. It is not possible to provide a straightforward interpretation of the mobility of the LILEs with regard to specific alteration types (Table 5). However, it is interesting to note that of the least altered rocks, the more equigranular, foid syenite samples (EB1809 and EB1810) have the lowest Ba/Nb, Ba/Th, and Ba/La ratios while the more porphyritic samples (EB1202A and EB1301A) are among the highest. Microprobe investigations show Ba concentrated in the sequential growth zones of the feldspar phenocrysts of the porphyritic samples. It is therefore suggested that high Ba abundance is related to direct precipitation from the magma, as well as later mobilisation during hydrothermal alteration.

Table 5.

Elemental ratios of the Howell Creek suite.

	Rb/Sr	Rb/Ba	La/Nb	Ba/Nb	Ba/Th	Rb/Nb	Th/Nb	Th/La	Ba/La	Zr/Nb
*EB1810	0.08	0.08	1.1	23.3	27.7	3.4	0.8	0.8	22.0	8.3
*EB1809	0.69	0.15	1.5	40.5	51.3	3.9	0.8	0.5	26.2	7.0
*EB1301A	0.33	0.08	2.1	182.7	296.8	9.3	0.6	0.3	85.9	7.6
*EB1202A	0.38	0.25	2.1	148.6	254.5	8.0	0.6	0.3	71.9	7.6
*EB0202	0.17	0.07	3.2	114.5	166.1	8.8	0.7	0.2	36.2	6.6
**HE4 94	0.07	0.04	1.1	151.0	534.2	10.9	0.3	0.3	139.3	7.3
**HE4 198	0.35	0.26	0.9	137.0	395.2	11.5	0.3	0.4	155.0	6.5
**HE2 59	0.28	0.07	1.8	275.9	380.2	9.8	0.7	0.4	149.2	10.6
**HE1-50/56	0.07	0.05	1.9	56.0	63.0	14.6	0.9	0.5	30.1	6.3
**HE1 68	0.16	0.10	1.6	60.8	77.7	15.0	0.8	0.5	37.8	6.6
**HE1 26	0.36	0.05	0.6	111.7	237.0	16.3	0.5	0.7	176.4	7.0
**HA7 169-171	0.09	0.14	1.2	74.4	134.4	5.4	0.6	0.5	62.3	3.2
**HA7 169	0.07	0.05	1.2	60.3	116.1	3.9	0.5	0.4	50.4	6.3
**EB0610	0.71	0.15	0.6	98.5	195.8	8.4	0.5	0.8	160.2	6.3

Table 5 cont.

***HE3 38.7	0.10	0.07	1.9	181.8	269.0	11.9	0.7	0.4	95.0	5.9
***HA1 154-6	0.20	0.06	1.3	117.3	180.2	6.0	0.7	0.5	89.7	8.3
***EB1901	0.45	0.15	2.2	118.3	170.2	17.7	0.7	0.3	53.9	9.9
***EB0603A	0.18	0.09	2.2	55.4	76.4	8.1	0.7	0.3	25.5	8.3

* Least altered ** Variable saussuritisation/sericitisation present ***Calcitisation present

Geochronology

The laser-microprobe $^{40}Ar/^{39}Ar$ dating method was chosen to analyse single grains of orthoclase selected from least altered igneous rock samples EB1301A (megacrystic syenite) and EB1810 (foid syenite) in order to obtain ages for the cooling of two separate phases of the Howell Creek suite (see 1:44 444 scale map and Plate 1 for sample sites). Alkali feldspar can have closure temperatures as low as 150°C (Harrison and McDougall, 1982) which may affect its ability to retain radiogenic argon. However, low closure temperatures also increase the sensitivity of alkali feldspar to record post-magmatic thermal events. The ability of the step heating process to assess the effect of possible overprinting was an important consideration as the Howell Creek suite has undergone a mineralising event and it was particularly important in obtaining precise and accurate ages that the thermal history of the intrusions could be determined.

In an attempt to determine the upper time limit of the plutonism in the Howell Creek area, samples were taken from the megacrystic syenite (Plates 4, 5 and 7), which from relative age dating (crosscutting field relationships) appeared to be a young member of the suite. The igneous rock sample EB1301A came from a site where it clearly intruded earlier phases of the suite within Precambrian country rocks (Plate 4). The orthoclase phenocrysts showed slight sericitic and argillic alteration.

To compare the ages of different members of the Howell Creek suite the second sample used for age dating purposes (EB1810) was chosen for its mineralogical and textural dissimilarity from EB1301A. Sample EB1810 (Plate 6) was taken from a foid syenite emplaced in Triassic strata in the southeastern quarter of the study area. The sample was relatively fresh, with the orthoclase phenocrysts showing no visible alteration minerals, although aegirine-augite crystals tended to occur within the outermost rim.

Method for $^{40}Ar/^{39}Ar$ analysis

From petrographic studies, two samples, EB1301A and EB1810, were selected for age dating. The samples were crushed separately and sieved to a grain size fraction of 0.5-1.0 mm. Approximately 100 of the least altered and fractured orthoclase crystals were then hand picked from each sample using a binocular microscope. No crystals with pyroxene inclusions were chosen from EB1810.

Final selection of the most suitable grains from samples EB1301A and EB1810 for dating purposes was made at the geochronology laboratory of the Geological Survey of Canada in Ottawa, by Mike Villeneuve.

The parameter J used in the process was determined using Fish Canyon Tuff sanidine, with an age of 28.03±1.0 Ma (Renne et al., 1994) as a flux monitor. The degree of error in the monitor is incorporated in the final calculations of the ages of the samples. There has recently been a call for a re-evaluation of the age of the Fish Canyon Tuff (FCT; used in this study to determine the J parameter) which if accepted would affect the value of the ^{40}K decay constant and the $^{40}Ar/^{39}Ar$ ages calculated from this commonly used geochronological standard. Schmidt and Bowring (2001) obtained similar dates for zircon and titanite grains from the FCT (~28.4 Ma) which suggest that the FCT is older than determined from previous studies (28.03 Ma; Renne et al., 1994; used in this study). However, the interpretation of these dates is debatable (e.g. the value of using U-Pb systematics on rocks of this age) and unless disproved, the ages calculated from FCT sanidine in this study (28.03 Ma; Renne et al., 1994) are believed to represent accurate age determinations for the Howell Creek suite.

$^{40}Ar/^{39}Ar$ age data

The apparent cooling ages of the analysed orthoclase crystals are taken from the inverse isochron data and are quoted in preference to the plateau ages, due to the greater degree of accuracy in the calculation obtained by isochron analysis. The ages differ by <0.5% (Figs. 10 and 11, and Appendix 5) between the inverse isochron and plateau data.

An assumption is made that the presence of non-radiogenic ^{40}Ar, either inherent in the crystal or produced during the experiment as blank, derives from present-day atmospheric argon, which has a fixed ratio to ^{36}Ar:

Figure 10.

Sample EB1301A (feldspar). (a) Inverse isochron plot of the most highly radiogenic steps. Data points are regressed through $^{40}Ar/^{36}Ar = 295.5$. (b) Plateau data plot. Heating steps used in the calculation of the final age are marked with an arrow above the data.

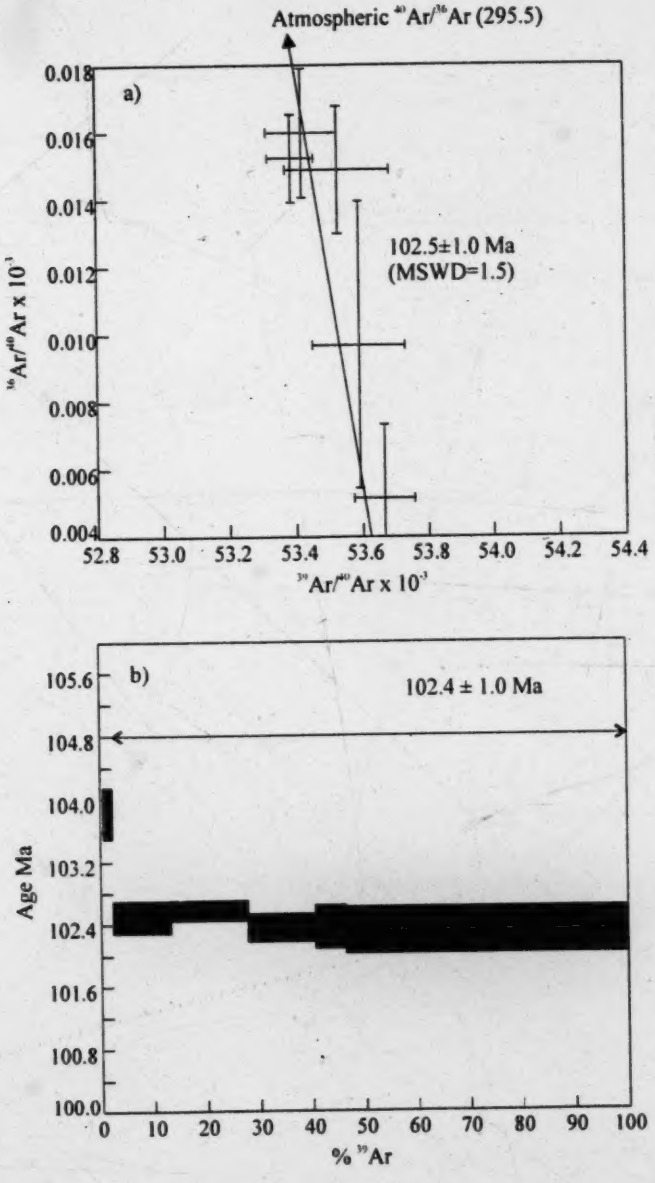

Figure 11.

Sample EB1810 (feldspar). (a) Inverse isochron plot of the most highly radiogenic steps. The data points were regressed through atmospheric $^{40}Ar/^{36}Ar$ = 295.5 (MSWD=1.5). Free regression through the data points produced a better fit (MSWD=1.1) with a line passing through $^{40}Ar/^{36}Ar$ = 488±122. The difference between the two resulting dates is minimal and within the calculated error. (b) Plateau data plot. Heating steps used in the calculation of the final date are marked with an arrow above the data.

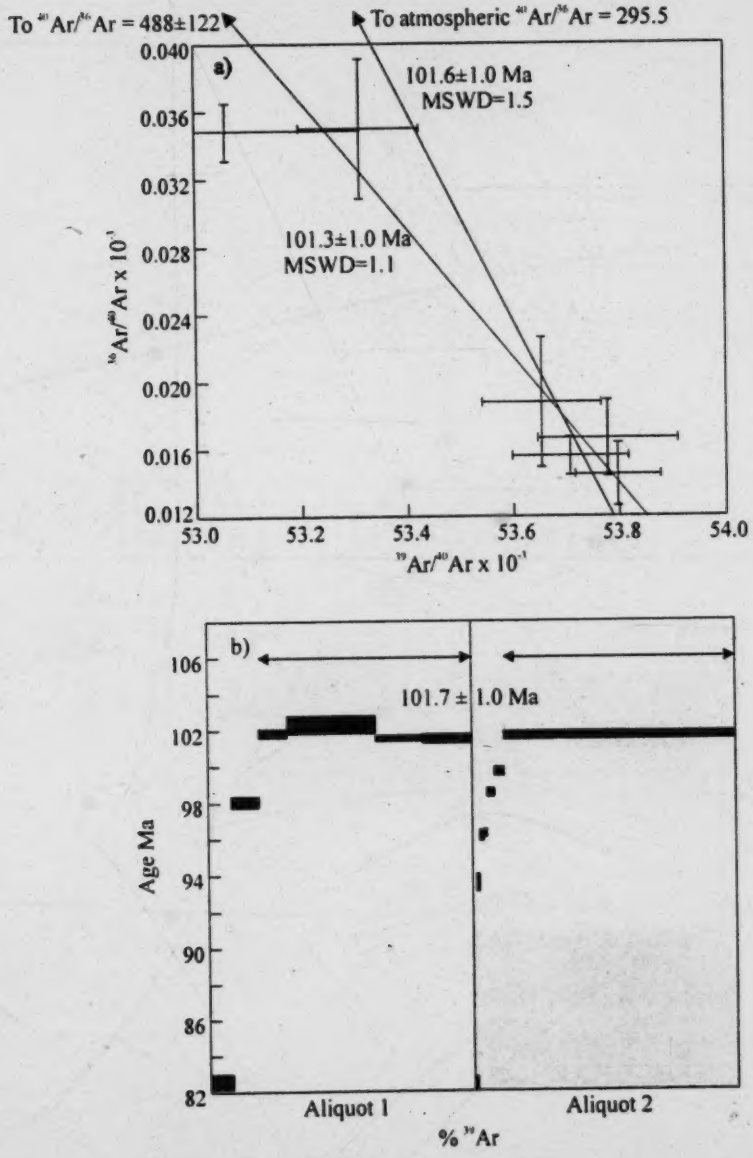

Atmospheric argon $^{40}Ar/^{36}Ar = 295.5$ (Steiger and Jäger, 1977)

To determine the total amount of non-radiogenic ^{40}Ar within the sample (and thereby deduce if there is an excess or deficiency of radiogenic ^{40}Ar in the crystal) the amount of ^{36}Ar produced during the experiment is measured and multiplied by 295.5. The ^{36}Ar is also assumed to be derived from present-day atmospheric argon. Present-day atmospheric argon is represented in the diagrams (Figs. 10a and 11a) as a line intersecting the $^{36}Ar/^{40}Ar$ axis at 1/295.5

From the value of the MSWD (mean squares of weighted deviates) the fit of the data points to a line of regression can be determined, and an assessment made of the uncertainty in the age dates (Rollinson, 1993). Isochrons with MSWD values of <2.5 are regarded as providing valid age determinations (Brooks et al. 1972).

Inverse isochron data

The analysis of sample EB1301A provides an apparent cooling age for the orthoclase of 102.5±1.0 Ma (2σ; assuming an intercept on the $^{36}Ar/^{40}Ar$ axis of 1/295.5; Fig. 10a) with an MSWD of 1.5.

Orthoclase from sample EB1810 provided an apparent cooling age of 101.6±1.0 Ma (2σ), with an MSWD of 1.5 when the intercept on the $^{36}Ar/^{40}Ar$ axis was assumed to be 1/295.5 (Fig. 11a). However, free regression through the data points produced a better fit, with an intercept on the $^{36}Ar/^{40}Ar$ axis at 1/488±122, and gave apparent cooling age of 101.3±1.0 Ma (2σ), with an MWSD of 1.1 (Fig. 11a).

A best-fit line for the data points which correlates to $^{40}Ar/^{36}Ar > 295.5$ (488±122, sample EB1810) indicates an apparent excess of radiogenic ^{40}Ar. However, the difference in the age dates obtained for sample EB1810 at different values of $^{40}Ar/^{36}Ar$ is minimal, and falls within the limits of error.

The MSWD values for both samples are low indicating the data are good, and that the apparent ages obtained are precise, while the agreement between the samples suggests the dates are also accurate.

Plateau data

98% of the released ^{39}Ar gas fraction of sample EB1301A and 65% of the released ^{39}Ar gas fraction of sample EB1810 provide stable plateaux forms (Figs. 10b and 11b). These are believed to express the undisturbed portion of the Ar gas release and can be used to determine the apparent age of cooling of the magma.

The plateaux give apparent cooling ages of 102.4±1.0 Ma (2σ) for sample EB1301A and 101.7±1.0 Ma (2σ) for sample EB1810.

The gas release plot for sample EB1310A shows an anomalously old apparent age for the early heating steps. In contrast, later gas releases yield uniform $^{40}Ar/^{39}Ar$ ratios providing a horizontal plateau, indicating no Ar loss or gain.

Both aliquots of sample EB1810 provide gas release plots suggesting anomalously young apparent ages for the early heating steps, in comparison to the later gas releases, which, as with sample EB1310A, indicate no Ar loss or gain.

The anomalous $^{40}Ar/^{39}Ar$ ratios were not included in the age calculations.

Interpretation of $^{40}Ar/^{39}Ar$ data

The early gas releases from both samples gave anomalous ages, which are of minor importance and do not detract from the reliability of the final calculated dates. However, they may give an indication of the thermal history of the intrusions.

The anomalously old apparent age given by the early gas releases from sample EB1310 could have a magmatic derivation from excess ^{40}Ar trapped during orthoclase crystallisation, or be due to post-emplacement infiltration of the rock by a fluid higher in ^{40}Ar. The fluid, possibly compositionally influenced by the country rocks as old as the Proterozoic, could be introduced during a period of hydrothermal alteration. The alteration visible on the surface of sample EB1310 suggests that this may be the case.

The apparent age obtained from the early gas releases in both aliquots of sample EB1810 is probably the result of a post-emplacement thermal disturbance.

The agreement between the results from samples EB1301A and EB1810, which overlap within error, indicate that the foid and megacrystic syenite are coeval, and were emplaced and cooled in the Howell Creek area ~102 Ma.

Discussion

In order to place the Howell Creek suite in a geological context within North America this discussion will first look at the complex magmatic history of the region and its environs. Selected intrusions of a similar composition and age, which occur along the length of the Canadian Cordillera, and younger intrusions from the northwest United States are then compared to the Howell Creek suite. A review of the work undertaken on the regional basement rocks is then provided, before the discussion culminates with a synthesis of the emplacement of the Howell Creek suite.

Regional igneous geology of southeastern British Columbia

Pre-Mesozoic

Proterozoic mafic dikes and sills, ranging in composition from alkaline to tholeiitic, are located in southwest Alberta, southeast British Columbia, and northeast Montana (Daly, 1912; Hunt, 1964; Goble et al., 1999a). Goble et al. (1999a) describe several generations of plagioclase-pyroxene-forsterite ± titaniferous phlogopite ± hornblende ± biotite sills, approximately 30 km east of the Howell Creek area. These intrusions are believed to be related to episodes of Middle to Late Proterozoic extensional faulting, occurring between 1200-1500 Ma, and approximately 1000 Ma and 800 Ma (Burchfiel, 1989; Harlan, 1989; Souther, 1991; Goble et al., 1999a and references therein). The earliest episode coincides with ages for the compositionally distinct Moyie sills (1445±11 Ma; U-Pb zircon; Höy, 1989) found to the west of the Howell Creek area in the Purcell and Kootenay Range mountains.

The development of a sedimentary rift basin abutting the western margin of the North American craton has been attributed to the separation of a landmass (1.5 Ma; Sears and Price, 1978; McMechan, 1981; Souther, 1991; Burrett and Berry, 2000), and evidence of various episodes of rifting along the Proterozoic/Paleozoic western Canada passive margin has been interpreted from the sedimentary rock record. The dominantly clastic sequences of the Windermere Supergroup (deposited between 780 and 570 Ma; Souther, 1991) which unconformably overlie basement rocks are thought to have originated in a rift setting. While from subsidence curves determined from lower Paleozoic miogeoclinal wedge sedimentary rocks, Bond and Kominz (1984) suggest a

later rifting event with an age of breakup and drift at 600 to 555 Ma. In general, the region experienced an extensional regime over a protracted time-span with further periodic alkalic igneous activity during the Paleozoic caused by local extensional stresses within the rift (Pell, 1987).

Mesozoic - Southern Omineca Belt

Currently lying approximately 500 km to the west of the study area, Late Triassic Nicola Group rocks were erupted in the Quesnellia terrane prior to the accretion of the more westward Insular Superterrane to the North American craton in the Middle Jurassic (Monger et al., 1982). The Nicola Group (Mortimer, 1987) and the Middle Jurassic Rossland Group have arc and back-arc geochemical signatures, respectively, that indicate an east dipping subduction zone, which Souther (1991) suggests separated the Quesnellia and Cache Creek terranes (Fig. 1). A temporary hiatus in the subduction process is proposed by Lang et al. (1995) in their study of alkalic intrusions emplaced between 210-200 Ma.

Among numerous Late Triassic to Middle Jurassic intrusions of the Quesnellia terrane are plutonic analogues of the Nicola Group, the Nelson Batholith and sub-alkaline to alkaline plutons of Copper Mountain, Similkameen and others, notable for their Cu±Au±Ag porphyry systems (Armstrong, 1988; Keep, 1992; Woodsworth et al., 1991; Panteleyev, 1991).

The more easterly region of the southern Omineca Belt (Fig. 1) experienced little igneous activity during the Mesozoic until the mid-Cretaceous period, when several calc-alkalic and alkalic plutons intruded the miogeoclinal sedimentary sequences between 122 Ma and ~90 Ma. The Bayonne Suite of intrusions (Fig. 12; Rice, 1941; Woodsworth et al., 1991; Brandon and Lambert, 1993, 1994) was emplaced at this time, and typically consist of LILE enriched, S-type, felsic plutons (Woodsworth et al., 1991) with initial $^{87}Sr/^{86}Sr$ ratios between 0.706 and ~0.720 (Armstrong, 1988; Brandon and Lambert, 1990). The Bayonne Suite is discussed in more detail later in the study, in association with other mid-Cretaceous intrusions occurring along the North American craton.

To the south east of the Bayonne Suite, and approximately 100 km north west of the Howell Creek suite, the Reade Lake (minimum 94 Ma) and Kiakho (122 Ma) quartz

monzonite stocks (Höy and van der Heyden, 1988) cut two ancient faults oriented northeast. The more northerly of these faults, the St. Mary fault (Fig. 13; St. Mary-Dibble Creek fault; McMechan, 1981), is sealed by the Reade Lake stock, and is thought to have been intermittently active since the Proterozoic (McMechan, 1981).

Figure 12.
Map showing location of selected mid-Cretaceous intrusions occurring along the Canadian Cordillera, as referred to in the text.

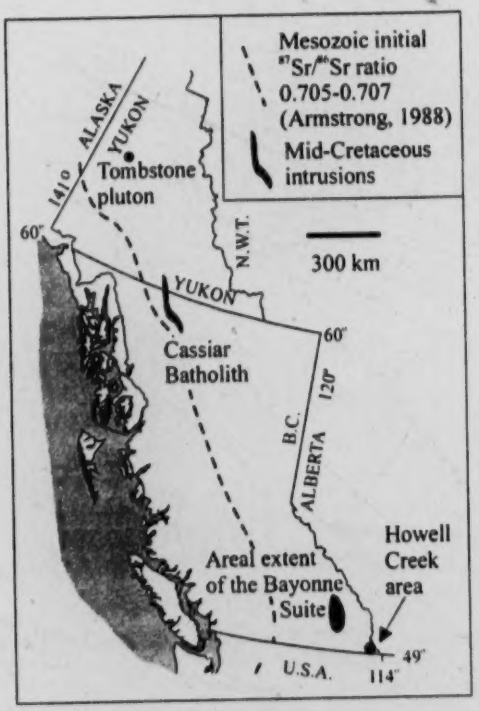

Mesozoic - Foreland Belt

Regional intrusions within 30 km east of the mapped area include: the Rainy Ridge phonolite sill (K-Ar; 118±2 Ma; Goble, personal communication, 2001); trachytes and syenites of Trachyte Ridge, (K-Ar; 105-66 Ma; Gordy and Edwards, 1962, recalculated;

Price, 1965), and the trachytes, syenites, and oversaturated monzonites of Commerce Mountain (Price, 1965; Goble et al., 1999b, and references therein). The igneous rocks of the Crowsnest Formation (K-Ar; ≥96 Ma; Folinsbee, 1957; Newland, 1963) consist of undersaturated blairmorites, phonolites, and trachytes, and crop out approximately 30 km to the north of the Howell Creek area (Fig. 2).

Figure 13.

Schematic map showing the regional tectonic features and Cretaceous intrusions in the Howell Creek area, as mentioned in the text.

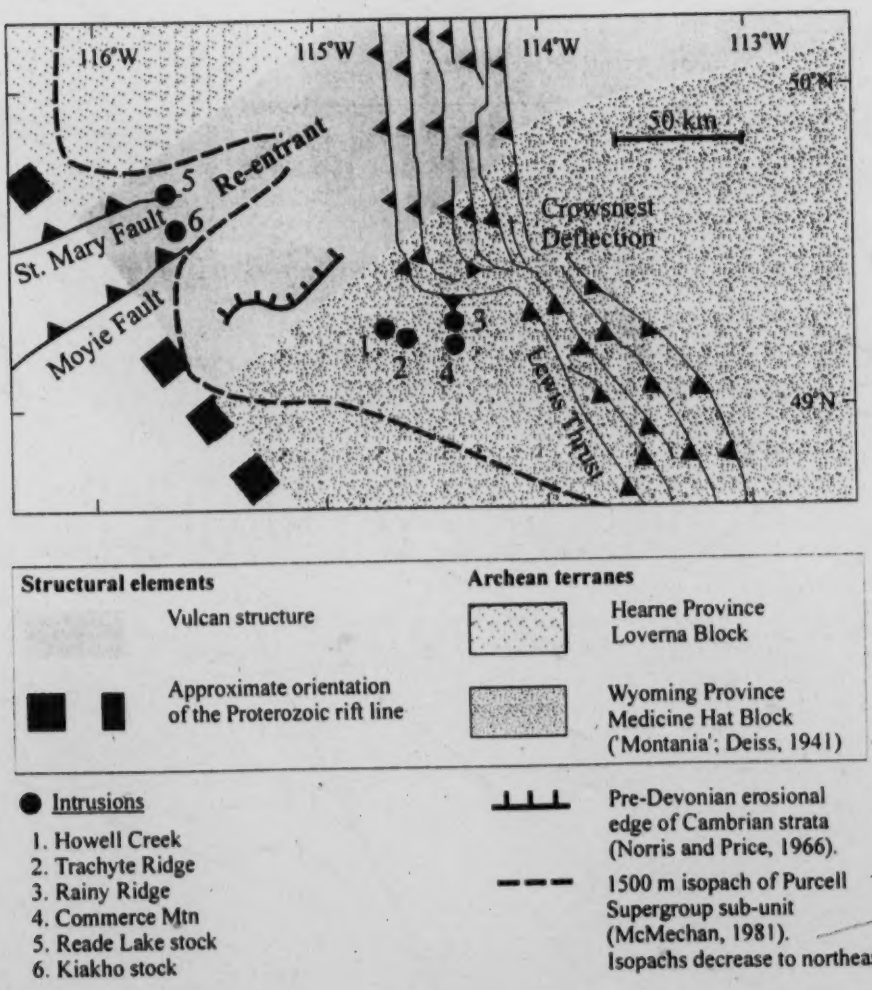

Work in progress at the University of Alberta by S. Ross and Dr. L. Heaman indicates a U-Pb age for the Crowsnest Formation, older than the previously reported age by several million years.

The results of $^{40}Ar/^{39}Ar$ dating undertaken for this study by Mike Villeneuve of the GSC on orthoclase phenocrysts (samples EB1301A and EB1810), has put precise age constraints on the magmatic event responsible for the Howell Creek suite. At 102.5±1.0 Ma (2σ) and 101.3±1.0 Ma (2σ) respectively, the results fall within the broad range of the less precise, recalculated K-Ar ages obtained from previous studies of the Howell Creek suite, 129±9 Ma (Leech et al., 1963) and 89±3 Ma (Gordy and Edwards, 1962). The results also overlap, within error, a more imprecise U-Pb date obtained for a syenite sample from Trachyte Ridge (98.5±5 Ma) reported in Skupinski and Legun (1989).

The advantage of using the $^{40}Ar/^{39}Ar$ step-heating procedure to interpret the thermal history of the intrusions is evident in this study. In contrast, conventional K-Ar dating which produces a single date for the sample cannot differentiate between areas of anomalous ^{40}Ar loss or gain within the crystal. The results obtained here provide an explanation of the broad range of dates obtained in previous studies. The possible infiltration of fluids containing excess ^{40}Ar and an unconstrained later thermal disturbance, identified in this study, could not be interpreted from earlier analyses.

Mid-Cretaceous magmatism of the Canadian Cordillera

Armstrong (1988) recognised episodic increases in magmatism within the Canadian Cordillera. He reported that between 130-84 Ma, the Omineca Belt (Fig. 1) was a site of extensive magmatic activity, and that during this period magmatism reached further inland than at any other period of the Mesozoic. The Howell Creek suite, together with regional intrusions and Crowsnest Formation volcanic rocks, represent the most easterly expression of magmatic activity in the southern Canadian Cordillera of this period. Armstrong (1988) correlated this period of Cordilleran magmatism with the formation of magmatic arcs resulting from Mesozoic terrane accretion to the west, and explained the variable but general easterly increase in alkalinity of the Cordilleran Cretaceous igneous

rocks in terms of increasing distance from subduction zones (Dickinson, 1975). Two temporally distinct subduction zones have been recognised amongst the assemblage of autochthonous and allochthonous terranes of Western Canada. The Late Triassic Nicola group in Quesnellia is believed to represent an arc complex with an easterly dipping subduction zone. The volcanic and volcaniclastic rocks of the Spences Bridge Group of southwestern British Columbia (Thorkelson, 1985) are identified as a magmatic arc related to an easterly dipping mid-Cretaceous subduction zone (Souther, 1991; Monger, personal communication, 2000).

Anatexis of the North American cratonic rocks represents an alternative theory put forward for the increased alkalinity of Cretaceous magmatic phases along the Cordillera. Anderson (1987), Woodsworth et al. (1991), Brandon and Lambert (1993 and 1994), and Driver et al. (2000) have all promoted the theory that the formation of a thickened crustal welt at the North American cratonic boundary induced by the compression of Mesozoic terrane accretion was the impetus behind Cretaceous anatectic melting.

Woodsworth et al. (1991) reviewed occurrences of calc-alkalic and alkalic plutonic rocks emplaced during the mid-Cretaceous, within the limit of the North American craton along the length of the Canadian Cordillera, coincident with the orientation of the miogeocline. The following section compares the lithology, geochemistry, and mineralisation of the Howell Creek suite to three selected mid-Cretaceous intrusions from the Canadian Cordillera (see Fig.12 for selected examples), selected younger intrusions of Montana, and the extrusive rocks of the Crowsnest Formation.

Tombstone pluton

In a geological setting similar to the Howell Creek area, the miogeoclinal rocks of the Selwyn Basin of western Yukon, host the diorite, tinguaite, quartz monzonite and syenitic intrusions of the Tombstone pluton (part of the Tombstone Range; ca. 90-110 Ma; Olade and Goodfellow, 1979; Anderson, 1987; Woodsworth et al., 1991 and references therein; Mortenson et al. 1996) which bear a striking resemblance to the Howell Creek suite in the major oxide geochemistry (Table 6), trace element profiles (Fig. 14), mineralogy.

The multi-element profile (Fig. 14) comparing the Howell Creek suite with selected Tombstone pluton samples shows that they have comparable curves and abundances of K, Nb, Sr, and Ti. In general, the Tombstone samples have slightly higher abundances of the other elements especially Y, Gd, Sm, Nd, Ce, La, U, and Th. The main mineralogical differences between the Howell Creek suite samples and the Tombstone pluton are the higher abundance of garnet, biotite, and amphibole, in the latter. These minerals may explain the increased levels of these elements, although Ba depletion in some of the Tombstone pluton samples, which is strongly partitioned into biotite (Arth, 1976) suggests that other processes are also involved. The Tombstone pluton, which includes fluorite–bearing tinguaite and syenite phases (cited as a U-mineralisation

Table 6.

Comparison of the major oxide abundances of the Howell Creek suite and the Tombstone pluton.

	SiO_2	Al_2O_3	TiO_2	Fe_2O_3	FeO	MnO	MgO	CaO	Na_2O	K_2O	P_2O_5
Howell Creek suite minimum	57.8	17.1	0.15	0.8	bd	bd	bd	0.03	0.5	4.4	0.01
Howell Creek suite maximum	63.7	20.6	0.47	3.8	1.9	0.17	1.0	5.17	7.4	12.7	0.22
***Tombstone pluton minimum**	56.3	15.4	0.33	0	1.4	0.03	0.1	1.16	2.5	6.69	0.02
***Tombstone pluton maximum**	63.8	21.2	0.61	2.2	3.0	0.13	1.2	4.24	6.0	12.6	0.27

*R. G. Anderson, unpublished data, 1987. 9 samples consisting of: hornblende syenite marginal phase, tinguaite groundmass, syenite, K-feldspar porphyry syenite, and a pseudoleucite porphyry dyke in syenite.

bd = below detection

targets by Olade and Goodfellow, 1979; Anderson, 1987) is the result of anatectic melting induced during the most recent of the cyclical periods of extension (200 m.y. duration) occurring in the area since 800 Ma (Anderson, 1987).

Figure 14.
Primitive mantle-normalised multi-element plot showing range of values for 18 samples from the Howell Creek suite in comparison with 9 samples from the Tombstone pluton (Anderson; unpublished data, 1987). Normalisation values from Jenner (NewPet, 1987-1994).

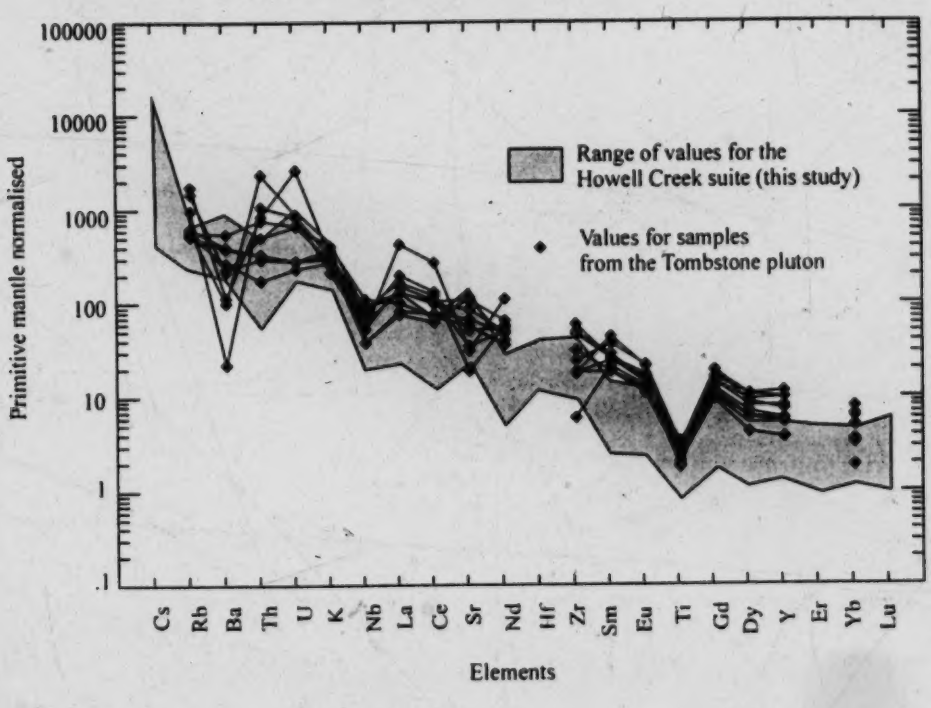

Mineralisation

In addition to the potential U-mineralisation of the Tombstone pluton, the numerous, scattered intrusions of the mid-Cretaceous Tombstone Range as a whole, are associated with various styles of gold mineralisation including: sheeted quartz veins and stockworks, skarns, carbonate and non-carbonate hosted disseminations, and quartz sulfide veins. These styles of mineralisation are thought to represent the evolution of a magmatic-hydrothermal system (Poulsen, 1997).

Poulsen (1996a, b, and 1997) compared the setting and examples of the mineralisation of the Tombstone Range to the highly economic, sediment-hosted, disseminated gold or 'Carlin-type' deposits within the miogeoclinal sedimentary rocks of the Great Basin of Nevada and Utah. Work by the British Columbia Geological Survey (BCGS) under their sediment-hosted gold mineralisation project further highlighted the

economic potential of disseminated gold mineralisation associated with the Brewery Creek intrusion within the Tombstone Range (Lefebure et al., 1999).

The Mineral Deposit Research Unit (MDRU) based at the University of British Columbia (UBC) have focussed on larger region which includes the Tombstone Range and extends approximately 500 km to the southeast, in their current 'Intrusion-Related Au Mineralisation' project. They are investigating the significance of the magmatic-hydrothermal systems of the Cretaceous 'Tombstone Plutonic Suite' with their Au-Bi-W-As±Sn±Mo association, which occur within a continental crustal setting, and suggest that the type of Au mineralisation in this area forms a distinct class of ore deposit.

Cassiar batholith

The Cassiar batholith (Fig. 12; ca. 100 Ma; Driver et al., 2000), which forms part of the Cassiar Suite (Woodsworth et al., 1991) consists of a range of variably felsic igneous rocks: granite, granodiorite, quartz monzodiorite, quartz monzonite, and quartz syenite.

Extended multi-element profiles comparing samples from the Howell Creek suite with those from the Cassiar Batholith (Driver et al., 2000; samples with <66 wt. % SiO_2 distinguished from samples with >66 wt. % SiO_2) are shown in Figure 15. The profiles show firstly, that there is no visible correlation between the SiO_2 abundance and the variation in elemental values of the Cassiar batholith. Secondly, and more importantly, the patterns of the Cassiar batholith and the Howell Creek suite are similar, although the Cassiar has a slightly less steep curve.

In the light of a range of analyses, including Nd, Sr and $\delta^{18}O$ isotopic data, Driver et al. (2000) do not emphasise the importance of relative depletions of Nb and Ti as signatures of subduction-related magmatism, but instead suggest an anatectic source of mixed crustal melts. They augment this theory with the observation that, in common with many other temporally and spatially related rocks of the Canadian Cordillera, the Cassiar batholith lacks mafic phases.

Figure 15.
Primitive mantle-normalised multi-element plot showing range of values for 18 samples from the Howell Creek suite in comparison with samples from the Cassiar Batholith (Driver et al., 2000). Normalisation values from Jenner (NewPet, 1987-1994).

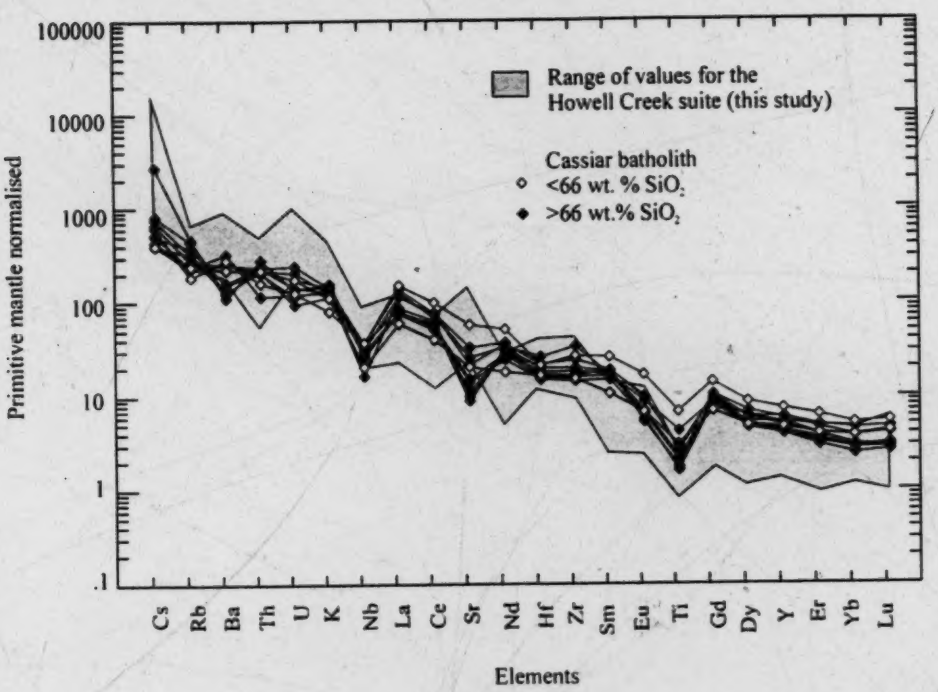

Bayonne Suite

The lithologies of the Cassiar batholith of Yukon-British Columbia (Woodsworth et al. 1991) bear a similarity to the mid-Cretaceous Bayonne Suite of southeastern British Columbia (Fig. 12; Table 7).

A relatively small number of geochemical analyses have been undertaken on the trace and REE composition of the intrusions of southeastern British Columbia. Brandon and Lambert (1993, 1994) analysed members of the Bayonne Suite; the Cretaceous Bugaboo, Fry Creek, Horsethief Creek and White Creek granitoid batholiths approximately 150 km to the northwest of the Howell Creek area (115-106 Ma; Brandon and Lambert, 1992).

Table 7.

Comparison of the Cassiar batholith and the Bayonne Suite lithologies (Driver et al., 2000; Brandon and Lambert, 1993, 1994).

	Lithologies
Cassiar batholith	bi and bi-musc granite, bi-hbl and bi-musc granodiorite, bi-hbl and bi quartz monzodiorite, bi quartz monzonite, and bi quartz syenite
Bayonne Suite	musc-bi granite, hbl-bi granite, and hbl-bi granodiorite

bi = biotite musc = muscovite hbl = hornblende

Multi-element profiles of selected samples from the White Creek, Fry Creek and Bugaboo batholiths of the Bayonne Suite (>70 wt. % SiO_2) are compared to samples from the Cassiar batholith (>68 wt.% SiO_2) in Figure 16. The Horsethief Creek batholith has not been included in this comparison as the trace element abundances are at variance with other members of the Bayonne Suite and the Cassiar batholith. The multi-element profiles highlight the similarities between these mid-Cretaceous intrusions, especially in the shape and slope of the profiles and the abundances of the LREE and MREE. Important differences lie in the variations in abundance of Nb, U, and Th. Nb is depleted in the Cassiar batholith while the selected Bayonne Suite samples show no sign of depletion. U and Th abundance is enhanced in the Fry Creek and Bugaboo pluton samples in comparison to the Cassiar batholith, and reach levels comparable to those of the Tombstone pluton and Howell Creek suite samples. Brandon and Lambert (1993) suggest that the Bugaboo, Fry Creek, and Horsethief Creek batholiths result from crustal anatexis in response to crustal thickening. Brandon and Lambert (1990) suggest a similar melting mechanism for the regional, peraluminous White Creek batholith (ca. 111 Ma?; Reesor, 1958; Wanless, 1968) adding that the variability of the initial $^{87}Sr/^{86}Sr$ ratios of various granodiorite (0.7069-0.7106) and granite (0.7169-0.7354) phases of the batholith denote variations in the degree of crustal assimilation.

The comparison of the Howell Creek suite to the Tombstone and Cassiar batholiths and the Bayonne Suite emphasises the similarities between the geochemical signatures of these mid-Cretaceous intrusions occurring along the Canadian Cordillera. In detail however, the Howell Creek suite has more in common with the Tombstone pluton

Figure 16.

Primitive mantle-normalised multi-element plot showing range of values for the Howell Creek suite, and 8 samples with >66 wt.% SiO_2 from the Cassiar Batholith in comparison with selected samples from the White Creek, Fry Creek and Bugaboo pluton of the Bayonne Suite (Driver et al., 2000; Brandon and Lambert, 1993, 1994). Normalisation values from Jenner (NewPet, 1987-1994).

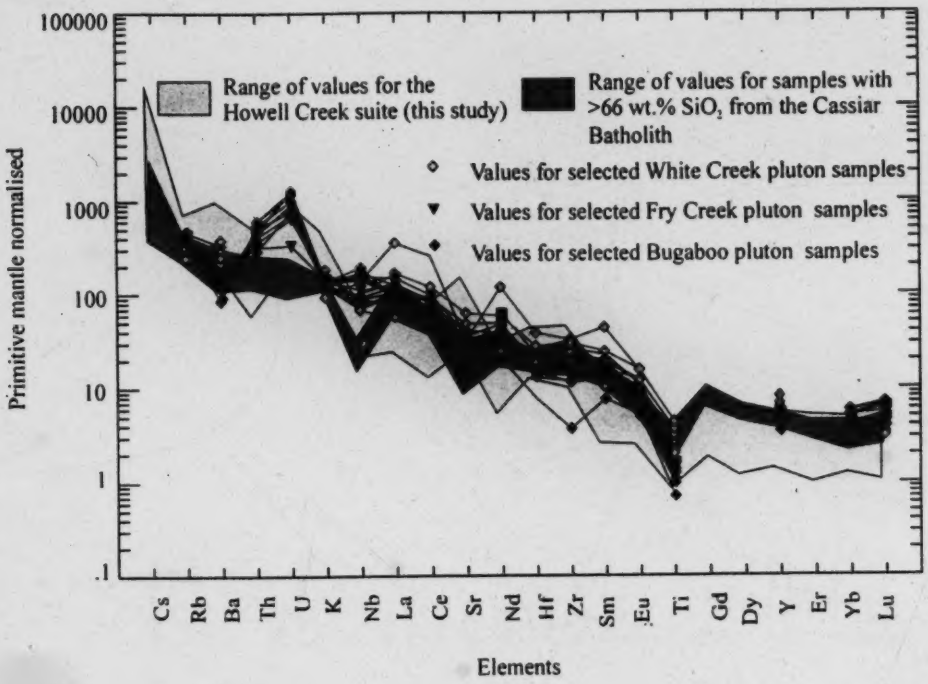

than either the Cassiar batholith or Bayonne Suite, which show stronger similarities to each other.

The lack of Nb depletion in the Bayonne Suite is an important distinction from the Howell Creek suite. These two suites of intrusive rocks are relatively proximal, with the Bayonne Suite occurring further to the west. The lack of Nb depletion in the Bayonne Suite would appear to contradict the assertion of Armstrong (1988) who related Cretaceous magmatism in this area of the Cordillera to subduction zone related processes (described above). If the geochemistry of the Bayonne Suite is not the result of concurrent subduction processes occurring to the west (Brandon and Lambert, 1993), then there is an implication that neither is the geochemistry of the Howell Creek suite. In

addition, the Nb-Ti depleted signature of the Cassiar batholith is not thought to be due to concurrent subduction processes but related to the composition of the source lithologies (Driver et al., 2000). The potential source lithologies of the Howell Creek suite include Proterozoic basalts (Daly, 1912; Hunt, 1964; Goble et al., 1999a) and possible subduction-related rocks (Lemieux et al., 2000) as well as more evolved crustal lithologies.

Although concurrent subduction processes appear to have had little influence on the geochemistry of Cretaceous magmatism along the Canadian Cordillera as described here, the intense compression induced by distal Triassic-Jurassic subduction and the consequent thickening of the North American craton edge appears to have had a profound affect.

Crowsnest Formation

The Cretaceous Crowsnest Formation crops out approximately 30 km north east of the Howell Creek area in the region of Crowsnest Pass, Alberta (Fig. 2). It consists of trachyte, analcite phonolite, and blairmorite in the form of agglomerates, bedded pyroclastic rocks, minor flows, and dikes. In recent years, various aspects of this compositionally unusual formation have been studied by Pearce (1970), Ferguson and Edgar (1978), Dingwall and Brearley (1985), Goble et al. (1993 and 1999b), Peterson and Currie (1993), Bégin et al. (1995), Adair and Burwash (1996), and Peterson et al. (1997).

The original vents responsible for these volcanically explosive deposits have yet to be discovered, although Pearce (1970) suggested three local sites from variations in lithologies and grain size, and the presence of flows and dikes. The predominant phenocrysts are sanidine, primary garnet, analcite, and aegirine-augite (Table 8).

The debate as to whether the Crowsnest Formation analcite phenocrysts are igneous, or the result of hydrothermal alteration after leucite, has continued since Pirsson (1915) disputed the assertion made by Mackenzie (1914) that the analcite of the Crowsnest Formation was primary. Analcite ($Na[AlSi_2O_6].H_2O$) as seen in the Crowsnest Formation rocks can have undisrupted inclusion trails, sharp crystal outlines (Ferguson and Edgar, 1978) and be so unaltered as to be of gem quality (Peterson et al., 1997). In

addition, the lack of any evidence of K-rich cores, as would be expected if Na had replaced K in the structure of leucite ($K[AlSi_2O_6]$), and $\delta^{18}O$ values which fall within the range of the lower crust, convinced Peterson et al. (1997) that the phenocrysts are primary. If so, the analcite helps define the physical parameters of the melt, because the assemblage of analcite + melt in the system $NaAlSi_3O_8$-$KalSi_3O_8$-$NaAlSiO_4$-H_2O exists only at lower crustal conditions of between 5-13 kbar, and 600-640°C (Deer et al., 1992; p. 516).

Table 8.

Phenocrysts of the Crowsnest Formation volcanic rocks. After Pearce (1970), and Ferguson and Edgar (1978).

Feldspar	Sanidine: up to 5 cm in length; Carlsbad > Baveno twinning; early dissolution textures commonly overgrown to form euhedral crystals; pink or white with pink/red patches or rims (albite); distinct, 50-100 µm wide chemical zonation, repeated up to 60 x in single crystal.
Garnet	Melanite and schorlomite, high-Ti varieties: <7.5 mm; euhedral; black; isotropic, light to dark brown under plane-polarized light; distinct chemical zonation especially in the trachytes, possibly due to variations in Ti content; contains inclusions of pyroxene, magnetite and titanite; appears as inclusions in analcite, feldspar and pyroxene.
Analcite	3 cm in diameter; well-developed trapezohedrons; rare chemical zonation in blairmorite and phonolite; also as interstitial matrix component; colour; brown, red, green, orange, originally brown; low Rb content.
Pyroxene	Aegirine-augite: <3 mm; black; rarely acicular; commonly zoned; with augite zones or cores; rarely altered; strongly pleochroic; extinction angle of pyroxene from analcite bearing rocks >30°;and <30° in non analcite bearing rocks; cores higher in Ca and Mg; rims higher in Na, Fe and Al; also in matrix.
Accessory minerals	Plagioclase, nosean, titanite, apatite, magnetite, ilmenite.
Alteration or replacement minerals	Albite, hematite, calcite, pyrite, clays, zeolites.

Peterson and Currie (1993), identified trace quartz in the Howell Creek phases, and although no free quartz was identified in the Howell Creek suite samples in this study, a comparison of major elements (Table 9) shows that the Crowsnest Formation is generally lower in SiO_2. Peterson et al. (1997) concluded that the area lacked any evidence of mineralisation.

Trace element profiles comparing the Howell Creek suite and the Crowsnest Formation volcanic rocks (Fig. 17; Peterson et al., 1997) illustrate the similarities

Table 9.

Comparison of the major oxide abundances of the Howell Creek suite and the Crowsnest Formation. Values for the Crowsnest Formation from Peterson et al. (1997).

	SiO_2	Al_2O_3	TiO_2	Fe_2O_{3t}	MnO	MgO	CaO	Na_2O	K_2O	P_2O_5
Howell Creek suite minimum	57.8	17.1	0.15	bd	bd	bd	0.03	0.5	4.4	0.01
Howell Creek suite maximum	63.7	20.6	0.47	5.7	0.17	1.0	5.17	7.4	12.7	0.22
Crowsnest Formation minimum	51.68	17.73	0.18	3.3	0.12	0.31	2.35	2.83	2.67	0.03
Crowsnest Formation maximum	60.18	20.71	0.63	8.65	0.27	1.62	8.64	7.61	9.22	0.14

bd = below detection Fe_2O_{3t} = total iron

between them. In general, the Crowsnest Formation rocks overlap the range of trace element abundances occurring in the Howell Creek suite, although, significant exceptions occur in the generally higher abundances of Nb, La, Ce, Sr, and Nd in the Crowsnest Formation rocks. The higher levels of these elements are probably due to the presence of clinopyroxene ± magnetite ± titanite, which have relatively high mineral/melt partition coefficients for these elements (Arth, 1976; Green and Pearson, 1983, 1987).

Examples of the Crowsnest Formation have initial $^{87}Sr/^{86}Sr$ ratios (Peterson et al., 1997; 0.704497 and 0.705105, blairmorite; 0.70479, analcite phonolite) which concur with Armstrong's (1988) initial $^{87}Sr/^{86}Sr$ ratio (0.703-0.705) for the Howell Creek suite, suggesting source rocks from lower crustal levels.

However, Peterson et al. (1997) determined a higher initial $^{87}Sr/^{86}Sr$ ratio for an intrusion from the Howell Creek suite (0.71018, trachyte) implying that various intrusive phases underwent varying degrees of crustal assimilation, with the analysed trachyte assimilating more crustal material than the rocks showing lower initial $^{87}Sr/^{86}Sr$ ratios.

From Nd-Sr isotopic compositions, Peterson et al. (1997) inferred an enriched mantle or contaminated crustal source for the Crowsnest Formation rocks, and suggested that enrichment occurred during the mid-Proterozoic. Metasomatic enrichment by

Figure 17.

Primitive mantle-normalised multi-element plot showing range of values for 18 samples from the Howell Creek suite compared with 7 samples from the Crowsnest Formation (Peterson et al., 1997). Normalisation values from Jenner (NewPet 1987-1994).

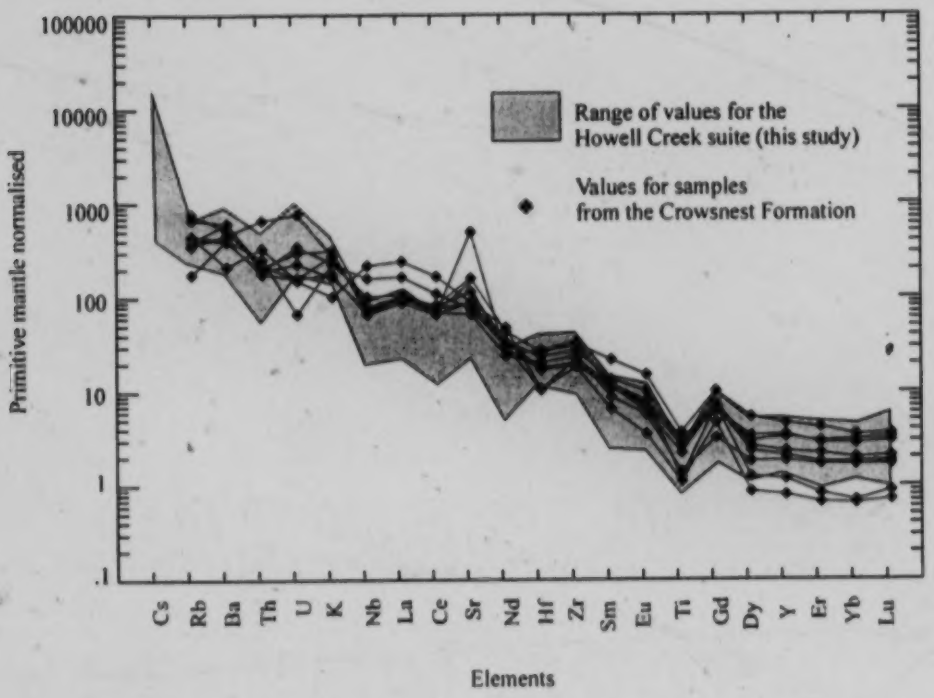

subduction processes and the approximate timing suggested by Peterson et al. (1997) would correlate with the formation of a Proterozoic suture zone (Fig. 13; and text below).

Peterson and Currie (1993) concluded that the lack of a spatial relationship between the Howell Creek suite and the Crowsnest Formation makes a co-magmatic theory tenuous. With palinspastic reconstruction of the movement on the Lewis Thrust, the original site of emplacement for the Howell Creek suite (west of the main trend of the Lewis Thrust; Figs. 2 and 13) lies approximately 80 km to the southwest of the Crowsnest Formation (east of the Lewis Thrust; Price, 1962). This distance is hard to

reconcile with a commonality of source, an interpretation supported by the disparity between the Sr abundances of the Crowsnest Formation and the Howell Creek suite.

Initial studies by S. Ross and Dr. L. Heaman (University of Alberta) on the Crowsnest Formation have provided a U-Pb age (melanite garnet phenocryst) older than the previous determination (96 Ma; K/Ar (sanidine); Folinsbee et al., 1957) by several million years. These results augment the findings of this study, that the region south of the Vulcan structure (Fig. 13) underwent a period of magmatism at ~102 Ma, which resulted in the emplacement of scattered, discrete alkalic igneous centres.

Mesozoic-Cenozoic magmatism of Montana

The Late Cretaceous to Miocene alkalic magmatism of Montana has been extensively studied (e.g. Giles, 1982; Wilson and Kyser, 1988; Hearn et al., 1989; Dudás, 1991; O'Brien et al., 1991; Baker, 1991; Russell, 1991; Hastings, 1992; Lange et al., 1994; Zhang and Spry, 1994) due in the most part to an interest in the associated ore mineralisation, especially of epithermal gold and silver. Concentrations of intrusive and extrusive rocks, including breccia pipes and diatremes, are scattered across central Montana and include (north to south) the Sweet Grass Hills, the Bearpaw and the Little Rocky Mountains (which include the Zortman-Landusky orebodies), the Missouri River Breaks, and the Highwood, Judith, Adel, Moccasin, Little and Big Belt, and the Crazy and Beartooth Mountains.

The origin of these alkalic igneous rocks is debated, and the rôle of flat-slab subduction of the Farallon plate during the Mesozoic is inconclusive, because igneous rocks display neither clear-cut temporal nor geochemical zonations (Dudás, 1991). However, the underlying craton, the Archean Wyoming Province, is frequently cited as a potential source for, or influence on, the magmas (e.g., O'Brien et al., 1991). Hearn et al. (1989) investigated the crystalline basement by analysing crustal and mantle xenoliths from various magmatic centres, and suggested that phlogopite in the upper mantle may be the potassium source for the magmas. They added that their results concurred with other studies that the craton had undergone a process of enrichment between 1.7 and 1.9 Ga. Also from the study of mantle xenoliths, O'Brien et al. (1991) concluded that the

geochemical signature of syenites and tinguaites from the Highwood Mountains (Fig. 18; Ba-LREE enriched, a relatively low Nb signature, negative Ti anomaly and depleted U-Th-HFSE) was derived from an ancient mantle enriched by metasomatic (glimmerite) veins.

In the case of the Crazy Mountains, Dudás (1991) stressed the inability of trace element patterns to positively identify magmatic source material in the absence of supportive geological evidence. He rejected the possibility that the geochemical subduction signature was generated during the Mesozoic, and proposed instead that they derived from a mantle source which had been modified, possibly during a mid-Proterozoic subduction event.

Figure 18.

Primitive mantle normalised multi-element plot showing the range of values for 18 samples from the Howell Creek suite, compared to two samples from the Highwood Mountains, Montana (O'Brien et al., 1991). Normalisation values from Jenner (NewPet, 1987-94).

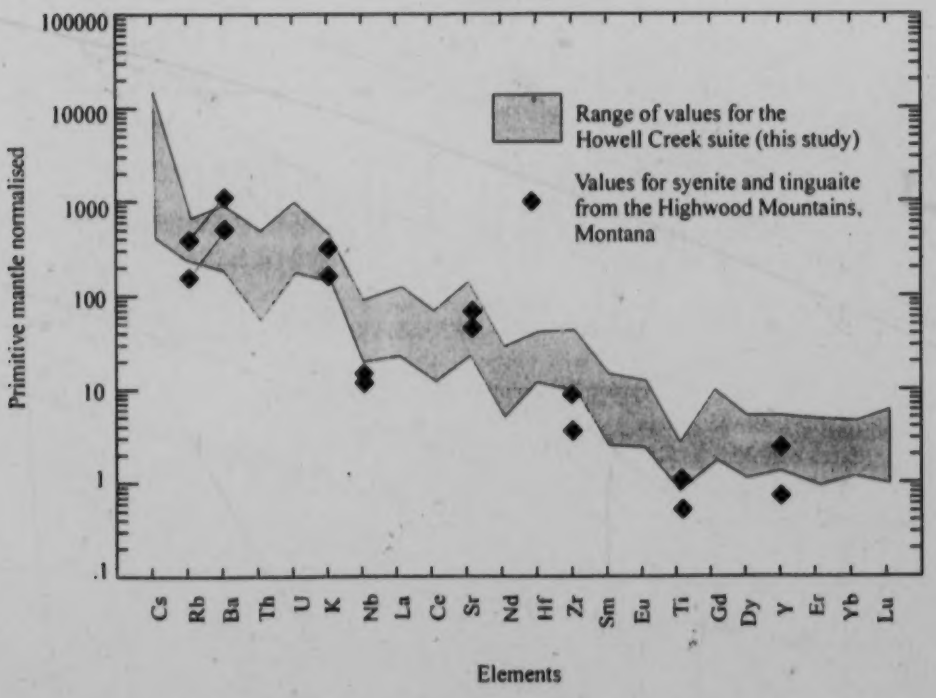

Mineralisation

In his review of alkalic intrusion-related epithermal gold deposits, Richards (1995) notes that the mineralisation associated with the intrusions of Montana occurs as disseminated gold-bearing pyrite in three different environments. The ore can be hosted by the intrusions, within replacement deposits in carbonate rocks, or occur in quartz stockworks or brecciated veins.

The gold and silver ore bodies responsible of the majority of the Zortman-Landusky deposits of the Little Rocky Mountains, are hosted by breccia dikes cutting porphyritic intrusions or by localised quartz stockworks. Ore consists of grains of native gold and silver (Au/Ag ratios averaging ~1:7; Wilson and Kyser, 1988) and trace amounts of electrum, tellurides and sulfosalts. Localised dark purple fluorite and widespread sulfide veins with pyrite>>marcasite>arsenopyrite are associated with highly mineralised areas (Russell, 1991).

Gold and silver±copper mineralisation associated with the Hog Heaven intrusions occurs within replacement deposits, veins, quartz stockworks, and to a lesser degree, vent breccias and open-space fillings. As in the Zortman-Landusky deposits the gold occurs in its native state, in electrum, as a coating on pyrite, or held intrinsically within the pyrite crystal structure (Lange et al., 1994).

Basement rock composition and structure

One of the most intriguing aspects of the Howell Creek area is the major crustal lineament which has been determined to run just north of the intrusions.

Deep crustal seismic profiles undertaken in the 1960s confirmed gravity and magnetic data showing an east-trending anomaly beneath the Western Canada Sedimentary Basin of southern Alberta. Kanasewich et al. (1969) interpreted the anomaly as the aulacogen or 'failed arm' of a Precambrian rift zone (see above). Sears and Price (1978) and McMechan (1981), amongst others, have also attributed the cause of the rift to the formation of a triple junction, which Bond and Kominz (1984) compared to the Afar region, East Africa.

More recent studies, conducted under the aegis of Lithoprobe, a multi-disciplinary geoscience program studying the geology of the crust in Western Canada, provided

further evidence of a west-trending linear anomaly running 350 km across southern Alberta and into southeastern British Columbia. Ross et al. (1991) proposed that this anomaly represents an Early Proterozoic collisional suture between the Medicine Hat and Loverna blocks of the Archean Wyoming and Hearne Provinces respectively. The major crustal suture lies to the north of the Howell Creek area, separating the Late Archean terranes: the Loverna Block of the Hearne Province to the north, and the Medicine Hat Block of the Wyoming Province to the south (Fig. 13).

Late Archean granitic gneiss has been dated from the Loverna Block (1.78 to 2.71 Ga; Villeneuve et al. 1993). U-Pb dates obtained by Davis et al. (1995) from Medicine Hat Block xenoliths, show evidence of a complex thermal history with samples providing younger dates from progressively increasing depths: tonalite gneiss (2.6 Ga), garnet-kyanite paragneiss (1.81-1.75 Ga), and mafic granulite rocks (1.75-1.70 Ga). Originating from depths between 5-15 km and approximately 41 km, these U-Pb dates indicate an Early Proterozoic thermal disturbance at lower crust/mantle boundary depths (Lemieux, 2000). The age of the source rocks in the Howell Creek area (inherited zircon; 2347±22 Ma, 2σ) reported by Don Murphy from the U-Pb analysis of a syenite sample from Trachyte Ridge (Fig. 2; Skupinski and Legun, 1989) is in line with dates obtained from the upper crust by Davis et al. (1995) and suggests that syenite from Trachyte Ridge was influenced by an upper crustal source.

In 1995, the Alberta Basement Transect program of Lithoprobe investigated the crystalline basement of Alberta. The resulting seismic refraction and reflection studies conducted across the Vulcan structure and proximal to it, in addition to magnetic and gravity surveys, were interpreted by Eaton et al. (1999) and Ross et al. (2000). They proposed that south-dipping reflectors seen in the vicinity of the 'Vulcan structure' (Fig. 13; Eaton et al., 1999) represent the subducted slab of the Loverna block.

At the western extent of the Alberta Basement Transect study area, the presence of the Vulcan structure is obscured due to the burial of the basement beneath the Paleozoic and Mesozoic sedimentary rocks of the Rocky Mountains, and the overprinting of potential field anomalies (gravity and magnetic) by Mesozoic faults and intrusions (Lemieux et al., 2000). Interpretation of an anomalous layer on seismic reflection profiles from less than 100 km to the east is suggested to represent the presence of mafic rocks

originally injected at a lower crustal level (≤51 km depth) into the Medicine Hat Block below the Vulcan structure (Ross, 1999), at a time of underthrusting and delamination of the Loverna Block during an Early Proterozoic collisional event (Lemieux et al., 2000).

The physical influence of this anomaly on the stratigraphic record of the area can be seen in isopach maps of the Proterozoic Purcell Supergroup which distinguishes the geometry of the western coastal margin of the North American craton at the time of deposition (McMechan, 1981). These maps outline a steep-sided, east-northeast-trending re-entrant (current orientation) in the crystalline basement whose proportions and orientation bear a strong similarity to the characteristics of the Vulcan structure independently determined in the Lithoprobe geophysical studies (Fig. 13).

Work by Norris and Price (1966) who reported that a geographically limited portion of the Cambrian sequence in this region had been eroded prior to deposition of Devonian sedimentary sequences (Fig. 13) implies that the re-entrant may have been the site of post-Proterozoic faulting. They claimed that the erosion was caused by movement of a fault-bounded 'gigantic trapdoor structure' in an area they called Montania. 'Montania' relates to a topographic high (Deiss, 1941) corresponding to the area now ascribed to the Medicine Hat block (Fig. 13). The fault along which this erosion of Cambrian strata occurred almost exactly follows the outline of the Vulcan structure as described by Ross et al. (2000).

The effect of the underlying basement geometry on the regional structural response to Mesozoic deformation has been studied by McMechan (1981), Kisilevsky et al. (1997), and Norris (2001), amongst others. In her work, McMechan (1981) describes four faults, which now cut the Purcell Anticlinorium to the west of Howell Creek, and which have been active since the deposition of the Windermere Supergroup in the Early to Late Proterozoic. Two of the faults, the St. Mary-Boulder Creek and the Moyie-Dibble Creek faults, parallel the orientation of the re-entrant (Fig. 13).

McMechan (1981) suggested that the topographic high in the basement rocks influenced the deformation of the Mesozoic fold and thrust belt by changing the trend of the faults in the Rocky Mountain belt from north to northwest at 49°50' N, forming the 'Crowsnest Deflection' (Norris, 1969; Figs. 2 and 13). From paleomagnetic studies Kisilevsky et al. (1997) determined that vertical-axis rotation had been minimal between

north and northwest-trending mountain ranges (the Flathead and Clark Ranges), which lie within the Lewis Thrust sheet in the vicinity of the study area. These results concur with kinematic data obtained by Norris (2001). Analysis of slickenlines measured in various strata in the vicinity suggested that only localised rotation of the beds had occurred, perhaps due in part to the heterogeneity of the strata. Any overall appearance of rotation in the trend of deformational structures was, Norris suggested, due to the underlying geometry of the basement.

The Howell Creek suite - synthesis

Setting

The alkalic Howell Creek suite occurs in a geographically limited area. The dominant basement feature in this region, coincident with these unique and compositionally distinct phases, is the presence of an Early Proterozoic collisional zone (Vulcan structure) at depth and the associated thickened and imbricated crust (Ross et al., 1991; Ross, 2000; Lemieux, 2000). Palinspastic calculations which reconstruct the area prior to movement on the Lewis Thrust, place the original site of intrusion of the Howell Creek suite into the sedimentary host rocks <100 km to the southwest, in a position similar to its present relationship in regard to the Vulcan structure. The phases of the Howell Creek suite show evidence of a subduction-related signature, in contrast to similarly aged plutons (Bayonne Suite) which lie to the north of the south dipping suture. It is therefore possible that the Howell Creek suite may have been influenced by metasomatic enrichment induced by the Early Proterozoic subduction zone. However, the similarity of the geochemical signature of the Howell Creek suite to that of the mid-Cretaceous intrusions along the Canadian Cordillera (see above) which are interpreted to be the result of anatectic melting, indicates that the source rocks for the Howell Creek suite were not unique. The influence of a specific subduction event during the Proterozoic on the geochemistry of the Howell Creek suite is therefore debatable at this point.

From analysis of initial Sr ratios undertaken in other studies (Armstrong, 1988; Peterson et al., 1997), it appears that the magma responsible for the Howell Creek suite was strongly affected by the underlying Archean crust. A strong crustal influence on Cretaceous alkalic magmatism occurring within the North American craton is seen along

the length of the Canadian Cordillera and in the later intrusions of Montana (see above). Armstrong (1988) reported that the intrusions in the Howell Creek area are the only igneous rocks along the length of the Canadian Cordillera that exhibit lower initial $^{87}Sr/^{86}Sr$ ratios (0.703-0.705) east of the intrusions found in the Omineca Belt (>0.707). However, Peterson et al. (1997) determined a higher initial $^{87}Sr/^{86}Sr$ ratio (0.71018) for a Howell Creek trachyte. Individual phases of the Howell Creek suite are therefore believed to have undergone varying degrees of crustal assimilation. This interpretation of the petrogenesis of the Howell Creek suite concurs with the conclusions of Anderson (1987), Woodsworth et al. (1991), Brandon and Lambert (1993 and 1994), and Driver et al. (2000) on the derivation of other mid-Cretaceous Canadian Cordilleran plutons from the thickened welt of the North American cratonic boundary.

The Vulcan structure has been a major structural influence on the region, both pre- and post- emplacement of the Howell Creek suite. Its presence is reflected in the thickness of Proterozoic sediments in the area (McMechan, 1981), and there is some justification for assuming it was a topographic high, at least prior to the Devonian period (Norris and Price, 1966). In addition, McMechan (1981), Kisilevsky et al. (1997), and Norris (2001) concur that the geometry of the basement had a major structural influence on the crustal response to Mesozoic deformation as reflected in the Crowsnest Deflection (Figs. 2 and 13). The presence of a robust, linear, deep crustal (and possibly topographic) anomaly with an east-northeasterly orientation, such as the Vulcan structure, could deflect the late-Cretaceous east verging thin-skinned structures to the present configuration.

The response of the crust prior to extensive movement along the Lewis Thrust, can only be speculated, however, during terrane accretion and the production of a thickened welt at the edge of the North American craton the suture would be expected to have introduced an area of heterogeneity to the crust. In these circumstances, the lineament could have acted in one of three ways. Firstly, it could have had no effect, neither restricting nor promoting movement. This is unlikely if the postulation that it was responsible for the formation of the Crowsnest Deflection is correct. Secondly, it could have acted as a plane of weakness, releasing the strain of compression by strike-slip movement in a similar manner to that observed in high-angle faults and shear planes of

the Great Falls tectonic zone of Idaho and Montana (O'Neill and Lopez; 1985). This would be the expected response, however, there is no evidence of major strike-slip movement in the miogeoclinal strata proximal to the Vulcan structure in the Howell Creek area. Although slickensides and bedding plane slippage are seen in the area (Norris, 2001) they are minor, localised occurrences as could be expected from regional compression of highly stratified lithologies. The third possibility is that during Mesozoic deformation the Vulcan structure behaved as a fixed, rigid anomaly. If so, it could have created an area of relatively low stress on its eastward flank. The Howell Creek suite would have originated in this area, in the 'pressure shadow' induced by the Vulcan structure, protected from the full extent of westerly compression. It could be described as an area of 'relative extension' in a highly compressed region. The resulting, isolated volume of relatively low stress in the crust, could assist melt production at depth (by de-pressurisation), and allow the Howell Creek suite phases to pool and assimilate crustal rock, prior to their subsequent ascent, possibly using the lineament as a conduit.

Whatever the rôle of the Vulcan structure during crustal thickening, melting may have been aided by additional heat supplied by the flow of hot mantle towards the subduction zones occurring to the west during the Mesozoic. Hot mantle is believed to flow into the mantle wedge to replace mantle which is displaced downwards as the colder subducted slab descends (Hamilton, 1995). Although modelling by Patiño Douce et al. (1990) of the ability of thickened crust to generate melting suggests that an additional heat source is not required. In their interpretation of the Cassiar Batholith, Driver et al. (2000) concluded that no additional heat was necessary to generate the magma responsible for the Cassiar Batholith from the thickened crust.

There is a spatial association of the intrusions in Howell Creek area with a complex system of faults, which include, for example, the obscure nature of the Twentynine Mile Fault/Lewis Thrust (Price, 1965; Skupinski and Legun, 1989; Legun, 1993). Although Paterson and Schmidt (1999) question the influence of faults on the location of intrusions, there is general agreement that high-level magma emplacement can cause fracturing and doming in the overlying strata (Jaroszewski, 1989; Price, 1990; Paterson et al., 1996; Petford, 1996). Regions of increased heat and liquidity caused by magma emplacement weaken the tensile strength of the host rock, which in the case of

rock with pre-existing mechanical anisotropies is already low (Clemens and Mawer, 1992). It is suggested that the introduction of areas of heterogeneity and weakness into the highly stratified sedimentary rocks of the miogeocline by the emplacement of the hypabyssal Howell Creek intrusions may have influenced fault generation and orientation. During a period of intense post emplacement compression, these weakened areas would respond differently to the surrounding strata, which were otherwise transported in a relatively predictable manner along bedding planes (Price, 1965).

Intrusions

The alkalic intrusions of the Howell Creek suite occur as small stocks, sills, dykes, and intrusive breccias within well-stratified miogeoclinal sedimentary sequences. The conformable nature of many of the sills and intrusive breccias affirms the strong anisotropic structural control of the intruded strata.

The major eastward thrusting in this area along the Lewis Thrust occurred post-emplacement. It has not been determined what faulting, if any, occurred in this region prior to this displacement. If the Howell Creek intrusions were emplaced into unfaulted strata, they would have crystallised at a depth of between 3.5 and 7 km, using the stratigraphical thicknesses calculated by Price (1965) for the intruded Triassic to Precambrian strata.

From age dating and field observations, the earliest intrusions appear to be the alkali feldspar syenite (K-Ar, 129±9 Ma; Leech et al., 1963), which occur throughout, with the largest outcrop occurring in the north west of the mapped area in the vicinity of the Twentynine Mile Fault/ Lewis Thrust. This highly leucocratic phase shows extensive alteration, with fluorite (Plate 8) and sulfides (Plate 9), and quartz stockwork veining (Plate 10). Its mineralogy and texture is comparable to the igneous fraction of the matrix of the intrusive breccias, and they are thought to be from the same phase. The megacrystic syenite (102.5±1.0 Ma (2σ), this study) commonly crosscuts the alkali feldspar syenite. The phenocrysts of the megacrystic syenite (especially the feldspar phenocrysts) display sequential growth zones, inferring a complicated thermal history, possibly including magma mixing, while the fine-grained groundmass indicates quenching, suggesting a rapid final emplacement. A rapid emplacement would concur

with localised areas rich in xenoliths derived from underlying lithologies, within the megacrystic syenite. The intimate spatial association of the alkali feldspar and megacrystic phases suggests that they may derive from the same plutonic body. The leucocratic (therefore less dense) phase, and the more mafic megacrystic phase, could represent the upper and lower levels respectively, of a magma chamber. A high F^- content in the magmatic aqueous phase of intrusions, as displayed in the disseminated and vein fluorite (Plate 8) of the alkali feldspar syenite, is recognised as significant in the final stages of crystallisation, especially in Ca-poor intrusions (Burnham, 1979; p. 116). The presence of F^- would act as an effective flux within the magma, depolymerising the melt by breaking the SiO_2 tetrahedra and forming stable SiF_4 molecules (Burnham, 1979; p. 77). The length of time the magma remained molten would thereby be increased and facilitate crystal growth as seen in the megacrystic syenite. The association of these phases is based on field relationships and requires confirmation, possibly from comparative analyses of the volatile content of the alkali feldspar phase and the amphibole phenocrysts of the megacrystic phase.

The presence of intrusive breccias in association with the alkali feldspar syenite suggests that the crystallising magma chamber eventually became overpressured by aqueous, F^--rich magmatic fluid, which explosively breached the chamber (Burnham, 1979; p. 115). Violently expulsed magma would entrain fragments both from the fractured carapace of the chamber and surrounding lithologies during its ascent. In addition, expulsion of the magmatic aqueous fluid would cause precipitation of disseminated minerals and veins in the country rock. This late-stage brecciation and mineralisation is also commonly seen in the epithermal gold-pyrite mineralisation of the Montana intrusions (see above). The commonly highly altered nature of the intrusive breccias and dissolution of the matrix, attests to the localised high permeability induced by the breccia pipes.

The emplacement of the foid syenite is temporally related to the megacrystic syenite (101.3±1.0 Ma (2σ), trachytic phase, this study), but is spatially and mineralogically distinct from the previously described phases and is therefore thought to have been derived from an isolated chamber. The foid syenite displays the lowest degree

of alteration and evidence of fluid ingress, and is not thought to be associated with mineralisation.

Mineralisation and alteration

In the Howell Creek area, gold mineralisation occurs in association with pyritisation of: carbonate and clastic rocks spatially associated with the intrusions on the north side of the Eastern Outlier, and the syenite intrusion in the northwest of the mapped area (1:44 444 scale map; Brown and Cameron, 1999). This style of mineralisation is redolent of that associated with the previously described alkalic intrusions of the Tombstone Range and Montana.

In addition to being cited as an example of intrusion-related sediment-hosted disseminated mineralisation by Lefebure et al. (1999) with similarities to alkalic epithermal deposit-types (Brown and Cameron, 1999; and references therein), the Howell Creek area has also been identified as an alkalic intrusion-associated Au-Ag deposit by Schroeter and Cameron (1996).

Various models of sediment-hosted deposits exist, with the rôle of magmatism having an obscure to an intrinsic influence on ore deposition; for example, 'Carlin-type' (Arehart, 1996; Ilchik and Barton, 1997) and 'distal-disseminated type' (Sillitoe, 1988). In his overview, Tosdal (2000) comments on the common association of distal-disseminated type deposits with porphyritic intrusions. Russell (1991) mentions that the mineralisation of the Zortman-Landusky mine is spatially related to porphyritic syenite, a relationship which is also implied in the Howell Creek area. Reviews by Richards (1995) and Müller and Groves (1995) have examined worldwide examples which typify the association of alkalic igneous rocks in epithermal deposits (Richards, 1995) and in alkalic (potassic) igneous rocks in general, from various tectonic settings (Müller and Groves, 1995). The 'sediment-hosted disseminated' and 'alkalic intrusion-associated' types of mineralisation into which the Howell Creek area has been categorised, are therefore not mutually exclusive (Poulsen, 1996a). Instead, the application of these various deposit models to the style of mineralisation in the Howell Creek area is a reflection of the strong chemical influence that sedimentary carbonate host rocks have in the precipitation of the ore minerals from magmatic fluid.

The disseminated style of the mineralisation in the Howell Creek area suggests that rapid depressurisation of the system during brecciation of the magmatic carapace was not the defining factor in ore deposition as this would be expected to produce higher ore concentrations. Instead, a process allowing dispersal of the expulsed aqueous magmatic fluid prior to a decrease in metal solubility is required to produce the precipitation of disseminated, fine-grained ore minerals. The most likely causes of metal precipitation from the magmatic fluid are interactions with the wallrock and groundwater causing oxidation and dilution.

For gold to be present within magmatic-hydrothermal fluids, it is important that the magma must not achieve sulfide saturation prior to the late-stage expulsion of the magmatic fluid, as gold is preferentially partitioned into immiscible sulfide phases within the magma (Richards, 1995 and references therein). Such conditions are possible in oxidised magmas where sulfur is present in the form of $SO_2 >> H_2S$ (Richards, 1995; Gammons and Williams-Jones, 1997). Geochemical analyses and the presence of magnetite in the samples, indicate that the magma responsible for the Howell Creek suite was relatively oxidised. Thus, gold may have been transported in the magmatic fluid as a chloride complex, $AuCl_2^-$, in preference to a gold bisulfide complex $Au(HS)_2^-$ which is more usual in less oxidised conditions (Barnes, 1979; Arehart, 2000). Although recent work by Loucks and Mavrogenes (1999) suggests that gold in the form of hydrosulfides would be compatible with these fluids. The occurrence of distal base-metal mineralisation in the Howell Creek area also suggests that chloride complexes were present in the magmatic fluid, as base metals are preferentially carried within these complexes (Barnes, 1979). The acidic magmatic fluids would be responsible for the sericitic alteration, and the dissolution of the carbonate host rocks, inducing extensive calcification and calcite veining. As the system evolved, groundwater would have been drawn into the convective cycle and Gammons and Williams-Jones (1997) suggest that 10-fold dilution of a magmatic fluid saturated in gold (as $AuCl_2^-$), by groundwater containing minimal chloride could result in 90% gold precipitation. The magmatic fluid would eventually be neutralised by reaction with the carbonate wallrock, which in the presence of F^- would precipitate fluorite.

$$2F^- + 2H^+ + CaCO_3 \rightarrow CaF_2 + CO_2 + H_2O$$

The resulting increase in pH would also contribute to the destabilisation of chloride complexes (Barnes, 1979) and therefore to gold precipitation.

From lithogeochemical analyses undertaken on the Howell Creek suite (Brown and Cameron, 1999; drill core HA-3) gold correlates with As (and Sb and W). This correlation suggests that other elements may also have complexed with gold in the magmatic-hydrothermal solution (Barnes, 1979; Yasuda and Mori, 1997).

Gold precipitation associated with fine-grained pyrite is a common feature of the mineralisation of disseminated or 'Carlin-type' gold deposits. As mentioned previously this style of gold mineralisation is also observed in association with the intrusions of the Tombstone Range and Montana. In his work, Arehart (1996 and 2000) recognises the concentration of microscopic gold within growth zones on pyrite and arsenian pyrite rims and highlights the association of gold with As in pyrite or marcasite. Arehart (2000) suggests that the incorporation of As in these iron sulfides induces Au deposition by creating reactive electrochemical sites which can potentially dissociate negatively charged ions i.e., $Au(HS)_2^-$. Although experimental evidence is lacking, Arehart (personal communication, 2001) concurs that gold precipitation from the dissociation of $AuCl_2^-$ in this environment would also be viable. Arehart (2000) stresses that due to structural differences between pyrite and its polymorph marcasite, an increased amount of As can enter the marcasite crystal structure, which may induce a higher degree of gold precipitation.

Commonly, coarse-grained pyrite, which is barren of gold (Brown and Cameron, 1999; Plate 9) occurs in association with late-stage, crosscutting calcite veins and adularia (low temperature hydrothermal minerals; Burnham, 1979) and reflects the evolution and cooling of the magmatic-hydrothermal system of the Howell Creek area.

Further studies

By its remit, this study has encompassed a broad range of topics concerning the Howell Creek suite and its geological environment. In addition to some important conclusions, several outstanding problems have been identified, the study of which could provide

valuable information on the magmatic and emplacement processes and mineralisation of the Howell Creek suite and the structural context of this area. Resolution of these questions may also have application in the geological interpretation of similar regional settings.

The structural complexity of the Howell Creek area remains unresolved in the main, making impossible accurate determinations of the economic potential of the site. Detailed mapping and palinspastic reconstructions of the area in the manner that Fermor and Price (1987) undertook on the Cate Creek and Haig Brook structural windows which occur approximately 20 km to the northeast, may answer some of the inconsistencies, including the true nature of the Twentynine Mile Fault / Lewis Thrust and the Howell Fault. Brown (1999, personal communication) expressed interest in confirming the presence of coal in the Triassic strata as mentioned by Price (1965) and the orientation of minor faults cut by the Harvey Fault. In addition, confirmation and interpretation of the presence of Alberta Group (this study) and Kishenehn Formation rocks (Jones, 1977) on the ridge of the Eastern Outlier and Cambrian carbonate lithologies on the Western Outlier (this study) would be of interest.

Regarding the mineralisation, work on the mineralogical association of gold and fine-grained pyrite could produce information important in the study of other intrusion-related disseminated gold deposits (Lefebure et al., 1999; Brown and Cameron, 1999). Extending the investigations to study the connection between the geochemistry of the intrusions and the mineralisation would be of enormous value, and could greatly assist in assessing the exploration potential of similar intrusions. In this regard, a review of, and comparison with the geochemical signatures and mineralisation of alkalic intrusions associated with Archean terranes (e.g., Smithies and Champion, 1999) may be of interest. The identification of the composition and interpretation of the rôle of volatiles (Webster and Holloway, 1990; Candela, 1990; Brenan, 1993; Coulson and Chambers, 1996) in the magma and the hydrothermal fluid of the Howell Creek suite would be useful, and may help explain the predominance of fluorite. Apatite is a ubiquitous mineral in the Howell Creek suite and its analysis could provide information on chloride and fluoride activities in the magma. Broadening the scope of the study to encompass the mineralisation of regional intrusions (e.g. Trachyte Ridge, Commerce Peak, etc.) which appear to be

temporally related, would enhance the application of the results. The striking similarity between the geochemistry and mineralisation of the Howell Creek suite and the Tombstone pluton, in the Tombstone Range, Yukon (Anderson, unpublished data, 1987) justifies a detailed comparison between the two areas, which could provide valuable insights on some of the geological processes affecting the Canadian Cordillera.

Radiogenic isotope studies using the Nd, Pb, and Sr systems would help identify the source of the magma and probable later contamination of the melt. Unfortunately, although previous studies have analysed the Nd and Sr ratios of intrusions in the Howell Creek area (Armstrong, 1988; Peterson, 1993) the identity of the sampled intrusive phases and precise locations of the sample sites are unknown. Therefore, radiogenic isotope studies probably constitute the most useful area for further magmatic-related studies. Although recent work by Davies and Tommasini (2000) suggests that disequilibrium melting during anatexis may affect especially the Sr and Nd isotopic ratios when the melt is able to migrate rapidly from the source, it is generally argued that the isotopic character of the protolith is unchanged in the resulting magma by partial melting (Rollinson, 1992). The presence of Archean basement rocks in the Howell Creek area make analysis by whole rock Nd isotopic ratios a suitable method, and results may help determine the possible influence and age of the protolith. Used in conjunction with analysis of Sr isotope ratios the results could provide a powerful tool in confirming the source rocks and the extent and source of later contamination. The mineralogy of the Howell Creek suite, with the preponderance of feldspar, makes Pb isotopic studies particularly applicable. The ability of the three common Pb systems ($^{206}Pb/^{204}Pb$, $^{207}Pb/^{204}Pb$, $^{208}Pb/^{204}Pb$) to identify lithospheric isotopic reservoirs (Doe and Zartman, 1979; Zartman and Haines, 1988) make it an ideal analytical tool to use in the determination of the source rocks and the magmatic processes involved in generation and emplacement of the Howell Creek suite.

Xenoliths identified in this study, occurring in the megacrystic and foid syenite (Brown and Cameron, 1999) and the breccia pipes, appear to have derived from upper crustal lithologies seen elsewhere in the area, and are interpreted here to be the result of high-level brecciation of the magmatic carapace. Sampling of the xenolithic clasts may confirm this theory or may additionally provide examples of deeper lithologies.

Geochemical and isotopic studies of the xenoliths, as well as details of the distribution and physical appearance, especially of any identified metamorphosed samples could provide insight into magmatic processes (contamination models) and possible source rocks for the intrusions, especially when compared to other regional studies of xenoliths (e.g., Buhlmann et al, 2000).

While these suggestions are by no means a comprehensive list of the possible directions that further studies of this area may take, additional work on any of these topics would greatly enhance the understanding of the geological environment of the Howell Creek area, and would provide important constraints on the mid-Cretaceous tectonic and magmatic evolution of the southern Canadian Cordillera.

Conclusions

- The mid-Cretaceous, alkalic Howell Creek suite consists of several coeval intrusive phases, emplaced at ~ 102 Ma.
- Geochemical and isotopic evidence suggests that the suite was derived from the anatectic melting of crustal material.
- The composition of the Howell Creek suite is comparable to other mid-Cretaceous intrusions occurring along the Canadian Cordillera. Petrogenetic interpretations of these intrusions suggest that they are derived from heterogeneous source rocks within the thickened crustal welt of the North American craton.
- The Howell Creek suite is located in a unique region of the Foreland Belt, underlain by a linear suture between Archean terranes. While the composition of the Howell Creek suite is compatible with metasomatic enrichment, the attribution of its geochemical signature specifically to Proterozoic metasomatism is debatable. The presence of this linear anomaly may have influenced the production and location of the magmatism responsible for the Howell Creek suite.
- The style of gold mineralisation associated with the alkalic Howell Creek intrusive suite resembles aspects of different deposit model types, including the 'distal-disseminated sediment-hosted gold deposit' type and the 'intrusion-related Au mineralisation' type, examples of which are recognised elsewhere along the Canadian Cordillera.

Acknowledgements

I would like to thank Hannah Kim for her excellent assistance in the field, and all fellow graduate students, undergraduate students, Faculty members and staff of the Department of Earth and Atmospheric Sciences at the University of Alberta who helped in the production of this thesis. I acknowledge the financial support provided by the British Columbia Geological Survey, and the Society of Economic Geologists through a McKinstry Award. It is a pleasure to acknowledge the support of various individuals who generously provided their time and expertise; Derek Brown, Dr. Ron Burwash, Dr. Charles Stelck, Dr. Larry Heaman, Dr. Tom Chacko, Glen Garratt, Bill Morton, Dr. Ron Goble, Dr. Terry Poulsen, Dr. Russell Hall, Chris Collom, Dr. Kirk Osadetz, Dr. Jim Monger, Dr. Frank Dickson, and especially my supervisor, Dr. Jeremy Richards, all contributed to the formulation of my ideas and the improvement of this work. However, I take full responsibility for the interpretations made here.

Finally, I would like to take this opportunity to express my heartfelt thanks to Dr. R. G. Anderson who not only generously permitted the use of previously unpublished data intrinsic to this study, but also provided the motivation to begin this study, and the encouragement and wise words that kept me going.

Plate 1. Inset of Howell Creek area 1:44 444 scale map showing Eastern Outlier. After Price (1965); Cameron et al. (unpublished map); Legun (1993).

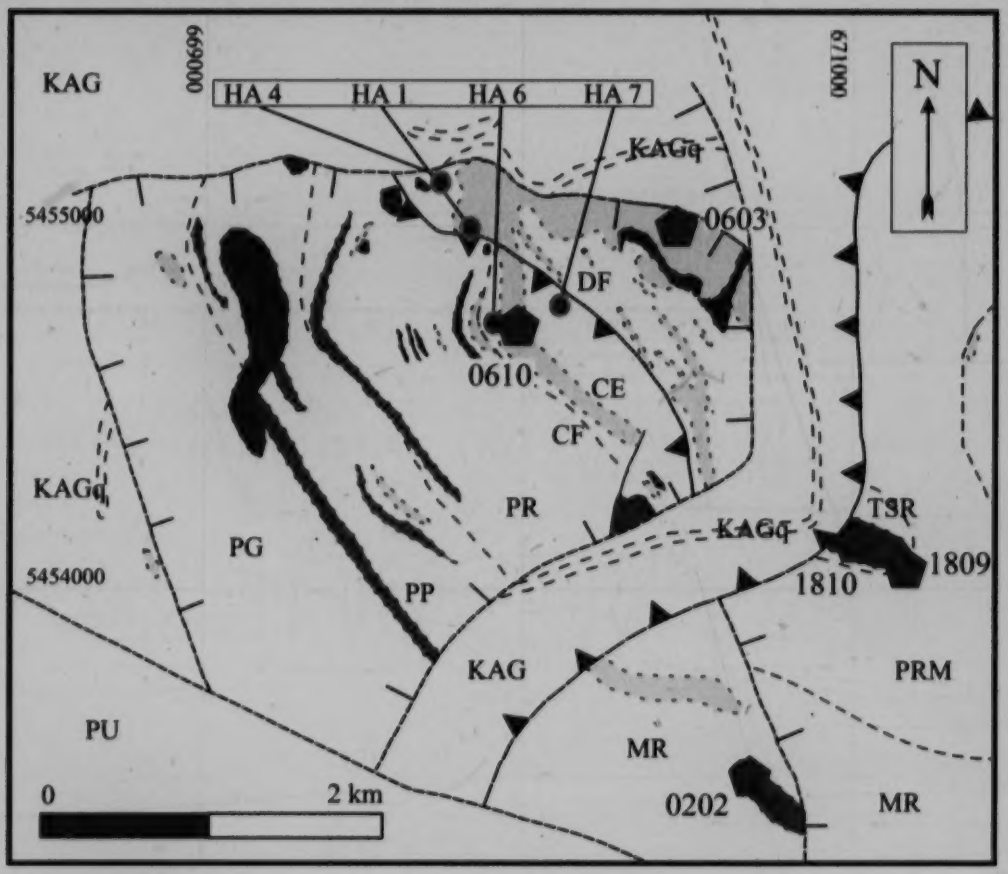

Legend

Stratified rocks

Cretaceous
KAG Alberta Group
KABq Alberta Group quartzite

Triassic
TSR Spray River Formation

Permian Pennsylvanian
PRM Rocky Mountain Group

Mississippian
MR Rundle Group

Devonian
DF Fairholme Formation

Cambrian
CE Elko Formation
CF Flathead Formation

Proterozoic
PR Roosville Formation
PP Phillips Formation
PG Gateway Formation

Intrusive rocks

Cretaceous

Gabbro
Intrusive breccia
Foid syenite
Alkali feldspar syenite

Symbols

Thrust fault-teeth on hanging wall
Thrust fault-approximate
Normal fault-approximate
Fault-undetermined movement orientation
Geological contact
Geological contact-approximate
Geological contact -inferred
0202 Station numbers
Drillhole identification

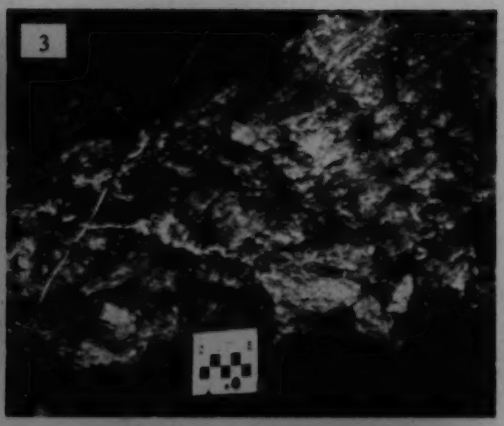

Plates 2-6.

Plate 2, examples of the Cretaceous fossils found at station EB0402 (black squares on scale card 1 cm.

Plate 3, flow textures visible in the alkali feldspar syenite.

Plate 4, pink alkali feldspar syenite crosscut by megacrystic syenite (scale card 3" x 2").

Plate 5, xenolithic syenite (width of image 5 cm).

Plate 6, foid syenite.

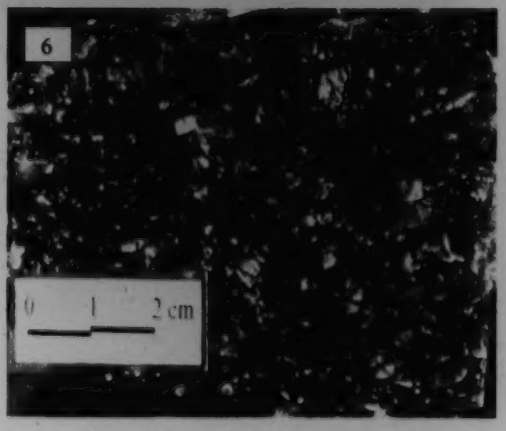

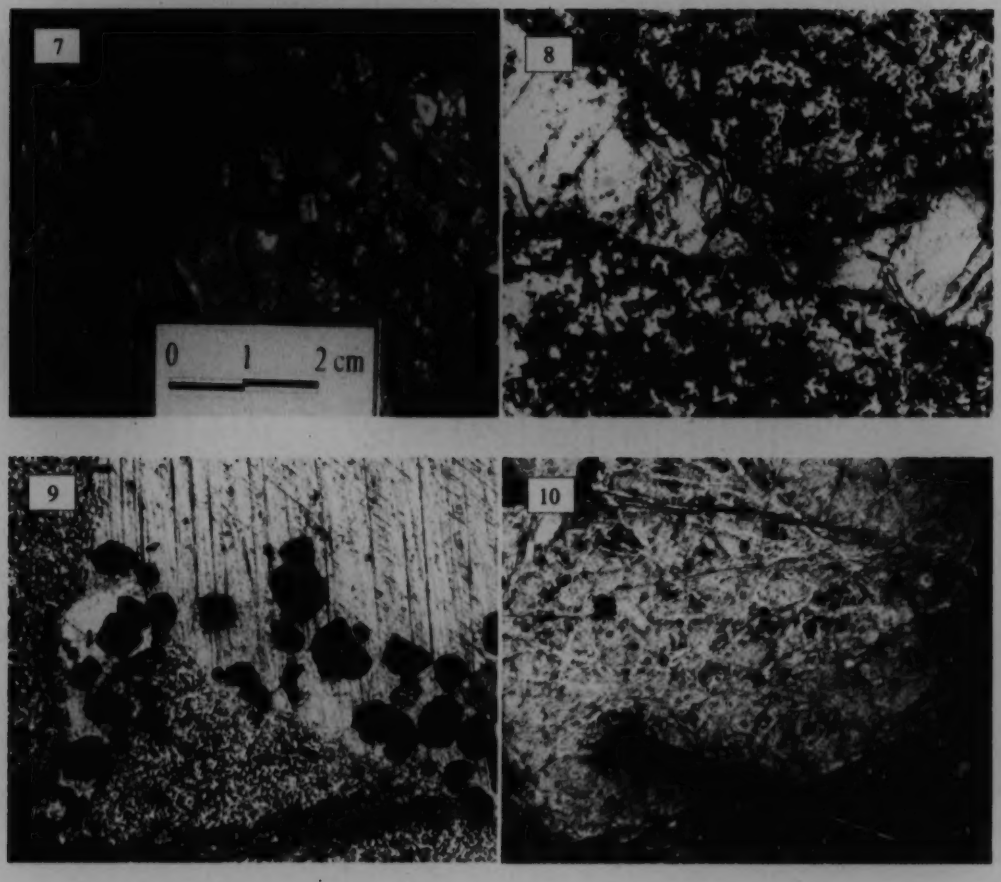

Plates 7-10.

Plate 7, megacrystic syenite.

Plate 8, purple fluorite vein cutting highly altered alkali feldspar syenite.

Plate 9, euhedral pyrite grains within sparry calcite vein, cutting fine-grained clastic country rock.

Plate 10, quartz stockwork crosscutting bleached alkali feldspar syenite.

Bibliography

Adair, R. N., and Burwash, R. A., 1996. Evidence for pyroclastic emplacement of the Crowsnest Formation, Alberta. Can. J. Earth Sci., v. 33, p. 715-728.

Anderson, R. G., 1987. Plutonic rocks in the Dawson map area, Yukon Territory. *In* Current Research, Part A. Geological Survey of Canada, Paper 87-1A, p. 689-697.

Arehart, G. B., 1996. Characteristics and origin of sediment-hosted disseminated gold deposits: a review: Ore Geology Reviews, v. 11, p. 383-403.

Arehart, G. B., 2000. PowerPoint diagrams for Carlin Short Course, Carlin-type Au deposits of the North American Cordillera: What are they? Where are they?, MDRU Short Course # 27, Vancouver, B.C., 2000, 27p.

Armstrong, R. L., 1988. Mesozoic and early Cenozoic magmatic evolution of the Canadian Cordillera. *In* Processes in Continental Lithospheric Deformation, S.P. Clark, Jr., B. C. Burchfiel, and J. Suppe, (ed.). The Geological Society of America, Special Paper 218, p. 55-91.

Arth, J. G., 1976. Behaviour of trace elements during magmatic processes - a summary of theoretical models and their applications. J. Res. U.S. Geol. Surv., v. 4, p. 41-47.

Baker, D. W., 1991. Central Montana Alkalic Province: Critical review of Laramide plate tectonic models that extract alkalic magmas from abnormally thick Precambrian lithospheric mantle. *In* Guidebook of the Central Montana Alkalic Province, Geology, Ore Deposits and Origin, D.W. Baker and R. B. Berg (ed.). Montana Bureau of Mines and Geology. Special Paper 100, p. 71-95.

Bally, A. W., Gordy, P. L., and Stewart, G. A., 1966. Structure, seismic data, and orogenic evolution of southern Canadian Rocky Mountains. Bull. Can. Petrol. Geol., v. 14, no. 3, p. 337-381.

Barnes, H. L., 1979. Solubilities of ore minerals. *In* Geochemistry of Hydrothermal Ore Deposits, H. L. Barnes (ed.) 2nd ed., John Wiley and Sons, p. 404-460.

Bégin, N. J., Ghent, E. D., and Beiersdorfer, R. E., 1995. Low-temperature metamorphism of the Crowsnest volcanic suite, southwestern Alberta. Can. Min., v. 33, p. 973-983.

Bond, G. C., and Kominz, M. A., 1984. Construction of tectonic subsidence curves for the early Paleozoic miogeocline, southern Canadian Rocky Mountains: Implications for subsidence mechanisms, age of breakup, and crustal thinning. Geol. Soc. Am. Bull., v. 95, p. 155-173.

Brandon, A. D., and Lambert R. StJ., 1990. Geochemistry of the 115 Ma White Creek batholith of southeast British Columbia: Implications for the origin of granitoids in the Omineca Crystalline Belt. Geological Association of Canada/Mineralogical Association of Canada, Annual Meeting, May16-18, 1990. Program with abstracts, v. 15, A14.

Brandon, A. D., and Lambert, R. StJ., 1992. Rb-Sr geochronology of Mesozoic granitoids in the southern Canadian Cordillera. *In* Project Lithoprobe Southern Cordillera Transect, Report 24, p. 95-104.

Brandon, A. D., and Lambert, R. StJ., 1993. Geochemical characterisation of mid-Cretaceous granitoids of the Kootenay arc in the southern Canadian Cordillera. Can. J. Earth Sci., vol. 30, p. 1076-1090.

Brandon, A. D., and Lambert, R. StJ., 1994. Crustal melting in the Cordilleran interior: The mid-Cretaceous White Creek batholith in the southern Canadian Cordillera. J. Petrol., v. 35, pt. 1, p. 239-269.

Brenan, J. M., 1993. Partitioning of fluorine and chlorine between apatite and aqueous fluids at high pressure and temperature: implications for the F and Cl content of high P-T fluids. Earth Plan. Sci. Lett., v. 117, p. 251-263.

Brooks, C., Hart, S. R., and Wendt, T., 1972. Realistic use of two-error regression treatments as applied to rubidium-strontium data. Rev. Geophys. Space Phys., v. 10, p. 551-577.

Brown, D. A., and Cameron, R., 1999. Sediment-hosted, disseminated gold deposits related to alkalic intrusions in the Howell Creek structure, southeastern British Columbia (82G/2,7). *In* Geological Fieldwork 1998, B.C. Ministry of Energy and Mines, Paper 1999-1, p. 1-14.

Buhlmann, A. L., Cavell, P., Burwash, R. A., Creaser, R. A., and Luth, R. W., 2000. Minette bodies and cognate mica-clinopyroxenite xenoliths from the Milk River area, southern Alberta: records of a complex history of the northernmost part of the Archean Wyoming craton. Can. J. Earth Sci., v. 37, p. 1629-1650.

Burchfiel, B. C., 1989. Tectonic framework of the Cordilleran orogenic belt of western North America. *In* Continental Magmatism, Abstracts, International Assoc. of Volcanology and Chemistry of the Earths Interior General Assembly, Santa Fe, NM, USA. New Mexico Bureau of Mines and Mineral Resources, Bull.13, p. 33.

Burnham, C. W., 1979. Magmas and hydrothermal fluids. *In* Geochemistry of hydrothermal ore deposits, H. L. Barnes (ed.) 2nd edition. John Wiley and Sons, p. 71-133.

Burrett, C., and Berry, 2000. Proterozoic Australia-western United States (AUSWUS) fit between Laurentia and Australia. Geology, v. 28, 2, p. 103-106.

Candela, P. A., Theoretical constraints on the chemistry of the magmatic aqueous phase. *In* Ore-bearing granite systems; Petrogenesis and mineralizing processes, H. J. Stein and J. L. Hannah (eds.), Geol. Soc. Am. Special Paper 246, p. 11-20.

Casselman, M., and Termuende, T. J., 1987. Howell Property, B.C. Ministry of Energy, Mines and Petroleum Resources, Assessment Report 16908.

Clark, L. M., 1964. Cross-section of Flathead Valley in vicinity of Sage Creek, B. C. Bull. Can. Petroleum Geology, v. 12, Field Conference Guide Book Issue, p. 345-349.

Clemens. J. D., and Mawer, C. K., 1992. Granitic magma transport by fracture propagation. Tectonophysics, v. 204, p. 339-360.

Coulson, I. M., and Chambers, A. D., 1996. Patterns of zonation in rare-earth-bearing minerals in nepheline syenites of the North Qôroq center, South Greenland. Can. Min., v. 34, p. 1163-1178.

Cox, K. G., Bell, J. D., and Pankhurst, R. J., 1979. The interpretation of igneous rocks. George, Allen and Unwin, London.

Dahlstrom, C. D. A., 1970. Structural geology in the eastern margin of the Canadian Rocky Mountains.

Bull. Can. Petrol. Geol., v. 18, No. 3, p. 332-406.

Daly, R. A., 1912. Geology of the North American Cordillera at the 49th parallel. Geological Survey of Canada, Memoir 38.

Davies, G. R., and Tommasini, S., 2000. Isotopic disequilibrium during rapid crustal anatexis: implications for petrogenetic studies of magmatic processes. Chem. Geol., v. 162, p. 169-191.

Davis, W. J., Berman, R., and Kjarsgaard, B., 1995. U-Pb geochronology and isotopic studies of crustal xenoliths from the Archean Medicine Hat block, northern Montana and southern Alberta: Paleoproterozoic reworking of the Archean crust. *In* 1995 Alberta Basement Transects Workshop, G. M. Ross (ed.). Lithoprobe Report 47, p. 330-335.

Deer, W. A., Howie, R. A., and Zussman, J., 1992. An introduction to the rock-forming minerals, 2nd ed. Longman Scientific and Technical, Longman Group, UK. 695p.

Deiss, C., 1941. Cambrian geography and sedimentation in the central Cordilleran region. Geol. Soc. Am. Bull., v. 52, p. 1085-1115.

Dickinson, W. R., 1975. Potash-depth (K-h) relations in continental margin and intra-oceanic magmatic arcs. Geology, v 3, 2, p. 53-56.

Dingwall, D. B. and Brearley, M., 1985. Mineral chemistry of igneous melanite garnets from analcite-bearing volcanic rocks, Alberta, Canada. Contrib. Min. Petrol., v. 90, p. 29-35.

Doe, B. R., and Zartman, R. E., 1979. Plumbotectonics I, The Phanerozoic. *In* Geochemistry of Hydrothermal Ore Deposits, H. L. Barnes (ed.) 2nd ed., John Wiley and Sons, Chap. 2, p 22-70.

Driver, L. A., Creaser, R. A., Chacko, T., and Erdmer, P., 2000. Petrogenesis of the Cretaceous Cassiar batholith, Yukon-British Columbia, Canada. Implications for magmatism in the North American Cordilleran Interior. GSA Bulletin, v. 112, p. 1119-1133.

Dudás, F. Ö., 1991. Geochemistry of igneous rocks from the Crazy Mountains, Montana, and tectonic models for the Montana Alkalic Province. J. Geophys. Res., v. 96, no. B8, p. 13,261-13,277.

Eaton, D. W., Ross, G. M., and Clowes, R. M., 1999. Seismic reflection and potential-field studies of the Vulcan structure, western Canada: a paleoproterozoic Pyrenees? J. Geophys. Res., v. 104, no. B10, p. 23,255-23,269.

Ferguson, L. J. and Edgar, A. D., 1978. The petrogenesis and origin of the analcite in the volcanic rocks of the Crowsnest Formation, Alberta. Can. J. Earth Sci., v. 15, p. 69-77.

Fermor, P. R., and Price, R. A., 1987. Multiduplex structure along the base of the Lewis Thrust Sheet in the Southern Canadian Rockies. Bull. Can. Pet. Geol., v. 35, no. 2, p. 159-185.

Folinsbee, R. E., Ritchie, W. D., and Stansberry, G. F., 1957. The Crowsnest volcanics and Cretaceous geochronology. *In* Guide Book, 7th Annual Field Conference, Waterton, Sept. 1957, E. W. Jennings and C.R. Hemphill (eds.). Alberta Society of Petroleum Geologists, Calgary, p. 20-26.

Fox, P. E., and Cameron, R. S., 1986. Howe Property B.C. Ministry of Energy, Mines and Petroleum Resources, Assessment Report 15035.

Fox, P. E., and Cameron, R. S., 1987. Howe Property B.C. Ministry of Energy, Mines and Petroleum

Resources, Assessment Report 16676.

Fox, P. E., and Cameron, R. S., 1989. Howell Property B.C. Ministry of Energy, Mines and Petroleum Resources, Assessment Report 18318.

Fujimaki, H., Tatsumoto, M., and Aoki, K., 1984. Partition coefficients of Hf, Zr, and REE between phenocrysts and groundmasses. Proc. 14th Lunar and Planetary Science Conf., Part 2. J. Geophys. Res., v. 89, Suppl., B662-B672.

Gammons, C. H., and Williams-Jones, A. E., 1997. Chemical mobility of gold in the porphyry-epithermal environment. Econ. Geol., v. 92, p. 45-59.

Giles, D. L., 1982. Gold mineralization in the Laccolith Complexes of Central Montana. *In* Proc. Denver Region Explor. Geol. Soc. Symposium, The genesis of Rocky Mountain ore deposits: Changes with Time and Tectonics, Nov. 4-5, Denver, CO, p. 157-162.

Goble, R. J., Ghazi, A. M., Treves, S. B., 1999a. Mineralogy and geochemistry of Proterozoic basaltic intrusions, Spionkop Ridge, southwestern Alberta. Can. Mineral. v. 37, p. 163-175.

Goble, R. J., Treves, S. B., and Ghazi, A. M., 1993. Comparison of the Rainy Ridge analcime phonolite sill and the Crowsnest volcanics, Alberta, Canada. Can. J. Earth Sci. v. 30, p. 1644-1649.

Goble, R. J., Treves, S. B., and Murray, V. M., 1999b. Cretaceous intrusions in the Commerce Mountain and adjacent areas of southeastern British Columbia and southwestern Alberta. Can. J. Earth Sci. v. 36, p. 1939-1956.

Goble, R., 1973. Commerce Property, B.C. Ministry of Energy, Mines and Petroleum Resources, Assessment Report 05070.

Gordy, P. L., and Edwards, G., 1962. Age of the Howell Creek intrusives. J. Alb. Soc. Petrol. Geol. v. 10, p. 369-372.

Green, T. H., and Pearson, N. J., 1883. Effect of pressure on rare earth element partition coefficients in common magmas. Nature, v. 305, p. 414-416.

Green, T. H., and Pearson, N. J, 1987. An experimental study of Nb and Ta partitioning between Ti-rich minerals and silicate liquids at high pressure and temperature. Geochim. Cosmochim. Acta, v. 51, p. 55-62.

Hamilton, W. B., 1995. Subduction systems and magmatism. *In* Volcanism associated with extension at consuming plate margins, J. L. Smellie (ed.). Geol. Soc. Spec. Publ. No. 81, p. 3-28.

Harlan, S. S., 1989. Paleomagnetism of Proterozoic mafic dikes, southwest Montana Foreland, USA. *In* Continental Magmatism, Abstracts, International Assoc. of Volcanology and Chemistry of the Earths Interior General Assembly, Santa Fe, NM, USA. New Mexico Bureau of Mines and Mineral Resources, Bull.13, p. 121.

Harrison, T. M., and McDougall, I., 1982. The thermal significance of potassium feldspar K-Ar ages inferred from $^{40}Ar/^{39}Ar$ age spectrum results. Geochim. Cosmochim. Acta, v. 46, p. 1811-1820.

Hastings, J. S., 1992. Gold deposits of Zortman-Landusky, Little Rocky Mountains, Montana. *In* Northwest Geology, J. E. Elliott (ed.), Guidebook for the Red Lodge-Beartooth Mountains-

Stillwater Area, Tobacco Root Geol. Soc. 17th Annual Field Conference, August 20-22, Red Lodge, MT., v. 20/21, p. 187-205.

Hearn, B. C. Jr., Collerson, K. D., MacDonald, R. A., and Upton, B. G. J., 1989. Mantle-crustal lithosphere of north-central Montana, USA: Evidence from xenoliths. *In* IAVCEI Continental Magmatism conference abstr., June 25-July 1, Santa Fe, NM, Bulletin 131, p. 125.

Höy, T., 1989. The age, chemistry and tectonic setting of the Middle Proterozoic Moyie sills, Purcell Supergroup, southeastern British Columbia. Can. J. Earth Sci., v. 26, p. 2305-2317.

Höy, T., and van der Heyden, P., 1988. Geochemistry, geochronology, and tectonic implications of two quartz monzonite intrusions, Purcell Mountains, southeastern British Columbia. Can. J. Earth Sci. v. 25, p.106-115.

Hume, G. S., 1932. Waterton Lakes - Flathead Valley area, Alberta and British Columbia. Geological Survey of Canada, Summary Report, Part B.

Hume, G. S., 1964. Oil seepages in the Sage Creek area, B. C. Bull. Can. Petroleum Geology, v. 12, Field Conference Guide Book Issue, p. 338-344.

Hunt, G., 1964. Chemical correlation of the Purcell igneous rocks. Bull. Can. Petroleum Geology, v. 12, Field Conference Guide Book Issue, p. 544-555.

Ilchik, R. P., and Barton, M. D., 1997. An amagmatic origin of Carlin-type gold deposits. Econ. Geol., v. 92, no. 3, p. 269-288.

Jaroszewski, W. 1989. Fault and fold tectonics. British Micropal. Soc. Series, p. 511.

Jones, P. B., 1964. Structures of the Howell Creek area. Bull. Can. Petroleum Geology, v. 12, Field Conference Guide Book Issue, p. 350-362.

Jones, P. B., 1969. Tectonic windows in the Lewis Thrust, southeastern British Columbia. Bull. Can. Petrol. Geol., v. 17, No. 2, p. 247-251.

Jones, P. B., 1977. The Howell Creek Structure – A Paleogene rock slide in the southern Canadian Rocky Mountains. Bull. Can. Petrol. Geol., v. 25, No. 4, p. 868-881.

Kanasewich, E. R., Clowes, R.M., and McCloughan, C.H., 1969. A buried Precambrian rift in western Canada. Tectonophysics, v. 8, p. 513-527.

Keep, M., and Russell, J. K., 1992. Mesozoic alkaline rocks of the Averill plutonic complex. Can. J. Earth Sci. v. 29, 2508-2520.

Kisilevsky, D. K., Enkin, R. J., Price, R. A., and Osadetz, K. G., 1997. Structural and Tectonic Implications of a paleomagnetic Study; Lewis Thrust sheet, southeast Canadian Rocky Mountains. Lithoprobe 1997, p. 171-172.

Labrecque, J. E., and Shaw, E. W., 1973. Restoration of the Howell Creek window and Flathead Valley of southeastern British Columbia. Bull. Can. Petrol. Geol., v. 21, no.1, p. 117-122.

Lang, J. R., Lueck, B., Mortenson, J.K., Russell, J. K., Stanley, C. R., Thompson, J. F. H., 1995. Triassic-Jurassic silica undersaturated and silica-saturated alkalic intrusions in the Cordillera of British Columbia: Implications for arc magmatism. Geology, v. 23, p. 451-454.

Lange, I. M., Zehner, R. E., and Hahn, G. A., 1994. Geology, geochemistry, and ore deposits of the Oligocene Hog Heaven Volcanic Field, Northwestern Montana. Econ. Geol. V. 89, p. 1939-1963.

Le Maitre, R. W., Bateman, P., Dudek, A., Keller, J., Lameyre Le Bas, M. J., Sabine, P. A., Schmid, R., Sorensen, H., Streckeisen, A., Woolley, A. R., and Zanettin, B., 1989. A classification of igneous rocks and glossary of terms. Blackwell, Oxford.

Leech, G. B., Lowdon, J. A., Stockwell, C. H., and Wanless, R. K., 1963. Age determinations and geological studies. Geological Survey of Canada, Paper 63-17, 140p.

Lefebure, D. V., Brown, D. A., and Ray, G. E., 1999. The British Columbia sediment-hosted gold project. *In* Geological Fieldwork 1998, B.C. Ministry of Energy and Mines, Paper 1999-1, p. 165-178.

Legun, A., 1993. The Howell Creek Structure, southeastern British Columbia. *In* Exploration in British Columbia 1992. Ministry of Energy, Mines and Petroleum Resources, p. 117-120.

Lemieux, S., Ross, G. M., and Cook, F. A., 2000. Crustal geometry and tectonic evolution of the Archean crystalline basement beneath the southern Alberta Plains, from new seismic reflection and potential-field studies, Can. J. Earth Sci. v. 37, p. 1473-1491.

Loucks, R. R., and Mavrogenes, J. A., 1999. Gold solubility in supercritical hydrothermal brines measured in synthetic fluid inclusions. Science, v. 284, p. 2159-2163.

MacKenzie, J. D., 1914. The Crowsnest Volcanics. Geol. Surv. Can. Mus. Bull. No. 4., Geol. Series, No. 20.

Maniar, P. D., and Piccoli, P. M., 1989. Tectonic discrimination of granitoids. Bull. Geol. Soc. Am., v. 101, p. 635-643.

McMechan, M. E., 1981. The Middle Proterozoic Purcell Supergroup in the southwestern Rocky and southeastern Purcell mountains, British Columbia and the initiation of the Cordilleran miogeocline, southern Canada and adjacent United States. Bull. Can. Petrol. Geol., v. 29, no.4, p. 583-621.

Miller, F. K., McKee, E. H., and Yates, R. G., 1973. Age and correlation of the Windermere Group in northeastern Washington. Geol. Soc. Am. Bull., v. 84, p. 3723-3730.

Monger, J. W. H., Price, R. A., and Tempelman-Kluit, D. J., 1982. Tectonic accretion and the origin of the two major metamorphic and plutonic welts in the Canadian Cordillera. Geology, v.10, p. 70-75.

Mortenson, J. K., Murphy, D. C., Poulsen, K. H., and Bremner, T., 1996. Intrusion-related gold and base metal mineralisation associated with the Early Cretaceous Tombstone plutonic suite, Yukon and east-central Alaska. *In* New Mineral Deposit Models of the Canadian Cordillera; 1996 Cordilleran Roundup Short Course Notes, section L, 13p.

Mortimer, N., 1987. The Nicola Group: Late Triassic and Early Jurassic subduction-related volcanism in British Columbia. Can. J. Earth Sci. v. 24, p. 2521-2536.

Müller, D., and Groves, D. I., 1995. Potassic igneous rocks and associated gold-copper mineralisation. Springer-Verlag, Berlin. 210p.

Netolitzky, R., 1972. Howell Property B.C. Ministry of Energy, Mines and Petroleum Resources,

Assessment Report 03785.

Newland, B. T., 1963. On the diffusion of radiogenic argon from potassium feldspars. Unpublished M.Sc. Thesis, University of Alberta, Edmonton, Alberta.

Noakes, S. B., 1984. Howell Property B.C. Ministry of Energy, Mines and Petroleum Resources, Assessment Report 13242.

Norris, D. K., 1969. The Crowsnest Deflection of the Eastern Cordillera of Canada. Geol. Soc. Am., abstract, Special Paper 121, p.221.

Norris, D. K., 2001. Slickenlines and the kinematics of the Crowsnest Deflection in the southern Rocky Mountains. Journal of Structural Geology, v. 23. Issues 6-7, p. 1089-1102.

Norris, D. K., and Price, R. A., 1966. Middle Cambrian stratigraphy of southeastern Canadian Cordillera. Bull. Can. Petrol. Geol., v. 14, p. 385-404.

O'Brien, H. E., Irving, A. J., and McCallum, I. S., 1991. Eocene potassic magmatism in the Highwood Mountains, Montana: petrology, geochemistry, and tectonic implications. J. Geophys. Res., v. 96, no. B8, p. 13,237-13,260.

Olade, M. A. and Goodfellow, W. D., 1979. Lithogeochemistry and hydrogeochemistry of uranium and associated elements in the Tombstone batholith, Yukon, Canada. *In* Proceedings of the 7th International Geochemical Symposium, Golden, Colorado, J. R. Watterson and T. K. Theobold (eds.), Association of Exploration Geochemists, p. 407-428.

O'Neill, J. M., and Lopez, D. A., 1985. Character and regional significance of the Great Falls tectonic zone, east-central Idaho and west-central Montana: Amer. Assoc. Petrol. Geologists, v. 69, p. 437-477.

Oswald, D. H., 1964a. The Howell Creek structure. Bull. Can. Petroleum Geology, v. 12, Field Conference Guide Book Issue, p. 363-377.

Oswald, D. H., 1964b. Mississippian stratigraphy of south-eastern British Columbia. Bull. Can. Petroleum Geology, v. 12, Field Conference Guide Book Issue, p. 452-459.

Panteleyev, A., 1991. Gold in the Canadian Cordillera-a focus on epithermal and deeper environments. *In* Ore deposits, tectonics and metallogeny in the Canadian Cordillera, W. J. McMillan (ed.). Ministry of Energy, Mines and Petroleum Resources. Paper 1991-4, p. 163-205.

Paterson, S. R., and Schmidt, K. L., 1999. Is there a close spatial relationship between faults and plutons? J. Struct. Geol., v. 21, p. 1131-1142.

Paterson, S. R., Fowler Jr., T. K., Miller, R. B., 1996. Pluton emplacement in arcs: a crustal-scale exchange process. Trans. Roy. Soc. Edin.: Earth Sci. v. 87, p. 115-123.

Patiño Douce, A. E., Humphreys, E. D., and Johnston, A. D., 1990. Anatexis and metamorphism in tectonically thickened continental crust exemplified by the Sevier hinterland, western North America: Earth Plan. Sci. Lett., v. 97, p. 290-315.

Pearce, J. A., and Norry, M. J., 1979. Petrogenetic implications of Ti, Zr, Y and Nb variations in volcanic rocks. Contrib. Mineral. Petrol., v. 69, p. 33-47.

Pearce, T. H., 1970. The analcite-bearing rocks of the Crowsnest Formation, Alberta. Can. J. Earth Sci., v. 7, p. 46-66.

Pell, J., 1987. Alkalic ultrabasic diatremes in British Columbia: petrology, geochronology and tectonic significance (82G, J, 83C, 94B). *In* Geological Fieldwork 1986, British Columbia Ministry of Energy, Mines and Petroleum Resources, Paper 1987-1, p. 259-267.

Peterson, T. D. and Currie K.L., 1993. Analcite-bearing igneous rocks from the Crowsnest Formation, southwestern Alberta. *In* Current Research, Part B; Geological Survey of Canada, Paper 93-1B, p. 51-56.

Peterson, T. D., Currie, K. L., Ghent, E. D., Begin, N. J., and Beiersdorfer, R. E., 1997. Petrology and economic geology of the Crowsnest Volcanics, Alberta. Geol. Surv. Can. Bull. 500, p. 163-184.

Petford, N., 1996. Dykes or diapirs? Trans. Roy. Soc. Edin. Earth Sci. v. 87, p. 105-114.

Pirsson, L. V., 1915. Scientific intelligence. Geology and Mineralogy-the Crowsnest volcanics. Amer. J. Sci., v. 39, p. 222-223.

Poulsen, K. H., 1996a. Carlin-type gold deposits and their potential occurrence in the Canadian Cordillera. *In* Current Research 1996-A, Geological Survey of Canada, p. 1-9.

Poulsen, K. H., 1996b. Carlin-type gold deposits: Canadian potential? *In* New Mineral Deposit Models for the Cordillera, Short Course Notes, Northwest Mining Association, p. E1-34.

Poulsen, K. H., Mortenson, J. K., and Murphy, D. C., 1997. Styles of intrusion-related gold mineralisation in the Dawson-Mayo area, Yukon Territory. *In* Current Research 1997-A; Geological Survey of Canada, p. 1-10.

Price, N. J., 1990. Analysis of geological structures. Press Syn. of the Univ. of Cambridge, p. 78.

Price, R. A., 1959. Flathead, British Columbia and Alberta. Geological Survey of Canada, Map 1-1959.

Price, R. A., 1962. Fernie Map-Area, East Half, Alberta and British Columbia. Geological Survey of Canada, Paper 61-24.

Price, R. A., 1965. Flathead Map Area, British Columbia and Alberta. Geological Survey of Canada, Memoir 336.

Reesor, J. E., 1958. Dewar Creek map-area with special emphasis on the White Creek batholith, B. C. Geol. Surv. Can., Memoir 292, 78p.

Renne, P. R., Deino, A. L., Walter, R. C., Turrin, B. D., Shisher, C. C. III, Becker, T. A., Curtis, G. H., Sharp, W. D., and Jaouni, A. –R., 1994. Intercalibration of astronomical and radioisotopic time. Geology, v. 22, p. 783-786.

Rice, H. M. A., 1941. Nelson map-area, east half, British Columbia. Geological Survey of Canada, Memoir 228, 86p.

Richards, J. P., 1995. Alkalic-type epithermal gold deposits-a review. *In* Magmas, fluids and ore deposits. Min. Assoc. Can. Short Course, v. 23, p.367-400.

Rollinson, H. R., 1993. Using geochemical data: evaluation, presentation interpretation. Longman Group, UK.

Ross, G. M., 2000. Introduction to special issue of Canadian Journal of Earth Sciences: The Alberta Basement Transect of Lithoprobe, Can. J. Earth Sci. v. 37, p. 1447-52.

Ross, G. M., Parrish, R. R., Villeneuve, M. E., and Bowring, S. A., 1991. Geophysics and geochronology of the crystalline basement of the Alberta basin, western Canada. Can. J. Earth Sci., v. 28, p. 512-522.

Russell, C. W., 1991. Gold mineralization in the Little Rocky Mountains, Phillips County, Montana. *In* Guidebook of the Central Montana Alkalic Province, Geology, Ore Deposits and Origin, D. W. Baker and R. B. Berg, (eds.), Montana Bureau of Mines and Geology, Special Paper 100, p. 1-18.

Schmidt, M. D., and Bowring, S. A., 2001. U-Pb zircon and titanite systematics of the Fish Canyon Tuff: an assessment of high-precision U-Pb geochronology and its application to young volcanic rocks. Geochim. et Cosmochim. Acta, v. 65, No. 59, p. 2571-2587.

Schroeter, T. G., and Cameron, R., 1996. Alkalic intrusion-associated Au-Ag, in Selected British Columbia Mineral Deposit Profiles, Vol. 2 – Metallic Deposits, D. V. Lefebure and T. Höy (eds.), British Columbia Ministry of Employment and Investment, Open File 1996-13, p. 49-51.

Sears, J. W. and Price, R. A., 1978. The Siberian Connection: A case for Precambrian separation of the North American and Siberian cratons. Geology, v. 6, p. 267-270.

Sillitoe, R. H., and Bonham, H. F., 1990. Sediment-hosted gold deposits-Distal products of magmatic-hydrothermal systems. Geology, v. 18, p. 157-161.

Skupinski, A. and Legun, A., 1989. Geology of alkalic rocks at Twentynine Mile Creek, Flathead River area, southeastern British Columbia. *In* Exploration in British Columbia 1988, B.C. Ministry of Energy, Mines and Petroleum Resources, p. B29-34.

Smithies, R. H., and Champion, D. C., 1999. Late Archean alkaline igneous rocks in the Eastern Goldfields, Yilgarn Craton, Western Australia: a result of lower crustal contamination? Jnl. Geol. Soc. London, v. 156, p. 561-576.

Sørenson, H., 1974. *In* The alkaline rocks, H. Sørenson (ed.). John Wiley and Sons, London.

Souther, J. G., 1991. Volcanic regimes, Chapter 14 in Geology of the Cordilleran Orogen in Canada, H. Gabrielse and C. J. Yorath (ed.); Geological Survey of Canada, Geology of Canada, N. 4, p. 457-490 (also Geological Society of America, the Geology of North America, v. G-2).

Thorkelson, D. J., 1985. Geology of the mid-Cretaceous volcanic units near Kingsvale, southwestern British Columbia. *In* Current Research, Part B, Geological Survey of Canada, Paper 85-1B, p. 333-339.

Tosdal, R. M., 2000. Overview of Carlin-type gold deposits in the Great Basin, Western USA. Carlin-type Au deposits of the North American Cordillera: What are they? Where are they?, MDRU Short Course # 27, Vancouver, B.C., 2000, 24p.

Villeneuve, M. E., Ross, G. M., Parrish, R. R., Theriault, R. J., Miles, W., and Broome, J., 1993. Geophysical subdivision, U-Pb geochronology and Sm-Nd isotope geochemistry of the crystalline basement of the Western Canada sedimentary basin, Alberta and northeastern British Columbia.

Geological Survey of Canada, Bulletin 447.

Wanless, R. K., Loveridge, W. D., and Mursky, G., 1968. A geochronological study of the White Creek batholith, southeastern British Columbia. Can. J. Earth Sci., v. 5, p. 375-386.

Webster, J. D., and Holloway, J. R., 1990. Partitioning of F and Cl between magmatic hydrothermal fluids and highly evolved granitic magmas. *In* Ore-bearing granite systems; Petrogenesis and mineralizing processes, H. J. Stein and J. L. Hannah (eds.), Geol. Soc. Am. Special Paper 246, p. 21-34.

Wheeler, J. O. and McFeely, P., compilers, 1991. Tectonic assemblage map of the Canadian Cordillera and adjacent parts of the United States of America. Geological Survey of Canada Map 1712A, scale 1:2 000 000, 2 sheets.

Williams, H., and James, E., 1971. Howell Property B.C. Ministry of Energy, Mines and Petroleum Resources, Assessment Report 03162.

Wilson, M. R., and Kyser, T. K., 1988. Geochemistry of porphyry-hosted Au-Ag deposits in the Little Rocky Mountains, Montana. Econ. Geol., v. 83, p. 1329-1346.

Woodsworth, G. J., Anderson, R. G., and Armstrong, R. L., 1991. Plutonic Regimes, Chapter 15 in Geology of the Cordilleran Orogen in Canada, H. Gabrielse and C. J. Yorath (ed.); Geological Survey of Canada, Geology of Canada, N. 4, p. 457-490 (also Geological Society of America, the Geology of North America, v. G-2).

Yasuda, H., and Mori, H., 1997. Spontaneous alloying of gold clusters into nanometer-sized antimony clusters. Zeitschrift für Physik D Atoms, Molecules and Clusters, v. 40, issue 1-4, p. 140-143.

Zartman, R. E., and Haines, S. M., 1988. The plumbotectonic model for Pb isotopic systematics among major terrestrial reservoirs-A case for bi-directional transport. Geochim. et Cosmochim. Acta, v. 52, p. 1327-1339.

Zhang, X. and Spry, P. G., 1994. Petrological, mineralogical, fluid inclusion, and stable isotope studies of the Gies gold-silver telluride deposit, Judith Mountains, Montana. Econ. Geol. v. 89, p. 602-627.

Appendix 1.

Sedimentary rock lithologies mapped for this study in the Howell Creek area.

Era	Period or Epoch	Group/Formation and lithology
Mesozoic	Cretaceous	**Belly River Formation** Medium-grained, massive sandstone, and shale
		Alberta Group Quartz arenite, conglomerate, dark grey to black shale, siltstone, sandstone
		Disconformity
	Triassic	**Spray River Formation** Carbonaceous shale, minor coal seams
		Disconformity
Paleozoic	Permian-Pennsylvanian	**Rocky Mountain Group** Quartz arenite, dolomitic sandstone, dolomite
	Mississippian	**Rundle Group** Pale to dark grey, bioclastic calcarenite
		Disconformity
	Devonian	**Fairholme Group** Argillaceous limestone
		Unconformity
	Cambrian	**Elko Formation** Mottled dolomite and limestone with shale unit at the base
		Flathead Formation Quartzite, quartz arenite
		Unconformity
Precambrian	Late Proterozoic-Upper Purcell Supergroup	**Roosville Formation** Green and maroon siltite, argillite, and minor carbonate
		Phillips Formation Red/maroon argillite
		Gateway Formation Green argillite and siltite
		Proterozoic undifferentiated Maroon and green siltite, argillite, quartzite and quartz arenite and minor carbonate

Appendix 2.

Fossils collected from field station 0402. Identified by Chris Collom and Dr. Russell Hall of the Department of Geology and Geophysics at the University of Calgary.

Age, Member and Formation	Identification	Fauna
Middle Coniacian Substage of Late Cretaceous, from the Muskiki Member of the Wapiabi Formation	*Scaphites ventricosus* *Cremnoceramus*?	ammonite inoceramid bivalve
Early Santonian Substage of Late Cretaceous, from the Dowling Member of the Wapiabi Formation	*Clioscaphites cf. Saxitonianus* *Clioscaphites vermiformis* *Sphenoceramus aff. lobatus* *Cordiceramus aff. cordiformis* *Pleuromya*	ammonite ammonite inoceramid bivalve inoceramid bivalve bivalve (possibly from underlying Marchybank Member
Late Santonian Substage of Late Cretaceous, from the Thistle Member of the Wapiabi Formation ('First White Specks' interval)	*Scaphites ventricosus* *Sphenoceramus cf. steenstrupi*	ammonite inoceramid bivalve

Appendix 3.

Petrographic observations of the 18 samples of the Howell Creek suite.

	Sample no. and rock type
	EB0202 foid syenite
Phenocrysts	Orthoclase; 20-25%, 5 - 8 mm x 3 - 4 mm, subhedral to euhedral, commonly with distinct growth zonations. Carlsbad and Baveno twinning present. Plagioclase; 5-10%, 2 - 5 mm x 1- 3 mm, subhedral to euhedral, An 60-80. Nepheline; <5%, ~ 2 x 2 mm, anhedral to euhedral. Apatite; 2 %, subhedral, up to 2 mm, disseminated throughout groundmass, also poikilitically held within feldspar crystals, and as clots. Relict hornblende; 15-20%, 3-4 x 1-2 mm, subhedral to euhedral, completely replaced by calcite, chlorite, muscovite?, and opaques, recognised by cleavage traces and habit.
Groundmass	30 %; feldspar crystals, also nepheline? Aegerine-augite; <1%, < 1 mm, acicular needles. Aphyric portion of groundmass extensively altered.
Alteration	Sericite; alteration of feldspar phenocrysts, widespread but not intensive, also muscovite associated with chlorite after hornblende. Chlorite; fine to medium grained after hornblende. Nepheline; <5%, <1 x 2 mm, euhedral, secondary, association with corroded feldspar phenocrysts. Biotite; <1 %, 1 - 2 mm, euhedral, reddish brown (high Ti?), associated with chlorite. Rare adularia (<<1%) and rutile (<<1%) in groundmass.
Mineralisation	Pyrite; <2 %, <1 x 1 mm, disseminated in groundmass, and localised in association with chlorite in relict hornblende. Magnetite; <1 % <1 x 1 mm, associated with pyrite. Calcite; localised areas, especially in groundmass.
	EB0603A megacrystic syenite
Phenocrysts	Orthoclase; 35%, 3-15 mm in length, pink, subhedral, mostly untwinned, rare perthitic texture, subaligned intense argillic alteration. Relict mafic minerals?; 35%, 2 mm, hexagonal prismatic crystal form.
Groundmass	Feldspar laths; 25%, <2 mm, trachytic texture.
Alteration	Feldspar phenocrysts and groundmass show saussuritisation and sericitic alteration. Limonitic veinlets.
Mineralisation	Calcite veins; 5%, associated with intensely altered areas.
	EB0610 alkali feldspar syenite
Phenocrysts	Orthoclase; 60%, 3-10 x 1-4 mm, trachytic texture, extensive argillic alteration. Completely replaced mafic minerals, 10%.
Groundmass	Feldspar laths; 10%, <1 mm, trachytic texture.

Appendix 3 cont.

Alteration	Illite; widespread. Zeolites; <5 %, 1-2 mm, anhedral form, pale green, cloudy, localised with replaced mafic minerals, and pyrite. Uralite; 20%, <2 mm acicular crystals, disseminated sheaves, pervasive, in groundmass. Apatite; < 2%, <1 mm, localised with replaced mafic minerals.
Mineralisation	Pyrite; <8%, 1 mm, subhedral to euhedral, localised within replaced phenocrysts. Marcasite; 5-7%, 1-2 mm, anhedral to euhedral, laths, localised within relict mafic crystal forms and throughout groundmass. Fluorite; <1%, 1-2 mm, dark purple, euhedral, localised.

EB1202A megacrystic syenite

Phenocrysts	Orthoclase; 25 %, 20 x 5 mm, subhedral to euhedral. Plagioclase; 10%, 3-5 x 1-2 mm, subhedral, as separate grains and within orthoclase. Hornblende; 7-8%, 2-3 mm, subhedral, variably altered, some glomerocrystic areas. Pyroxene; 7-8%, 3-4 mm, completely replaced or intensely altered. Titanite; 1-2 %, <5 mm, euhedral, simple twinning, as separate grains and within orthoclase. Apatite; 1%, <1 mm, euhedral to subhedral.
Groundmass	Feldspar laths; 35-40 %, <1.5 mm.
Alteration	Sericite; pervasive in groundmass and on edges of feldspar phenocrysts. Chlorite; fine-grained, replaces hornblende and pyroxene. Biotite; <1%, <1 mm, secondary, clotted appearance, associated with pyrite and adularia?
Mineralisation	Calcite; extensive replacement of mafic phenocrysts. Pyrite; 5%, <1 mm, disseminated, associated with calcite and alteration and replacement of mafic minerals. Fluorite; <<1%, < 2 mm, dark purple, associated with calcite.

EB1301A megacrystic syenite

Phenocrysts	Orthoclase and sanidine; 30%, 5-10 mm x 4-6 mm, euhedral, shows dissolution textures, growth zones in optical continuity, common poikilitic texture with plagioclase, clinopyroxene and smaller orthoclase crystals. Augite; 15%, 3-4 mm, highly altered or relict (identification from crystal form). Aegerine augite; <<1%, < 2mm acicular crystals, within orthoclase poikiloblasts. Titanite; <5%, 2 mm, subhedral, held within orthoclase crystals.
Groundmass	Feldspar laths; 25%, <2 mm.
Alteration	Sericite; ~ 5%, coarse to fine grained, concentrated in the groundmass and as fringes on orthoclase phenocrysts. Saussuritisation; <5%, extensive, concentrated in orthoclase phenocrysts. Rutile; <5%, 1-2 mm, honey-brown, euhedral. Adularia; <1%, < 1 mm, euhedral.

Appendix 3 cont.

Mineralisation	Calcite; replacement of mafic phenocrysts. Pyrite; 5-10%, <1 mm, disseminated, associated with calcite and alteration and replacement of mafic minerals.
	EB1809 foid syenite
Phenocrysts	Orthoclase; 55%, 5 x 2 mm, Carlsbad twinning. Aegerine-augite; 10 %, dark green, prismatic needles, <0.1- 8 mm in length; also as stubby, equant, zoned, euhedral phenocrysts, 2-4 mm, distinct dark green-mid brown pleochroism. Plagioclase; 10%, <1 mm. Analcite; 5%, 2-4 mm, highly altered, equant, disordered twinning. Nepheline; <5%, 1-3mm, equant.
Groundmass	Aphanitic; 10-15 %.
Alteration	Sericite; <5%, associated with leucocratic minerals. Uralite; <5%, associated with mafic minerals. Biotite; <10%, reddish, associated with mafic minerals.
Mineralisation	None observed
	EB1810 foid syenite
Phenocrysts	Orthoclase; 50%, two average sizes, 5 x 2 mm and <3 x 1 mm, perthitic textures, Carlsbad twinning. Aegerine-augite; 10-15 %, dark emerald green, prismatic needles, <0.1- 8 mm in length; also as stubby, equant, zoned, euhedral phenocrysts, 2-4 mm, distinct dark green-mid brown pleochroism. Analcite; 5%, 2-4 mm, highly altered, equant, disordered twinning. Andradite; <5%, 0.3-0.6 mm, euhedral, mid yellow brown, intensely corroded. Plagioclase; <5%, <1 mm. An 60-75. Nepheline; <5%, 1-3mm, equant.
Groundmass	Aphanitic; 10-15 %.
Alteration	Biotite; <10%, reddish, associated with mafic minerals. Orthopyroxene; <5%, mantling garnet. Sericite; <5%, associated with leucocratic minerals. Uralite; <5%, associated with mafic minerals.
Mineralisation	None observed
	EB1901 alkali feldspar syenite
Phenocrysts	Orthoclase; 20%, 10-20 mm in length, subhedral, fractured.
Groundmass	70%; highly altered, but appears to be same composition as phenocrysts.
Alteration	Sericite; complete replacement of phenocrysts, and alteration of groundmass. Undulatory quartz; <10%, replacing minerals. Adularia; <5%. Biotite; <1%, <1 mm, subhedral to euhedral.
Mineralisation	Pyrite; 3-5%, 1-2 mm, disseminated.

Appendix 3 cont.

HA1 154-6 alkali feldspar syenite

Phenocrysts	Orthoclase; 30%, 5-10 mm, euhedral. Apatite; 1-3%, 2 mm.
Groundmass	65% highly altered.
Alteration	Sericite?; minor argillic alteration. Adularia; euhedral, 1%, lining vugs produced by dissolution of phenocrysts, associated with calcite.
Mineralisation	Sheeted calcite veins.

HA7 169-171 alkali feldspar syenite

Phenocrysts	Orthoclase; 35%, 5-15 x 5-10 mm, tabular, euhedral, Carlsbad twinning, subaligned. Apatite; ~1%, 1-2 mm, anhedral to euhedral.
Groundmass	Feldspar; 45%, <1 mm, subaligned.
Alteration	Sericite; 5-7%, fine grained. Uralite?; 10% after mafic minerals.
Mineralisation	Pyrite; ~5%, <1 mm, disseminated in groundmass and associated with replacement of mafic minerals. Calcite; <1-5%, as vug filling, associated with pyrite.

HA7-169 alkali feldspar syenite

Phenocrysts	Orthoclase; 40%, 5-20 x 7-10 mm, elongate, tabular, euhedral, Carlsbad (contact and interpenetrant) twinning, subaligned. Apatite; ~2%, 1-2 mm, anhedral. Hexagonal, prismatic mineral; ~10%, replaced by fine grained alteration minerals.
Groundmass	Feldspar; 30%, <1 mm, subaligned, with eddies in flow patterns around individual crystals causing random orientation.
Alteration	Sericite?; 5-7%, fine-grained alteration minerals.
Mineralisation	Pyrite; ~5%, <1 mm, disseminated in groundmass and associated with replacement of amphibole? Calcite; <1%, as vug filling, associated with pyrite and rarely as core replacement of orthoclase phenocrysts.

HE1-50/56 alkali feldspar syenite

Phenocrysts	Orthoclase; 20%, 5-10 mm x 4-6 mm, euhedral. Relict mafic minerals; pyroxene, <10-15%, 2-3 mm; hornblende, <10 %, 2-3 mm.
Groundmass	Feldspar; 50%, laths.
Alteration	Argillic alteration; <5%, extensive, concentrated in orthoclase phenocrysts. Rutile; <5%, 1-2 mm, honey-brown, euhedral. Epidote; 2-3%, 2 mm, euhedral.
Mineralisation	Marcasite; 5-7%, 1-2 mm, anhedral to euhedral, laths, localised within relict mafic crystal forms and throughout groundmass. Fluorite; <1%, 1-2 mm, dark purple, euhedral, localised, spatially associated with rutile. Pyrite; <1%, subhedral, localised within relict mafic crystal forms.

Appendix 3 cont.

HE1-26 alkali feldspar syenite

Phenocrysts	Orthoclase; 55%, 3-5 mm in length, subhedral to euhedral, commonly untwinned, perthitic, saussuritic alteration. Relict mafic minerals?; 10%, 2 mm, hexagonal prismatic crystal form.
Groundmass	Feldspar; 25%, subaligned laths.
Alteration	Extensive saussuritisation of phenocrysts and groundmass. Sericitic alteration along fractures and in feldspar phenocrysts. Biotite; 5%, red-brown. Oxidation of pyrite.
Mineralisation	Pyrite; 5%, 2 mm. Rutile; <1%, <2 mm. Both euhedral and concentrated in areas of replaced mafic minerals.

HE1-68 alkali feldspar syenite

Phenocrysts	Orthoclase; 45-50%, 5-7 mm in length, subhedral, saussuritic alteration. Titanite; 1%, euhedral, 2 mm. Relict mafic minerals; 10%.
Groundmass	Feldspar; 20-25%, laths.
Alteration	Extensive saussuritisation of phenocrysts and groundmass. Sericite associated with feldspar phenocrysts.
Mineralisation	Pyrite; <10%, disseminated. Calcite; 5%, associated with alteration of mafic minerals.

HE2-59 alkali feldspar syenite

Phenocrysts	Orthoclase; 50%, 5-10 mm in length, subhedral to euhedral, saussuritic alteration. Titanite; 1%, euhedral, 2 mm. Relict mafic minerals; 15%.
Groundmass	Feldspar; 25%, laths.
Alteration	Extensive saussuritisation of phenocrysts and groundmass. Sericitic of feldspar phenocrysts.
Mineralisation	Pyrite; <10%, disseminated. Rutile; 2%, 2 mm.

HE3-38.7 alkali feldspar syenite

Phenocrysts	Orthoclase; 25-30%, 10-20 x 5-8 mm, argillic alteration of rims. Aegerine-augite; 15-20%, <1 mm, acicular needles. Titanite; <1%, <2mm, subhedral to euhedral. <10%, pyroxene/amphibole, totally replaced by secondary minerals, recognised only by relict form.
Groundmass	Feldspar; 30-35%, 3 x 1 mm.
Alteration	Extensive argillic alteration of groundmass and feldspar crystal edges. Adularia; <2%, <2 mm, associated with areas of calcite and with veinlets.

Appendix 3 cont.

Mineralisation	Pyrite: <5%, <2 mm, disseminated. Calcite; <3%, replaces mafic? minerals, and as veinlets. Rutile; <1%, <2 mm, subhedral to euhedral, associated with alteration of mafic minerals.

HE4-198 alkali feldspar syenite

Phenocrysts	Orthoclase; 60%, 2-12 x up to 5 mm, subhedral. Plagioclase; 20-25%, 2-12 mm in length, subhedral, An 65-75. Both feldspars show extensive illite and sericite alteration. Apatite; <1%, <1 mm, euhedral.
Groundmass	Feldspar crystals; 3-8 mm in length, subhedral, perthitic texture. Original rock has granular texture of intergrown subhedral feldspar crystals. Groundmass apparent only in cm-sized vein with hypidiomorphic granular texture of same composition as the early phenocrysts.
Alteration	Extensive sericitic and argillic alteration. Rare calcite filling miarolitic cavities in vein and forming veinlets. Actinolite?; <<1%, <1 mm.
Mineralisation	Pyrite; 5%, 1-2 mm, associated with intense alteration.

HE4-94 alkali feldspar syenite

Phenocrysts	Orthoclase; 60%, 5 x 7 mm, subhedral. Plagioclase; 20%, 7-10 mm in length, subhedral. Apatite; <1%, <1 mm, euhedral.
Groundmass	Feldspar crystals; 15%, 3-8 mm in length, subhedral, perthitic texture. Original rock has granular texture, with intergrown subhedral feldspar crystals.
Alteration	Sericitic and argillic alteration.
Mineralisation	Pyrite; 5%, 1-2 mm, disseminated.

Appendix 4.

Geochemical analyses of 18 samples of the Howell Creek suite.

wt. % = weight percent.

bd = below detection limits.

na = not applicable (analysis not undertaken).

Mg# = 100[MgO/(MgO+FeO ^{total})].

wt. %	EB0202	EB0603A	EB0610	EB1202A	EB1301A	EB1809	EB1810	EB1901	HA1 154-6	HA7 169-171	HA7 169	HE1 26	HE1 50-56	HE1 68	HE2 59	HE3 38.7	HE4 198	HE4 94
SiO_2	59.6	60.6	61.9	60.1	60.3	58.6	59.5	63.7	58.0	58.5	58.8	61.5	59.9	60.9	60.4	57.8	63.4	62.9
TiO_2	0.47	0.20	0.22	0.31	0.34	0.17	0.15	0.38	0.20	0.24	0.23	0.17	0.18	0.18	0.29	0.22	0.18	0.16
Al_2O_3	17.1	20.0	19.9	18.1	18.2	19.2	20.1	19.5	18.8	20.5	20.6	19.6	18.8	19.1	18.3	18.6	18.5	18.8
FeO	1.9	0.4	0.2	1.1	1.3	0.5	0.4	0.1	0.9	0.1	bd	0.1	0.3	0.1	0.3	0.5	bd	bd
Fe_2O_3	2.9	2.0	2.1	2.2	2.1	1.7	1.7	0.8	1.4	2.5	2.0	1.9	1.9	2.1	3.8	1.9	2.7	2.4
MnO	0.13	0.07	bd	0.11	0.12	0.06	0.06	0.02	0.05	0.02	0.02	bd	0.07	0.04	0.09	0.17	0.03	bd
MgO	0.68	0.37	0.27	0.57	0.56	0.47	0.16	0.26	0.99	0.32	0.28	0.12	0.44	0.22	0.41	0.49	0.12	bd
CaO	5.17	0.56	0.03	3.59	3.31	0.68	1.05	0.08	2.51	2.48	2.88	0.03	1.12	0.51	1.07	2.85	0.65	0.2
Na_2O	4.1	1.2	1.1	5.4	4.4	5.8	7.4	0.5	2.6	1.0	0.8	1.3	1.5	1.6	3.9	2.8	5.0	4.9
K_2O	4.4	12.6	11.8	5.7	6.5	8.6	6.9	12.7	10.0	11.1	11.1	12.6	12.2	11.9	8.5	10.1	7.2	7.5
P_2O_5	0.22	0.04	0.02	0.09	0.09	0.04	0.02	0.03	0.04	0.06	0.07	0.01	0.04	0.03	0.05	0.05	0.06	0.05
Cr_2O_3	bd	bd	bd	bd	bd	bd	bd	bd	bd	bd	0.02	0.01	bd	0.01	0.02	bd	0.03	0.02
LOI	3.2	1.8	2.2	2.4	2.5	2.9	2.4	1.6	2.3	2.6	2.9	1.8	1.9	1.9	1.7	3.2	1.8	1.7
Total	**99.9**	**99.8**	**99.6**	**99.7**	**99.8**	**98.7**	**99.8**	**99.6**	**99.7**	**99.3**	**99.6**	**99.0**	**98.4**	**98.6**	**98.9**	**98.6**	**99.5**	**98.6**
S	na	0.03	na	0.17	na	na	na	0.02	0.07	na	1.22	1.24	1.14	1.27	0.05	1.12	1.77	1.73
CO_2	na	0.34	na	bd	na	na	na	0.01	2.09	na	na	na	na	na	na	2.93	na	na
CO_3	na	na	na	na	na	na	na	na	na	na	2.71	0.01	1.75	0.66	0.53	na	0.72	0.01
H_2O^+	na	na	na	na	na	na	na	na	na	na	1.4	0.9	0.7	0.7	1.2	na	0.4	0.5
H_2O^-	na	na	na	na	na	na	na	na	na	na	0.2	0.2	0.1	0.2	0.2	na	0.1	0.2
Mg#	12.3	13.6	10.7	14.6	14.0	17.7	7.2	23.4	30.2	11.0	12.5	5.8	16.4	9.1	9.0	17.1	4.3	0.0
Fe^{3+}/Fe^{2+}	1.5	4.9	10.3	2.0	1.6	3.4	4.1	7.5	1.5	24.9	0.0	18.6	6.5	21.0	12.8	3.7	0.0	0.0

Appendix 4 cont.

Geochemical analyses of 18 samples of the Howell Creek suite.

ppm = parts per million.

$Eu/Eu^* = (Eu_N/\sqrt{[(Sm_N).(Gd_N)]})$ – using normalisation values from Jenner (NewPet; 1987-1994).

ppm	EB0202	EB0603A	EB0610	EB1202A	EB1301A	EB1809	EB1810	EB1901	HA1 154-6	HA7 169-171	HA7 169	HE1 26	HE1 50-56	HE1 68	HE2 59	HE3 38.7	HE4 198	HE4 94
Li	23.9	25.5	46.4	23.7	21.3	42.3	27.2	28.3	75.8	26.5	31.9	58.5	41.5	38.4	189.8	48.8	2.1	2.3
Be	2.48	6.25	4.61	3.59	3.36	8.85	7.55	2.17	6.38	5.73	5.21	4.54	3.08	3.02	4.39	2.85	2.35	2.25
Sc	10.11	1.56	2.71	3.93	4.32	1.40	0.84	2.22	1.63	2.07	1.71	0.75	1.48	1.16	1.91	2.26	2.04	1.65
V	97.6	100.8	100.1	77.6	79.0	89.5	70.8	93.4	91.7	106.3	108.5	80.2	47.9	55.8	109.4	68.5	29.4	32.1
Rb	114	305	300	143	161	172	144	296	205	260	206	343	292	305	184	227	176	177
Sr	1349	441	1675	2104	2270	1044	1642	419	571	1495	1052	755	836	796	2673	2230	528	637
Y	19.2	17.7	10.8	15.7	16.3	12.0	12.6	15.6	8.4	11.8	11.7	4.9	5.7	5.3	8.9	10.2	6.1	7.1
Zr	86	312	225	136	133	315	356	166	285	154	336	147	126	134	200	112	99	118
Nb	12.9	37.5	35.7	17.8	17.4	44.6	42.9	16.8	34.3	47.9	53.3	21.0	19.9	20.3	18.9	19.0	15.2	16.2
Mo	0.4	0.5	0.7	0.8	0.3	0.8	0.5	0.4	0.8	0.2	0.6	0.5	0.8	0.6	0.4	0.4	1.8	16.4
Cs	11.9	12.1	6.5	7.0	11.1	8.5	9.2	7.1	88.7	9.7	6.9	5.1	2.8	3.2	35.4	3.7	2.8	3.2
Ba	1482	2080	3520	2652	3185	1807	1000	1983	4019	3563	3212	2346	1117	1232	5201	3462	2087	2447
La	40.9	81.5	22	36.9	37.1	69.1	45.5	36.8	44.8	57.2	63.7	13.3	37.1	32.6	34.9	36.5	13.5	17.6
Ce	75	97	37	65	67	98	70	66	70	93	107	19	61	52	56	61	28	28
Pr	8.2	11.2	3.9	7.3	7.5	8.7	6.2	7.6	6.6	9.2	11.1	1.7	5.7	4.8	5.5	6.2	3.2	2.9
Nd	30.8	35.5	12.8	26.7	27.6	25.6	18.2	27.9	20.0	28.7	32.8	5.3	17.5	15.0	16.8	20.3	12.2	10.2
Sm	5.68	5.25	2.30	4.70	4.99	3.35	2.61	5.40	2.88	4.06	3.88	0.89	2.02	1.69	2.28	3.26	2.03	1.87
Eu	1.81	1.33	0.79	1.40	1.50	0.88	0.73	1.58	0.75	1.04	0.97	0.33	0.52	0.41	0.55	0.91	0.59	0.69
Gd	4.78	4.12	1.82	3.67	3.76	2.64	1.95	3.89	2.32	2.75	2.85	0.85	1.48	1.28	1.69	2.39	1.57	1.65
Tb	0.59	0.48	0.24	0.44	0.43	0.28	0.25	0.44	0.25	0.30	0.33	0.11	0.15	0.12	0.17	0.24	0.19	0.21
Dy	3.52	2.82	1.44	2.51	2.57	1.74	1.59	2.7	1.29	1.67	2.02	0.73	0.86	0.79	1.07	1.43	1.22	1.3
Ho	0.69	0.54	0.29	0.47	0.48	0.35	0.33	0.56	0.27	0.33	0.4	0.12	0.16	0.13	0.19	0.27	0.24	0.26
Er	2.00	1.51	0.83	1.39	1.39	1.07	1.09	1.73	0.90	1.01	1.14	0.39	0.45	0.38	0.54	0.79	0.71	0.74
Tm	0.29	0.22	0.14	0.22	0.21	0.18	0.19	0.26	0.14	0.16	0.17	0.06	0.06	0.06	0.09	0.11	0.12	0.12
Yb	1.82	1.42	0.99	1.47	1.48	1.25	1.27	1.76	0.94	1.00	1.17	0.47	0.47	0.44	0.72	0.74	0.77	0.86
Lu	0.36	0.28	0.19	0.29	0.29	0.24	0.24	0.37	0.20	0.22	0.17	0.06	0.07	0.06	0.10	0.16	0.12	0.13
Hf	3.80	7.41	5.86	3.83	4.02	8.32	8.05	5.40	6.87	5.26	10.01	4.15	4.11	3.49	6.43	3.76	3.11	3.06
Ta	0.70	0.87	1.43	0.81	0.81	1.27	1.20	0.60	0.80	1.38	1.59	0.62	0.63	0.62	0.73	0.76	0.76	0.84
Tl	1.07	4.64	10.21	2.02	1.50	1.83	1.61	11.21	2.49	9.16	7.77	11.06	7.95	7.99	2.06	4.40	4.01	3.93
Pb	16.4	17.1	28.2	20.0	33.5	61.0	64.8	142.6	35.6	43.5	36.5	74.5	48.9	55.5	52.7	68.3	85.9	51.7
Bi	0.20	0.27	0.23	0.14	0.19	0.34	0.19	0.13	0.26	0.13	0.11	0.28	0.19	0.21	0.23	0.14	0.97	1.24
Th	8.9	27.2	18.0	10.4	10.7	35.3	36.1	11.7	22.3	26.5	27.7	9.9	17.7	15.9	13.7	12.9	5.3	4.6
U	3.4	14.6	8.6	5.4	5.4	14.4	18.7	5.3	12.0	3.7	11.1	10.0	12.3	13.1	8.4	7.1	5.4	7.0
Eu/Eu*	1.06	0.87	1.18	1.03	1.06	0.90	0.99	1.05	0.89	0.95	0.89	1.16	0.92	0.85	0.86	1.00	1.01	1.20

Appendix 5.

Geochronological data for sample EB1301A and EB1810.

a: As measured by laser in % of full nominal power (10W).
b: Fraction ^{39}Ar as percent of total run.
c: Errors are analytical only and do not reflect error in irradiation parameter J.
d: Nominal J, referenced to FCT-SAN=28.03 Ma (Renne et al., 1994).

*: Step not included in age determination.
**: Step not included in regression through atmospheric air.

All uncertainties quoted at 2σ level.

Power[a]	Vol. ^{39}Ar x^{10-11} cc	$^{36}Ar/^{39}Ar$	$^{37}Ar/^{39}Ar$	$^{38}Ar/^{39}Ar$	$^{40}Ar/^{39}Ar$	%^{40}Ar (atmos)	$^{*40}Ar/^{39}Ar$	f_{39}[b] (%)	Apparent Age Ma[c]
Aliquot: A		**EB1301A Feldspar; J =.00313760[d] (49° 12' 33" N, 114° 42' 20" E)**							
2.4*	1.4486	0.0094±0.0006	0.075±83.654	0.026±0.001	28.969±0.228	9.5	26.203±0.211	0.5	142.54±1.10
2.8*	4.8581	0.0012±0.0002	0.018±54.909	0.005±0.001	19.229±0.065	1.8	18.879±0.061	1.8	103.82±0.33
3.5	29.8497	0.0003±0.0000	0.012±50.113	0.002±0.000	18.719±0.037	0.5	18.630±0.038	11	102.49±0.20
3.9	39.3984	0.0003±0.0000	0.012±25.723	0.002±0.000	18.730±0.024	0.4	18.646±0.024	14.5	102.57±0.13
4.2	34.846	0.0001±0.0000	0.011±32.205	0.002±0.000	18.634±0.032	0.2	18.606±0.033	12.8	102.36±0.18
4.6	15.8603	0.0002±0.0001	0.012±81.933	0.001±0.000	18.659±0.049	0.3	18.606±0.051	5.8	102.36±0.27
12	145.6232	0.0003±0.0000	0.011±53.517	0.002±0.000	18.681±0.055	0.4	18.599±0.056	53.6	102.32±0.30
Aliquot: A		**EB1810 Feldspar; J =.00312800[d] (49° 13' 05" N, 114° 39' 05" E)**							
2.4*	0.2962	0.0185±0.0028	0.061±90.373	0.032±0.003	30.157±0.796	18.1	24.692±0.647	0.1	134.22±3.39
3.0*	12.2083	0.0005±0.0001	0.012±56.744	0.002±0.000	15.124±0.074	1	14.976±0.077	2.6	82.59±0.42
3.5*	15.2557	0.0005±0.0001	0.002±40.937	0.002±0.000	17.990±0.056	0.8	17.855±0.057	3.2	98.05±0.31
3.9	15.6278	0.0007±0.0001	0.002±91.227	0.001±0.000	18.758±0.040	1	18.564±0.043	3.3	101.83±0.23
4.2**	48.7287	0.0007±0.0000	0.001±51.326	0.002±0.000	18.847±0.090	1	18.653±0.090	10.3	102.31±0.48
4.6	26.0714	0.0003±0.0000	0.002±88.682	0.002±0.000	18.588±0.028	0.4	18.509±0.028	5.5	101.54±0.15
12.0	26.665	0.0003±0.0000	0.001±81.370	0.002±0.000	18.595±0.046	0.5	18.504±0.046	5.6	101.51±0.25
Aliquot: B									
2.4*	0.0495	0.1136±0.0222	0.365±207.340	0.170±0.065	49.424±5.656	67.9	15.857±6.542	0	87.34±35.17
3.0*	0.4211	0.0138±0.0022	0.116±85.995	0.020±0.005	20.657±0.515	19.7	16.578±0.501	0.1	91.21±2.69
3.5*	0.7016	0.0107±0.0010	0.134±56.808	0.015±0.002	17.001±0.362	18.6	13.841±0.249	0.2	76.46±1.35
3.9*	4.0448	0.0013±0.0002	0.016±61.332	0.003±0.000	15.344±0.067	2.6	14.952±0.062	0.9	82.47±0.33
4.2*	3.9691	0.0012±0.0003	0.007±64.262	0.004±0.000	17.385±0.083	2.1	17.019±0.091	0.8	93.58±0.49
4.6*	5.5775	0.0008±0.0002	0.007±56.063	0.003±0.001	17.749±0.056	1.4	17.506±0.055	1.2	96.18±0.29
5.0*	4.06	0.0013±0.0002	0.011±47.627	0.003±0.000	17.921±0.058	2.2	17.531±0.040	0.9	96.32±0.22
5.5*	9.6189	0.0004±0.0001	0.009±107.271	0.003±0.000	18.057±0.040	0.6	17.947±0.044	2	98.54±0.23
6.0*	12.0797	0.0004±0.0001	0.005±22.733	0.003±0.000	18.284±0.046	0.7	18.161±0.044	2.6	99.68±0.24
6.5	149.6495	0.0003±0.0001	0.001±25.782	0.002±0.000	18.638±0.039	0.6	18.535±0.044	31.7	101.68±0.24
12.0	137.7617	0.0003±0.0000	0.001±166.234	0.002±0.000	18.619±0.038	0.5	18.534±0.039	29.1	101.67±0.21

Elspeth Barnes - Curriculum Vitae

Education

1999-2002 **Master of Science, Earth and Atmospheric Sciences**
University of Alberta

Courses taken:

- 'METALLIFEROUS ORE DEPOSITS' (Dr. J. P. Richards).
- 'GEOCHEMISTRY OF ORE DEPOSITS' (Dr. J. P. Richards).
- 'STRUCTURAL GEOLOGY AND TECTONICS' (Dr. P. Erdmer).
- 'GRANITES AND CRUSTAL EVOLUTION' (audited; Dr. T. Chacko and Dr. R. Creaser).

1996-1999 **Bachelor of Science (Hons) 2.1, Geology and Applied Geology**
University of Glasgow, Scotland

1996-1997 **Exchange Student**
University of British Columbia

Work Experience

Academic Experience

Teaching Assistant
University of Alberta
'METALLIFEROUS ORE DEPOSITS'- 4th year course, 2000 and 2001

- **Received Graduate Student Association Teaching Award, 2001**

'INTRODUCTORY GEOLOGY' – 1st year course, 2000
'MINERALOGY' – 2nd year course, 1999

Field School Teaching Assistant
University of Alberta
'ADVANCED GEOLOGY FIELD SCHOOL – A GUIDE TO THE GEOLOGY OF THE SOUTHEASTERN CANADIAN CORDILLERA, ALBERTA AND BRITISH COLUMBIA' - 3rd year course, May 2001.

Fieldwork Leader
University of Alberta
Fieldwork component of thesis

1996-1997 **Field Assistant**
Geological Survey of Canada
Volunteer for the NATMAP project in central British Columbia working under the guidance of Dr. R.G. Anderson. Summer field seasons.

Business, Marketing, and Research Experience

1995-1996 **Research Assistant**
Fundraising Department,
Royal Opera House, Covent Garden, London

1987-1995 **Subscription Department Supervisor**
and **Premium Services Supervisor**
Box Office, Marketing Department and Trust Department
Royal Opera House, Covent Garden, London

Awards and Grants

Faculty of Science Teaching Assistant bursary, 1999-2000 and 2000-2001
Bruce E. Nesbitt Memorial Graduate Award, 2000
Graduate Intern Tuition Supplement, 2000
British Columbia Geological Survey, 1999-2000
(*also* Graduate Student Association Teaching Award, 2001 *and*
Society of Economic Geologists-McKinstry Research Grant, 2000)

Academic Presentations

Talks

'The role of magmatism in gold deposition: the Howell Creek area, southeastern British Columbia', presented during 'New Ideas for a New Millennium' Cranbrook, B.C., 2000

Posters

'Cretaceous alkalic intrusions of the Howell Creek area', Cordilleran Roundup, Vancouver, B.C., 2001

'Gold deposition and magmatism: the Howell Creek area, southeastern British Columbia', Cordilleran Roundup, Vancouver, B.C., 2000

'Gold and magmatism: the Howell Creek area, southeastern British Columbia', Geological Association of Canada/Mineralogical Association of Canada conference, Calgary, Alberta, 2000.

Short Courses

'Structural controls on ore genesis', Society of Economic Geologists Short Course, Toronto, Ontario, 2001

Carlin-type Au deposits of the North American Cordillera: What are they? Where are they?, MDRU Short Course # 27, Vancouver, B.C., 2000

Publications

Anderson, R. G., Snyder, L. D., Grainger, N. C., Resnick, J., Villeneuve, M. E., and **Barnes**, E. M., 2001. Eocene – Neogene magmatism in the Nechako River area, Central British Columbia; (abstract) in F. Cook and P. Erdmer (compilers), Slave – Northern Cordillera Lithospheric Evolution

(SNORCLE) transect and Cordilleran Tectonics Workshop Meeting, (February 22-25) Pacific Geoscience Centre, Lithoprobe Report No. 79, P. 199-201.

Anderson, R. G., Snyder, L. D., Resnick, J., Grainger, N. C., **Barnes**, E. M., and Pint, C. D., 2000. Mesozoic geology of the Takysie Lake and Marilla map areas, central British Columbia. *in* Current Research 2000A, Geological Survey of Canada, (online; http://www.nrcan.gc.ca/gsc/bookstore)

Anderson, R. G., Snyder, L. D., Resnick, J., Grainger, N. C., and **Barnes**, E. M., 2000. Tertiary geology of the Takysie Lake and Marilla map areas, central British Columbia. *in* Current Research 2000A, Geological Survey of Canada, (online; http://www.nrcan.gc.ca/gsc/bookstore)

Barnes, E. M., and Anderson, R. G., 1999. Mineralogy of amygdaloidal, mafic flow rocks of the Endako Group in the Kenney Dam area, northeastern Nechako River map area, central British Columbia. *in* Current Research 1999-A/B, Geological Survey of Canada, p. 9-20.

Barnes, E. M., and Anderson, R. G., 1999. Bedrock geology of the Uncha Mountain area, northwestern Nechako River area, central British Columbia. *in* Current Research 1999-A/B, Geological Survey of Canada, p. 129-138.

Anderson, R. G., Snyder, L. D., Resnick, J., Grainger, N. C., and **Barnes**, E. M., 1999. A reconnaissance of the Knapp Lake map area, central British Columbia. *in* Current Research 1999A, Geological Survey of Canada, p.109-118.

Anderson, R. G., Snyder, L. D., Resnick, J., and **Barnes**, E. M., 1998. Geology of the Big Bend area, central British Columbia. *in* Current Research 1998-A/B, Geological Survey of Canada, p.145-154.